Ultrastructural and immunohistochemical studies of the development of the nervous system and the mesoderm in Enteropneusta and Pterobranchia in order to elucidate deuterostome evolution

Dissertation
zur Erlangung des Grades des
Doktors der Naturwissenschaften (Dr. rer. nat.)
am Fachbereich Biologie, Chemie und Pharmazie
der Freien Universität Berlin

vorgelegt von
Sabrina Kaul-Strehlow

aus Husum

Oktober 2011

Gutachter

Erster Gutachter:	Prof. Dr. Klaus Hausmann Institut für Biologie Fachbereich Biologie, Chemie und Pharmazie Freie Universität Berlin
Zweiter Gutachter:	PD Dr. Thomas Stach Institut für Biologie Fachbereich Biologie, Chemie und Pharmazie Freie Universität Berlin
Datum der Disputation:	2. Dezember 2011

Erklärung

Hiermit erkläre ich, dass ich die vorliegende Arbeit ohne die unzulässige Hilfe Dritter und ohne die Verwendung anderer als der angegebenen Hilfsmittel angefertigt habe.
Diese Arbeit wurde bisher weder im In- noch im Ausland in gleicher oder ähnlicher Form einer anderen Prüfungsbehörde vorgelegt.

Berlin, den 31. Oktober 2011

Sabrina Kaul-Strehlow

Danksagung

Herrn PD Dr. Thomas Stach möchte ich für die Aufnahme in seine Arbeitgruppe und die Betreuung dieser Dissertation herzlich danken. Herrn Prof. Dr. Klaus Hausmann danke ich an dieser Stelle für die abschließende Betreuung und die Übernahme der Kommissionsleitung.

Diese Arbeit wurde durch eine Finanzierung seitens der Deutschen Forschungsgemeinschaft im Rahmen des SPP „Deep Metazoan Phylogeny“ ermöglicht. Ich danke der DFG freundlichst für die umfassende Förderung meines Dissertationsvorhabens.

Ganz besonders danken möchte den Mitglieder der AG Stach und den Tutoren der Zoologie der FU Berlin. Mein besonderer Dank gehört an dieser Stelle nochmals meinem Betreuer PD Dr. Thomas Stach, der mir die Anregung für diese Arbeit gab und mich, wann immer es ging, mit anregenden Diskussionen versorgte. Allen voran möchte ich außerdem Dipl.-Biol. Fanny Leubner und Katrin Braun (M. Ed) danken, die mit mir nicht nur eine Begeisterung für die Tierwelt teilen, sondern darüber hinaus auch zu wertvollen Freundinnen für mich geworden sind. Nicht vergessen werden dürfen in diesem Zusammenhang die zahllosen „Tutoren-Grillereignisse“, die wir auf der Terrasse des EBS veranstaltet haben, sie waren immer eine erfreuliche Ablenkung. Außerdem möchte ich Dr. Esther Ullrich-Lüter und Dipl.-Biol. Tobias Kaller danken, die mir stets ihr Gehör geschenkt haben, nicht nur bei inhaltlichen Diskussionen sondern auch bei Anliegen außerhalb der Universitätswelt.
Waltraud Brackwehr möchte ich für ihre unbezahlbare Hilfe zur Überwindung von bürokratischen Hindernissen danken, aber auch für die vielen erheiternden und interessanten Gespräche.

Meinen Eltern möchte ich ganz herzlich dafür danken, dass sie nie aufgehört haben, an mich zu glauben, und außerdem dafür, dass ich bei Ihnen immer ein zu Hause haben werde. Besonders meiner Mutter bin ich zu tiefem Dank verpflichtet, ohne ihre vorbehaltlose Unterstützung wäre ich jetzt nicht hier.

Mein spezieller und innigster Dank gilt meinem Mann Benjamin Strehlow. Ohne sein grenzenloses Verständnis und seine fortwährende Unterstützung wäre diese Arbeit so nicht zustande gekommen, weshalb sie ihm gewidmet ist. Danke.

Table of Contents

1. General Introduction

1.1 Deuterostomia

Deuterostomia comprise one of the major groups of the Bilateria and is a sister group to the Protostomia, including e.g. molluscs, annelids, and arthropods (Edgecombe et al. 2011, Nielsen 2001, Peterson & Eernisse 2001). Deuterostomia consists of five higher groups, Echinodermata, Hemichordata, Cephalochordata, Tunicata, and Craniata, of which the three latter ones form the taxon Chordata. Xenoturbellida represents probably a sixth taxon (Bourlat et al. 2006), but see Hejnol et al. (2009) or Edgecombe et al. (2011) for a different view.

The monophyly of Deuterostomia is supported by at least two well-defined apomorphies, which are deuterostomy and enterocoely (Nielsen 2001, Schaeffer 1987). During early development, gastrulation occurs at the vegetal pole and the blastopore typically becomes the anus in adults, whereas the mouth develops secondarily from the archenteron as a new opening (MacBride 1896, Spengel 1893). The other character, that is uniting deuterostome animals as a monophyletic taxon, is the origin of the third germ layer, mesoderm from the archenteron by a process called enterocoely (Ax 2001, Hyman 1951, Technau & Scholz 2003). The mesoderm then typically develops into three pairs of coelomic cavities, named from anterior to posterior protocoel, mesocoel, and metacoel (Ax 2001, Nielsen 2001, Schaeffer 1987). Accordingly, body organization is predominantly trimeric within non-chordate deuterostome taxa consisting of a prosome, mesosome and metasome, respectively.

Other presumed deuterostome characteristics, such as radial cleavage pattern (Burdon-Jones 1952, Hörstadius 1973), lack of incorporation of larval nervous system into the adult (Cameron & Hinegardner 1974, Chia & Burke 1978), or a dipleurula-like larval stage (Nielsen 1987; 2005), are either plesiomorpic, because radial cleavage pattern is inherited from the metazoan ancestor (Ax 2001); whereas the lack of incorporation of the larval nervous system into the adult is controversially discussed (Hay-Schmidt 2000) and was recently documented not to be true for tunicates (Horie et al. 2011); and the dipleurula-like larval stage is considered to represent a synapomorphy uniting two higher taxa of deuterostomes together as sister groups, Echinodermata and Hemichordata (Cameron 2005, Ruppert 2005).

1.2 Chordata

Chordata comprises a well-defined taxon, consisting of Tunicata, Cephalochordata, and Craniata. Chordates are characterized by exhibiting a notochord, a skeletal rod that serves as a central stiffening element that ensures length constancy by allowing alternate contractions of the bilateral longitudinal muscles into lateral undulations. The notochord is always derived from the dorsal region of the archenteron during early development (Hausen & Riebesell 1991, Hirakow & Kajita 1994, Munro & Odell 2002). The cells composing the notochord differ drastically from highly vacuolated to non-vacuolated cells in the three groups though (Welsch 1968, Welsch & Storch 1969, Stach 1999), homology of the notochord among

chordate taxa is further supported by the expression of *brachyury* during determination of the notochord (Holland et al. 1995, Wilkinson et al. 1990, Yasuo & Satoh 1994).

In Chordata, the notochord is dorsally accompanied by the neural tube, a strand of nervous tissue that, together with an anterior brain, comprises the central nervous system (Stach 2008). Furthermore, all neural tubes possess a central fluid-filled canal with cilia. This canal is continuous with the endodermal lumen at the posterior end during early development and called the neurenteric canal (Müller & O'Rahilly 1985, Salvini-Plawen 2000). The neural tube of chordates is formed during ontogeny by a characteristic process called neurulation (Keller 1975; 1976, Nicol & Meinertzhagen 1988, Hirakow & Kajita 1994, Stach 2000). First, a longitudinal fold is formed along the dorsal midline of early ontogenetic stages. A hollow neural tube is then be formed by classical invagination of a monolayered, a bilayered, or a multilayered epithelium (Nicol & Meinertzhagen 1988, Saveliev 2009, Schoenwolf & Smith 1990), or by sinking in of the neural plate that subsequently is overgrown from the lateral epidermis (Hirakow & Kajita, 1994, Stach, 2000), or by the delamination of a solid tissue rod underneath the epidermis (Lowery & Sive 2004, Watters 2006). Thus, despite its final subepidermal position, the neural tube is ectodermal in origin.

In Chordata, the pharynx is perforated and possesses gill slits for filter-feeding and respiration (Ruppert 1997a). Furthermore, within the ventral midline of the pharyngeal region, the endostyle is present. It incorporates iodine and produces a continuous mucous net for food-capture (Fiala-Médioni 1978a; b, Jorgensen 1966, Mallat 1979; 1981, Olsson 1963, Riisgard & Svane 1999). Beside the three most prominent chordate apomorphies, notochord, neural tube and gill slits with a ventral endostyle (Benito & Pardos 1997, Boorman & Shimeld 2002, Lemaire et al. 2008, Stach 2008), *left-right (LR) asymmetry* in the organization of certain structures is a typical chordate feature as well (Boorman & Shimeld 2002, Gerhart et al. 2005).

Based on the preceding characters, Chordata itself is well supported as a monophyletic taxon. However, the origin and evolution of the aforementioned chordate features is currently far from being understood, when it comes to find potentially homologous rudiments in non-chordate deuterostomes, i.e. echinoderms and hemichordates.

1.3 Hemichordata

Hemichordata is a taxon of non-chordate deuterostomes that consists of two subgroups, the colonial and small pterobranchs on the one hand, and the solitary, wormlike enteropneusts (Benito & Pardos 1997, Hyman 1959, van der Horst 1939). About 100 species are currently described of these exclusively marine and benthic invertebrates that are distributed worldwide (Cameron 2005). Both hemichordate groups possess a trimeric body organization divided into a short prosome and mesosome, followed by the metasomal region (Fig. 1.1, 1.2A, B). The prosome is called "proboscis" in enteropneusts and "cephalic shield" in pterobranchs and followed by the "collar" or "mesosome" that surrounds the mouth bearing a tentacular crown in pterobranchs (Benito & Pardos 1997, van der Horst 1939). Within the anterior

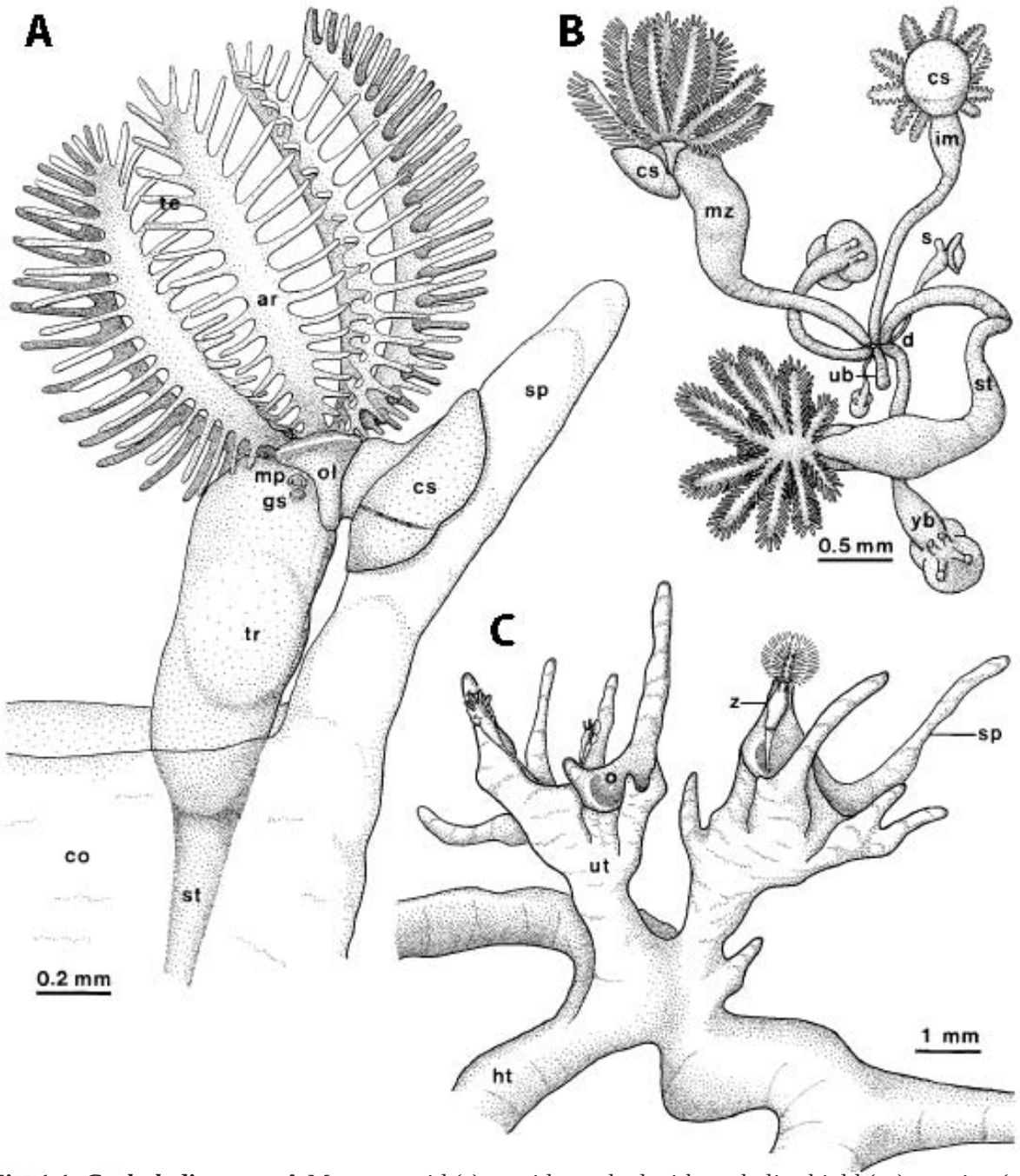

Fig. 1.1. ***Cephalodiscus*** **sp. A** Mature zooid (*z*); zooid attached with cephalic shield (*cs*) to spine (*sp*) of coenecium (*co*); arms (*ar*) and tentacles (*te*) arched to form feeding basket. **B** Cluster of zooids at various stages of development; basal disc (*d*) at ends of stalks (*st*) is also the budding zone; note arm tip swellings (*s*) of young buds (*yb*) without tentacles. **C** Colony formation; hollow coenecium consists of horizontal tubes (*ht*), contacting the substrate and uptight tubes (*ut*), which possess distal ostia (*o*) and spines. *gs* gill slit, *im* immature bud with developing tentacles, *mz* mature zooid, *mp* mesocoel pore, *o1* oral lamella, *tr* trunk, *ub* undifferentiated bud (from Lester 1985).

protocoel of hemichordates, a characteristic excretory structure is present, the stomochord-pericardium-glomerulus complex (Dohle 2004). The stomochord is a rod-like extension of the buccal cavity that projects into the protocoel. It is filled with vacuolated cells and serves as a support of the heart sinus and pericardium which are situated above the stomochord (Balser & Ruppert 1990, Kaul-Strehlow & Stach 2011, Chapter 4). The glomerulus is spanning the anterior tip of the stomochord and is a highly dilated blood sinus that receives input from the posterior heart sinus. Because of its endodermal origin and the presence of vacuolated

cells, the stomochord has been suggested to be a homologue of the chordate notochord early on (Bateson 1885, Barrington 1965, Komai 1951).

Pterobranchia comprises a comparably species-poor group, consisting of less than 30 described species (Cameron 2005, Nielsen 2001). All species are colonial and almost sessile animals living in secreted tubes attached to hard substratum (Fig. 1.1) (Anderson 1907, van der Horst 1939). Body length usually ranges only between 1 to 5 mm of the individual zooids and all zooids within a colony are produced by asexual reproduction (budding) from a single larva. Most species live in deep waters, although several species have been described from the shallow tropical waters as well (Lester 1985; 1988). The nervous system of pterobranchs is a simple intraepidermal nerve net spanning the entire body with a more prominent condensation between the branches of the tentacles within the dorsal mesosome (Dilly et al. 1970, Rehkämper et al. 1987, Stach, Gruhl & Kaul-Strehlow submitted, Chapter 5).

The majority of pterobranchs belongs to one of the two genera, i.e. *Cephalodiscus* M'Intosh, 1882 or *Rhabdopleura* Allman, 1868. A presumed third genus is monotypic with *Atubaria heterolopha* Sato, 1936 as a single species from deeper Japanese waters and the validity of this genus is debated (Mierzejewski 2004). Almost all species of *Cephalodiscus* are individual zooids that live in finger-like branched coenecia (Fig. 1.1C), although in some *Cephalodiscus* species the zooids stay interconnected by the stalk (Lester 1985) (Fig. 1.1B). *Cephalodiscus* spp. exhibits five to nine pairs of tentacles on the mesosoma and furthermore one pair of gill slits, two gonads, and gonopores on the globular trunk region, or metasome (Fig. 1.1A) (Hyman 1959). At the posterior end of the trunk region, a muscular stalk is developed and used when the zooid withdraws swiftly into its tube. *Rhabdopleura* spp. only bear one pair of tentacles on the mesosome, one gonad and no gill pores at all on the metasome (Schepotieff 1907, van der Horst 1939). Individuals of one colony live in tubular coenecia and are, in contrast to most *Cephalodiscus* spp., interconnected permanently by the stalk at their posterior end of the trunk (Hyman 1959, Lankester 1884).

Enteropneusta comprise the second group of Hemichordata and consists of about 70 described species (Cameron 2005) ranging from 2 to 250 cm in size. All enteropneusts are marine, solitary species, distributed around coastal areas from temperate to tropical waters worldwide (Hyman 1959, Nielsen 2001), with few species living at great depths (Holland et al. 2005, Woodwick & Sensenbaugh 1985). They are usually living in benthic habitats, buried in sand or mud, or live associated with the underside of rocks (Cameron 2005, Spengel 1893, Hyman 1959).

The wormlike body of enteropneusts is divided into three distinct regions, corresponding to the tripartite subdivision of the coelom (Morgan 1984, Spengel 1893). The anterior portion, known as the proboscis or prosoma, varies in shape from short and conical (Fig. 1.2A) to long and slender (Fig. 1.2B) (van der Horst 1939). It is attached to the collar (mesosome) by a stout stalk. The proboscis is very muscular, and it is used for burrowing and foraging (Benito & Pardos 1997, van der Horst 1939). The short, narrow and cylindrical collar is

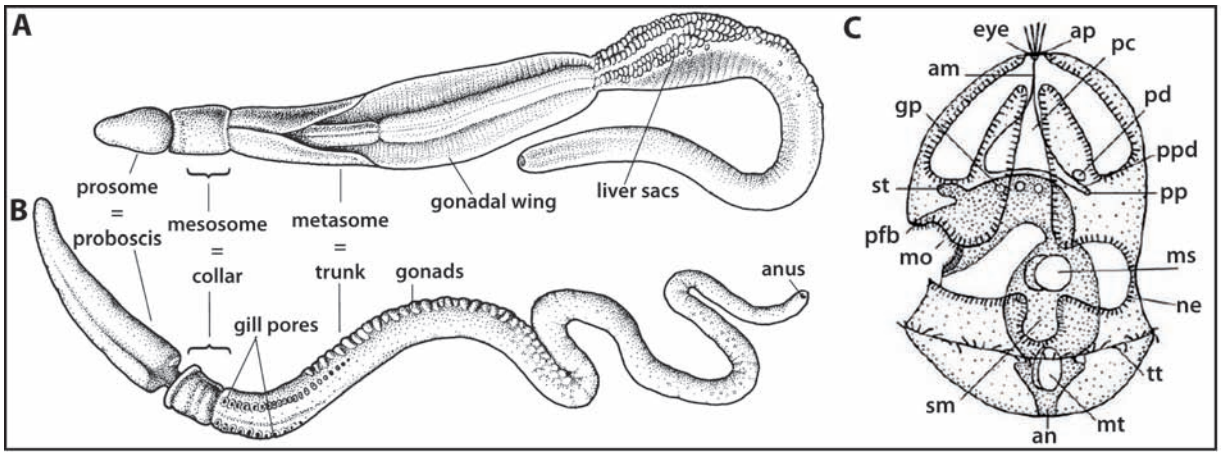

Fig. 1.2: Enteropneusts. A Anatomy of *Balanoglossus clavigerus* Delle Chiaja ,1829, a ptychoderid enteropneust. The proboscis is comparably short, gonadal wings and liver sacs are present within the trunk region. **B** Anatomy of *Saccoglossus mereschkowskii* (Nic. Wagner, 1885), an enteropneust of the family Harrimaniidae. The proboscis is long and slender (A, B from Westheide & Rieger 2007). **C** Scheme of a tornaria larva present in the families Ptychoderidae and Spengelidae (from Cameron 2005). *am* apical muscle, *an* anus, *ap* apical plate, *gp* gill pore, *mo* mouth, *ms* mesocoel, *mt* metacoel, *ne* neotroch, *pc* protocoel, *pd* pericardium, *pfb* perioral feeding band, *pp* protocoel pore, *ppd* protocoel pore duct, *sm* stomach, *st* stomochord, *tt* telotroch.

situated posterior to the proboscis, surrounding and overlapping the proboscis stalk and the posterior part of the proboscis (Fig. 1.2A, B). The mouth opening is situated ventrally between the constriction separating proboscis and collar region (Bateson 1885, Spengel 1893). The posterior portion, the trunk (metasoma), is the largest part of the body. It is subdivided into an anterior branchio-genital region, a middle hepatic region and a posterior abdominal (gut) region (Hyman 1959, Spengel 1893). On either side of the branchio-genital region there is a row of gill slits. In the specialised hepatic region of many large species there are numerous liver sacs, i.e. hollow projections of the gut and body wall (Fig. 1.2A). The long, cylindrical abdominal region extends back to the anus at the posterior end of the trunk.

The nervous system of enteropneusts is developed as an intraepidermal nerve net as present in pterobranchs (Bullock 1965, Silén 1950). Local condensations of the nervous tissue are present in form of a dorsal and a ventral longitudinal nerve cord running within the midlines in the trunk region (Bullock 1946; 1965, Knight-Jones 1952). The dorsal nerve cord further extends through the collar region to form a concentrated area of nervous tissue at the base of the proboscis, the proboscis stem. Within the collar region the dorsal cord is invaginated to form a subepidermal, hollow nerve cord, reminiscent of the neural tube present in chordates (Kaul & Stach 2010, chapter 3, Morgan 1894, van der Horst 1939).

The majority of the described enteropneust species belongs to one of the three main families: Harrimaniidae Spengel, 1901, Spengelidae Willey, 1898 and Ptychoderidae Spengel, 1893. Harrimaniid enteropneusts possess the simplest anatomy of all Enteropneusta as they lack liver sacs and genital wings within the dorsal trunk region (Fig. 1.2B). Moreover, the gill slits in harrimaniids are not supported by stabilizing synapticles as present in other enteropneust families (Cameron 2005, van der Horst 1939). Harrimaniid enteropneusts are so-called direct developer, because they do not develop through a pelagic, planctotrophic tornaria larva (Fig. 1.2C) (Cameron 2002). For the reason of a comparably simple body organization,

Harrimaniidae has been regarded as primitive within Enteropneusta (Burdon-Jones 1956). In contrast, the family Ptychoderidae is known by the presence of gill slit synapticles and a pronounced trunk region possessing liver sacs and genital wings (Fig. 1.2A). Members of the Spengelidae again lack genital wings whereas liver sacs are only present in the genus *Schizocardium* Spengel, 1893 (Cameron 2005). Both families, Ptychoderidae as well as Spengelidae develop indirectly through the aforementioned tornaria larva (Fig. 1.2C).

1.4 Echinodermata

Currently, about 6500 extant species are known, whereas the fossil record of Echinodermata is overwhelming by containing of about more than 13000 described morphospecies (Goldschmid 2007, Nielsen 2001). All echinoderms are marine, and almost all are benthic in the adult stage, whereas a planktotrophic larval stage is known in almost all groups (Hyman 1955, Nielsen 2001). The tripartite coelomic cavities characteristic for deuterostomes is developed bilaterally in the larva with three pairs of coelomic cavities, axocoel, hydrocoel and somatocoel (Gemmill 1912, MacBride 1896, von Ubisch 1913).

The Echinodermata are one of the most well-defined animal taxa as there are three apomorphies that are uniquely found in echinoderms (Ax 2001, Chia & Harrison 1994, Hyman 1955, Nielsen 2001). First to name is a specialized coelomic compartment, the water vascular system that distinguishes them from all other taxa (Delage & Hérouard 1903). It is composed of the ring canal as well as five radial canals, indicative of pentameric symmetry. The radial canals develop numerous podia along the ambulacra that function for filter-feeding or locomotion within the subgroups of Echinodermata (Hyman 1955, Goldschmid 2007).

The pentamery, another apomorphy of this taxon, is a secondary character of the adult organism since the larval stage displays a bilateral symmetry (Ax 2001, Nielsen 2001, Schaeffer 1987). In the adults, most structures, such as gonads, gut diverticulae or arms are developed as a multiple of five (Hyman 1955).

The third character supporting Echinodermata as a monophyletic group is a calcareous endoskeleton that is formed mesodermally and has a lattice-like structure, called stereom. The nervous system of echinoderms lacks a distinct brain, nerve cords around the mouth and along the ambulacra are present, but no central, coordinating nervous centre (Cobb 1995).

The extant Echinodermata consists of five higher taxa, Crinoidea (sea lilies and feather stars), Asteroidea (star fish), Ophiuroidea (brittle stars), Echinoidea (sea urchins), and Holothuroidea (sea cucumbers).

1.5 Phylogenetic relationships of the Deuterostomia

The preceding paragraphs gave overviews over the morphology of higher deuterostome taxa, Chordata, Hemichordata and Echinodermata. With only three clearly distinguished taxa, deuterostome phylogeny and particularly chordate evolution from invertebrate animals should in principle be a solvable scientific problem for phylogenetic systematists. However, despite the fact that each of these groups is well supported by different autapomorphic fea-

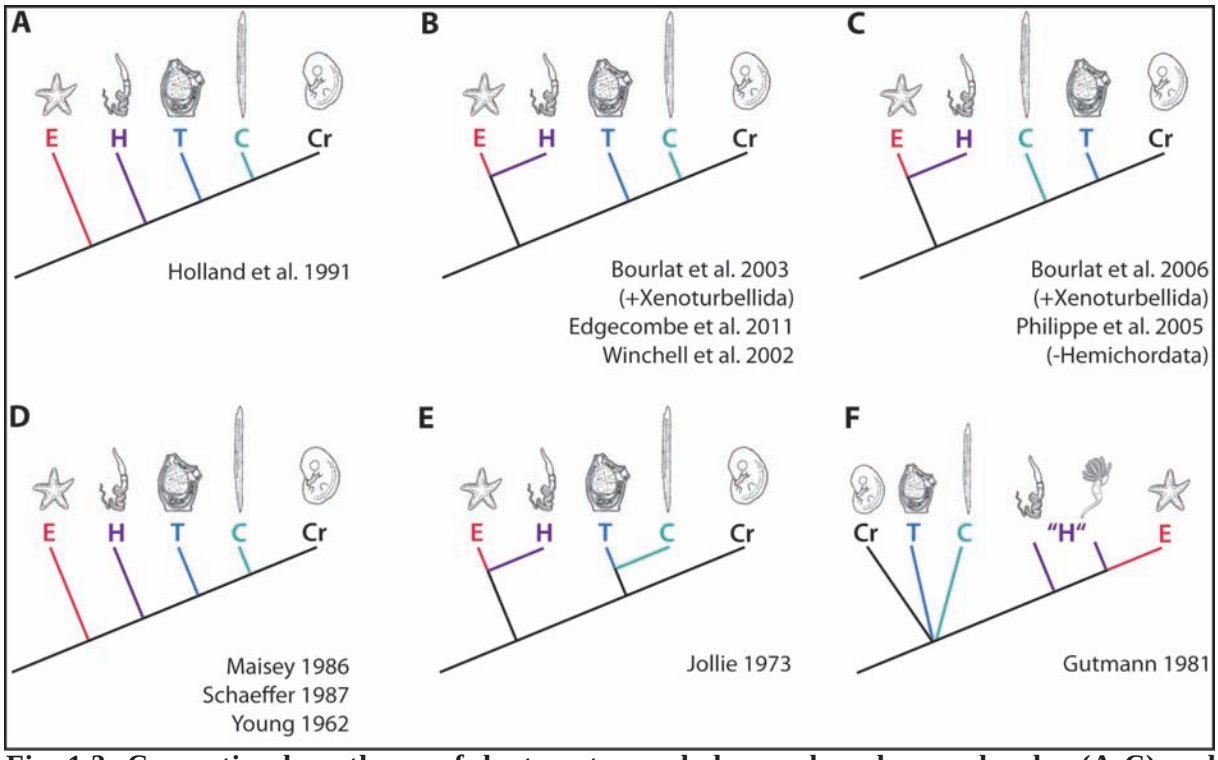

Fig. 1.3: Competing hypotheses of deuterostome phylogeny based on molecular (A-C) and morphological (D-F) data. B, C Xenoturbellida is not shown, but forms the sister group of Ambulacraria (Echinodermata and Hemichordata) according to Bourlat et al. (2003, 2006). Hemichordata were not included in the analysis of Philippe et al. 2005. **F** Hemichordata form a paraphyletic group in Gutmann 1981. E = Echinodermata, C = Cephalochordata, H = Hemichordata, T = Tunicata, V = Vertebrata.

tures, the most puzzling issue is to reconstruct the origin of chordate features, because the phylogenetic position of non-chordate deuterostomes in particular is less clear. At first side, this is not too surprising, as one is confronted with highly diverse body plans and life habits within each group of Deuterostomia, e.g. the pentamerous echinoderms, motile, solitary and wormlike enteropneusts, sessile and colonial pterobranchs, or fish-like chordates with segmented myotomes, to name but a few (Brusca & Brusca 1990, Chia & Harrison 1994, Hyman 1955; 1959, Ruppert 1997a; b).

Indeed, the earliest molecular phylogenetic studies revealed a monophyletic Deuterostomia (Lake 1992, Turbeville 1992), and the taxon has been recognized early by morphologists as well (e.g. Garstang 1928, Grobben 1908, Hyman 1955, Schaeffer 1987). However, scenarios evaluating deuterostome evolution changed during the last years as forthcoming new interrelationships of deuterostome taxa were generated by molecular systematists (Fig. 1.3A-C) (e.g. Bourlat et al. 2003: 2006, Delsuc et al. 2006, Edgecombe et al. 2011, Holland et al. 1991, Philippe et al. 2005). Nevertheless, even by using larger datasets of multigene analyses or large genomic data sets (ESTs), the emerging picture of deuterostome evolution is not as clear as some authors claim (Bromham & Degnan 1999, Swalla et al. 2008, Halanych 2004). On the other hand, by looking at available analyses based on morphological data, it becomes evident that morphologists face similar problems in evaluating deuterostome evolution (Fig. 1.3D-F) (e.g. Ax 2001, Gutmann 1981, Jefferies 1986, Jollie 1973, Maisey 1986, Ruppert 2005, Schaeffer 1987). However, the discrepancies between different

hypotheses based on morphology have certain causes. On the one hand, in large-scale studies attempting to resolve deuterostome or even metazoan phylogeny often uncritically recycle characters from traditional textbooks leading to incorrect primary homology hypotheses as already profoundly criticized by Jenner (2004). In other studies, morphological characters are mapped on a preferred hypothesis derived from molecular data (e.g. Rychel et al. 2006, Winchell et al. 2002, Zeng & Swalla 2005), though polarity of morphological characters can not be determined with certainty. On the other hand, modern and detailed morphological studies are often lacking especially from non-chordate deuterostome groups (e.g. Enteropneusta or Pterobranchia) and therefore, comparison of specific structures or developmental processes among deuterostome taxa is limited, again causing incongruent and ambiguous hypotheses. Concerning the origin of chordate features, such as the notochord, neural tube or pharyngeal gill slits, it is necessary to investigate if similar structures are present within non-chordate deuterostomes.

The previous introduction on hemichordates shows that some similarities between the aforementioned chordate features with certain structures in hemichordates are indeed present, e.g. the stomochord, invaginated collar cord in enteropneusts, or pharyngeal gill slits. Moreover, hemichordates and in particular enteropneusts exhibit a comparably simple bilaterally symmetric body plan and may therefore be a promising group allowing insights into early chordate evolution (Brown et al. 2008, Gerhart et al 2005, Lacalli 2010). Other non-chordate deuterostomes as echinoderms in contrast, display widely divergent body plans including pentaradial symmetry. Indeed, the above mentioned similarities between hemichordates and chordates have not gone unnoticed previously, as already Bateson (1885) and Barrington (1965) suggested a closer relationship between Hemichordata and Chordata. However, others propose a closer relationship of Hemichordata and Echinodermata based on larval characters (Cameron 2005, Metschnikoff 1881, Ruppert 2005) or similarities in 18S rRNA sequences (Bourlat et al. 2006, Cameron et al. 2000, Cannon et al. 2009, Halanych 1995; 2004, Winchell et al. 2002). Accordingly, the invaginated collar cord of enteropneusts and the stomochord have been interpreted as examples of homoplasy rather than being homologues to the neural tube and notochord of chordates (Cameron & Mackie 1996, Ruppert 2005). Although the similarities between hemichordates and chordates have long been acknowledged, this group is still understudied with recent progress from developmental biological studies (Lowe et al 2003, Lowe et al. 2006). Unfortunately, the majority of morphological studies were restricted to light microscopical techniques (e.g. Anderson 1907, Bateson 1884, Bourne 1889, Colwin & Colwin 1953, Davis 1908, Morgan 1891; 1894, Schepotieff 1907, Spengel 1893, Stiasny 1914, see van der Horst 1939 for a review). On the other hand, although ultrastructural studies are available as well (see Benito & Pardos 1997 for a summary), particularly ultrastructural studies on the nervous system are limited to a few (e.g. Dautov & Nezlin 1992, Dilly et al. 1970, Kaul & Stach 2010, Rehkämper et al. 1987, Stach, Gruhl & Kaul-Strehlow submitted), and the development of mesoderm has not been documented using electron microscopy, either in enteropneusts or in pterobranchs.

In summary, with current limitations in all datasets and obvious conflicts concerning phylogenetic hypotheses in the limited number of higher deuterostome taxa, it will be necessary to supplement morphological datasets, to achieve progress in the study of deuterostome phylogeny and evolution. In particular, this study will focus on detailed descriptions of the development of the nervous system and mesoderm in hemichordates, as these structures are most likely to be homologous among the drastically differing body plans of deuterostomes.

1.6 Aims of the present study

As stated in the previous paragraph, hemichordates share some similarities with chordates and may allow insights into early chordate evolution. For this purpose, the present study elucidates the development of the mesoderm and nervous system in enteropneusts and pterobranchs using TEM, SEM, histology, computer aided 3D-reconstruction, and immunohistochemical analyses using confocal laser scanning microscopy in order to approach this aim. For the investigations on enteropneusts, *Saccoglossus kowalevskii* (Agassiz, 1873), a direct developer was chosen. *S. kowalevskii* belongs to the Harrimaniidae and allows a steady following of the development of organ systems as there is no tornaria larval stage developed. This study provides a detailed description of the development of the collar cord, mesoderm with coelomic cavities and pharyngeal gill slits and reveals further arguments supporting homology with characteristic features of Chordata, e.g. neurulation, mesoderm formation or pharyngeal gill slits. Moreover, the organization of the nervous system in *Cephalodiscus gracilis* M'Intosh, 1882, a pterobranch is investigated by ultrastructural and immunohistochemical methods and discussed phylogenetically. The obtained data are compared among deuterostomes as a contribution to elucidate deuterostome evolution.

2. The post-anal tail of *Saccoglossus*

2.1 Contribution to this paper

Project conception: S K 30%; performance of practical work: S K 80%;
writing of manuscript: S K 40%.

2.2 Publication

Stach T, Kaul S (2011) The postanal tail of the enteropneust *Saccoglossus kowalevskii* is a ciliarly creeping organ without distinct similarities to the chordate tail. Acta Zoologica 92: 150-160.

http://dx.doi.org/10.1111/j.1463-6395.2010.00462.x

3. Neurulation in *Saccoglossus*

3.1 Contribution to this paper

Project conception: S K 70%; performance of practical work: S K 80%;
writing of manuscript: S K 60%.

3.2 Publication

Kaul S, Stach T (2010) Ontogeny of the collar cord: Neurulation in the hemichordate *Saccoglossus kowalevskii*. Journal of Morphology 271: 1240-1259.

http://dx.doi.org/10.1002/jmor.10868

4. Schizocoely in the deuterostome *Saccoglossus kowalevskii*

4.1 Contribution to this paper

Project conception: S K-S 80%; performance of practical work: S K-S 90%;
writing of manuscript: S K-S 60%.

4.2 Publication

Kaul-Strehlow S, Stach T (2011) The pericardium in the deuterostome *Saccoglossus kowalevskii* (Enteropneusta) develops from the ectoderm via schizocoely. Zoomorphology 130: 107-120.
http://dx.doi.org/10.1007/s00435-011-0125-0

5. The nervous system of *Cephalodiscus gracilis*

5.1 Contribution to this paper

Project conception: A G 20%, S K-S 20%, T S 60%; performance of practical work: A G 30%, S K-S 20%, T S 50%; writing of manuscript: A G 20%, S K-S 20%, T S 60%.

5.2 Manuscript

Stach T, Gruhl A, Kaul-Strehlow S. The central and peripheral nervous system of *Cephalodiscus gracilis* (Pterobranchia: Deuterostomia). Zoomorphology (submitted)

Zoomorphology

The central and peripheral nervous system of Cephalodiscus gracilis (Pterobranchia, Deuterostomia)

--Manuscript Draft--

Manuscript Number:	
Full Title:	The central and peripheral nervous system of Cephalodiscus gracilis (Pterobranchia, Deuterostomia)
Article Type:	Original Paper
Keywords:	nervous system evolution; neurophylogeny; hemichordate; cns
Corresponding Author:	Thomas Günther Stach, PhD Freie Universität Berlin Berlin, GERMANY
Corresponding Author Secondary Information:	
Corresponding Author's Institution:	Freie Universität Berlin
Corresponding Author's Secondary Institution:	
First Author:	Thomas Günther Stach, PhD
First Author Secondary Information:	
All Authors:	Thomas Günther Stach, PhD
	Alexander Gruhl, PhD
	Sabrina Kaul-Strehlow, Dipl. biol.
All Authors Secondary Information:	
Abstract:	Nervous systems are important in assessing interphyletic phylogenies because they are conservative and complex. Regarding nervous system evolution within deuterostomes two contrasting hypotheses are currently discussed. One that argues in favor of a concentrated, structured, central nervous system in the last common ancestor of deuterostomes (LCAD); the other reconstructing a decentralized nerve net as the nervous system of the LCAD. Here we present a morphological analysis of the nervous system of the pterobranch deuterostome Cephalodiscus gracilis Harmer, 1905 based on transmission electron microscopy, confocal laser scanning microscopy, immunohistochemistry, and computer-assisted 3D-reconstructions based on complete serial histological sections. The entire nervous system constitutes a basiepidermal plexus. The prominent dorsal brain at the base of the mesosomal tentacles contains an anterior concentration of serotonergic neurons and a posterior net of neurites. Predominant neurite directions differ between brain regions and synapses are present, indicating that the brain constitutes a centralized portion of the nervous system. Main structures of the peripheral nervous system are the paired branchial nerves, tentacle nerves, and the ventral stalk nerve. Serotonergic neurites are scattered throughout the epidermis and are present as concentrations along the anterior border of the branchial nerves. Serotonergic neurons line each tentacle and project into the brain. We argue that the presence of a centralized brain in C. gracilis supports the hypothesis that a nerve center was present in the LCAD. Moreover, based on positional and structural similarity we suggest that the branchial nerves in C. gracilis could be homologous to branchial nerves in craniates, a hypothesis that should be further investigated.

The central and peripheral nervous system of *Cephalodiscus gracilis* (Pterobranchia, Deuterostomia)

Thomas Stach[1], Alexander Gruhl[2*], Sabrina Kaul-Strehlow[1*]

[1]Freie Universität Berlin, Fachbereich Biologie, Chemie, Pharmazie, Institut für Biologie, Systematik und Evolution der Tiere, Königin-Luise-Straße 1-3, 14195 Berlin, Germany

[2]Natural History Museum, Department of Zoology, Cromwell Road, London SW16 1QJ, UK

[*]These authors contributed equally to this work

[1]Corresponding author

Email addresses:

TS: tstach@zoosyst-berlin.de

AG: a.gruhl@nhm.ac.uk

SK: skaul@zoosyst-berlin.de

Abstract

Nervous systems are important in assessing interphyletic phylogenies because they are conservative and complex. Regarding nervous system evolution within deuterostomes two contrasting hypotheses are currently discussed. One that argues in favor of a concentrated, structured, central nervous system in the last common ancestor of deuterostomes (LCAD); the other reconstructing a decentralized nerve net as the nervous system of the LCAD. Here we present a morphological analysis of the nervous system of the pterobranch deuterostome *Cephalodiscus gracilis* Harmer, 1905 based on transmission electron microscopy, confocal laser scanning microscopy, immunohistochemistry, and computer-assisted 3D-reconstructions based on complete serial histological sections. The entire nervous system constitutes a basiepidermal plexus. The prominent dorsal brain at the base of the mesosomal tentacles contains an anterior concentration of serotonergic neurons and a posterior net of neurites. Predominant neurite directions differ between brain regions and synapses are present, indicating that the brain constitutes a centralized portion of the nervous system. Main structures of the peripheral nervous system are the paired branchial nerves, tentacle nerves, and the ventral stalk nerve. Serotonergic neurites are scattered throughout the epidermis and are present as concentrations along the anterior border of the branchial nerves. Serotonergic neurons line each tentacle and project into the brain. We argue that the presence of a centralized brain in *C. gracilis* supports the hypothesis that a nerve center was present in the LCAD. Moreover, based on positional and structural similarity we suggest that the branchial nerves in *C. gracilis* could be homologous to branchial nerves in craniates, a hypothesis that should be further investigated.

Introduction

Nervous systems have traditionally been given special value in evolutionary considerations and two main reasons can be advanced for this. Firstly, nervous systems are considered conservative and secondly, nervous systems can be sufficiently complex to result in numerous phylogenetically informative characters (Hay-Schmidt 2000; Holland 2003; Nieuwenhuys 2002). Additionally, nervous systems are interesting because they are constitutive elements of eumetazoans and intrinsically correlated with all animal behaviors (Pflüger and Stevenson 2005). Technical advances have but increased the scientific interest in the evolution of animal nervous systems, especially with the widespread use of confocal laser scanning microscopy (Harzsch 2007; Harzsch et al. 2009; Loesel and Heuer 2010; Wanninger et al. 2007) and molecular studies of developmental processes (Arendt and Nübler-Jung 1999; Holland 2009; Holland et al. 2008; Lowe et al. 2006; Lowe et al. 2003).

Within the wider field of nervous system evolution, the evolutionary origin of the peculiarly tubular central nervous system of chordates has been especially puzzling for researchers (Kaul and Stach 2010; Lacalli 2008; Nielsen 1999; Nieuwenhuys 2002). Two more general, yet incompatible hypotheses are currently debated: one holds that the central nervous system of chordates is derived from a complex centralized nervous system already present in the last common ancestor of the bilaterians (Arendt et al. 2008; Nomaksteinsky et al. 2009; Tomer et al. 2010) whereas the other proposes a net-like nervous system in the last common ancestor of the deuterostomes (Holland 2003; Lowe et al. 2006; Lowe et al. 2003). Both hypotheses invoke developmental gene expression data to support their respective

argumentations. While it is well established that the so-called lesser animal taxa are crucial in evolutionary considerations (Jenner 2004; Kristensen 2002), most of the modern discussions rely on very few selected model organisms resulting in a picture that is at the same time precise on a technical level and crude on the phylogenetic level. In addition, the hypothesis that a complex centralized nervous system was present in the last common ancestor of the bilaterians confounds levels of primary homology statements (Bolker and Raff 1996; de Pinna 1991; Dickinson 1995; Nielsen and Martinez 2003; Richter 2005), when it equates "molecular finger-prints" during early ontogeny with complex adult structures (Arendt et al. 2008; Tomer et al. 2010). This is unfortunate in the light of accumulating evidence that ontogenetic gene expression patterns can vary in homologous morphological structures (Kugler et al. 2011; Lemaire 2006, 2009; Swalla 2006). Therefore we argue that morphological characters should be evaluated, if the primary homology of a morphological unit like "brain" or "central nervous system" is under consideration.

Pterobranchia, especially of the genus *Cephalodiscus*, have always played a central role in scientific scenarios of deuterostome evolution (Ax 2001; Nielsen 2001). They combine an almost sessile life form as a tentacle-based filter feeder reminiscent of the stalked crinoids with some characters found in enteropneusts such as the stomochord or paired mesocoelic pores. Moreover the dorsally situated brain and the pair of gill slits are also similar to so-called key chordate features (Satoh 2008; Swalla and Smith 2008). Schepotieff, Dilly and also Rehkämper et al. already described the brain in the mesosome of pterobranchs as similar to brains in enteropneusts and chordates in their dorsal position (Dilly 1975; Rehkämper et al. 1987; Schepotieff 1907). However, these authors at the same time emphasized the primitiveness of pterobranch brains in respect to their basiepithelial position. In order to advance our current understanding

of the evolution of deuterostome nervous systems and eventually distinguish between the two aforementioned competing evolutionary hypotheses, we investigated the nervous system of the pterobranch *Cephalodiscus gracilis* Harmer, 1905 using transmission electron microscopy, computer-assisted 3D-reconstructions of complete series of histological sections, and confocal laser scanning microscopy in conjunction with immunohistochemistry.

Materials and Methods

Specimen collection

Coralline pebbles and cobbles with adult specimens of *Cephalodiscus gracilis* Harmer, 1905 attached to their undersides were collected from 1 – 2 m depth around the southern end of the bridge of the Castle Harbor Causeway (Bermuda Islands, geotagged geo:lat=32.358589 geo:lon=-64.706334; http://www.gorissen.info/Pierre/maps/googleMapLocationv3.php) in October 2008. The pebbles covered with seawater were brought to the laboratory and kept in sea tables with running ambient seawater. Individual colonies attached via their stolons were dissected out of their tubes and relaxed in 7% $MgCl_2$ for 5-10 minutes prior to processing for transmission electron microscopy (TEM), scanning electron microscopy (SEM), histology, and immunohistochemistry.

Immunohistochemistry and confocal laser scanning microscopy

Specimens were fixed in 4% paraformaldehyde for 30 minutes at 4°C, subsequently rinsed three times in 0.1M phosphate buffer with added 0.33M NaCl (PBS) and stored in storage buffer (PBS + 0.01% NaN_3). In order to permeabilize cell membranes and to quench unspecific antibody binding sites specimens were treated with blocking buffer (PBS + 1% bovine serum albumine + 0.1% Triton-X 100) for 2h at room temperature prior to antibody staining. Incubation with primary antibodies (anti-5HT, Sigma S5545, anti acetylated α-tubulin Sigma T-6199) took place at final dilutions between 1:250 - 1:500 in blocking buffer for 6-12h at room temperature. Unbound primary antibodies were removed by several rinses with PBS + 0.1% Triton-X 100 over 8h. Fluorescent-coupled secondary antibodies (Molecular Probes A11004,

A21050) were applied at a dilution of 1:200 in blocking buffer for 6h and washed out with PBS. Counterstaining for nuclei was done with propidium iodide for 20 min at a dilution of 1:250 after treatment with ribonuclease A (2h, room temperature). Specimens were either directly mounted on slides in 90% glycerol, 10% PBS, 0.25% DABCO or cleared and mounted in Murray Clear. Confocal image stacks of 16 individuals were acquired using Leica TCS SP and TCS SPE confocal laser scanning microscopes. Negative controls in which either the primary or secondary antibodies were omitted resulted in no relevant signal. Image data were processed and analyzed using the freely available software packages MBF ImageJ (McMaster Biophotonics Facility, Ontario, Canada), Voxx2 (Indiana Center for Biological Microscopy, Indianapolis, USA) and v3d (H. Peng, Howard Hughes Medical Institute, Ashburn, VA, USA).

Transmission electron microscopy, light microscopy, and 3D-reconstruction

For TEM most of the relaxation agent was removed and replace with ice-cold primary fixative containing 2.5% glutaraldehyde in 0.2M sodium cacodylate buffer (pH 7.2), adjusted to an osmolarity of approximately 800mosm by addition of NaCl. Primary fixation was stopped after 45 minutes with three buffer rinses for 10, 15, and 20 minutes. Primary fixation was followed by 30 minutes of postfixation with 2% OsO_4 in sodium cacodylate buffer. Postfixation was stopped with three buffer rinses (15, 30, 30 minutes) followed by two rinses with ddH_2O (15, 30 minutes). After dehydration through a graded series of ethanol specimens were embedded in Araldite for TEM and light microscopy. For SEM specimens were critical point dried in a CPD 030 (Balzers Union, Liechtenstein). Dried specimens were sputter coated with gold in a SCD 040

(Balzers Union, Liechtenstein) and viewed with a Fei Quantum 200 scanning electron microscope at 15 kV (FEI Co. Netherlands)

Complete longitudinal and transverse serial sections of three adult individuals were prepared. One specimen was completely serially sectioned sagittally using a diamond knife on a Reichert Ultracut S (Reichert Labtec, Germany) and combining semi-thin sections (0.5µm) with ultrathin sections (60-70nm). Eight semi-thin sections were followed by 30 ultrathin sections. Semi-thin sections were stained with toluidine blue for light microscopy. Ultrathin sections were stained with 2% uranylacetate and 2.5% lead citrate in an automatic stainer (Nanofilm Technologie GmbH, Göttingen) for TEM. Two additional specimens were fixed with Bouin's fixative for 1 hour, embedded in paraffin, sectioned at 6µm thickness and stained with Azan for conventional histological light microscopical analysis in order to assess relevant individual morphological variability.

Light microscopic images were recorded with a digital camera (Olympus BX-UCB) mounted on an OlympusBX51 (Olympus, United Kingdom) compound microscope. TEM pictures were documented with a Philips CM120 BioTWIN (FEI, Netherlands) electron microscope at 60 kV on Ditabis Digital Imaging. Plates were read by a Ditabis Micron IP-Scanner (Ditabis, Germany). Images were aligned using Imod align Software on a Linux computer. Based on the resulting stack of images 3D-models of the anatomy of all organ systems was created in Amira 3.0 software (Mercury Computer Systems, Berlin).

Statistic analysis

In order to get a rough estimate of predominant neurite fiber directions in different brain regions of *Cephalodiscus gracilis* we divided a large composite printout of

transmission electron micrographs of a mid-sagittal section of the brain in three regions (anterior third, middle third, posterior third) of equal distance along the anterior-posterior axis. Three cross sections of neurites were selected randomly for each third and the 20 cross sections closest to the respective randomly selected neurite section measured. We measured the angle between the longitudinal axis of the respective neurite to the longitudinal horizontal line approximating the base of the brain. The angles were counted in 6 categories as indicated in Figure 6. The median of the three respective counts is given for the respective category and brain region in Figure 6.

Results

General 3D anatomy of the nervous system

Cephalodiscus gracilis is a trimeric animal with an anterior mouth shield (protosome), a small collar region that dorsally bears ten conspicuous pinnate tentacles (mesosome), and a large trunk that posteriorly tapers into a muscular stalk (metasome; Fig. 1). The externally visible trimeric body partition is mirrored in the internal organization, where three prominent coelomic cavities are found: proto-, meso-, and metacoel (Fig. 1b, c). The nervous system of *C. gracilis* is a plexus (sensu Richter et al. 2010) present throughout the entire epidermis. The thickness of the plexus varies from single neurite fibers to local condensations up to about 15 – 20 µm in thickness. 3D-reconstructions of the more substantial parts of the nervous systems, i.e. those elements above 5 µm in thickness, based on light micrographs of complete serial sections reveal several distinct condensations (Fig. 1d). The most prominent condensation is the anterior dorsal brain. It is situated mid-dorsally at the base of the tentacles in the region of the collar. It spreads out anteriorly at the dorsal epidermis of the mouth shield becoming gradually thinner. Smaller fibers, most below the 5 µm threshold leave the brain dorsolaterally and enter each of the tentacles. Two more prominent nerves leave the brain posteriorly. They project bilaterally symmetrically backwards dorsal to the conspicuous mesocoel pores and the less conspicuous branchial pores. These branchial nerves also become thinner as they run along the sides of the trunk towards the ventral side until they merge with the general basiepidermal plexus. Slightly posterior two nerves emerge from the general nerve net on the ventrolateral sides. These two nerves unite as they run into the posterior stalk. Here, they run along the ventral side of the stalk. A bilaterally symmetrical pair of

plexus is situated in the epidermis of the lateral lips that project underneath the tentacles along the dorsal margin of the mouth opening.

Distribution of serotonergic immunoreactivity

Immunohistological staining with antibodies against acetylated α-tubulin confirms the general arrangement of the elements of the nervous system presented above, although in addition to the neurite bundles this method also stains cilia (Fig. 2). Thus, the most prominent features stained with these antibodies are the branchial nerves, the mesocoel pores, and the intestinal tracts (Fig. 2a-c, f). In addition the cilia of the epidermis, including the tentacles are stained and in the nervous system the posterior part of the dorsal brain is clearly labeled (Fig. 2). Closer inspection reveals that the neurite-like immunostaining in the posterior part of the brain reveals a net like arrangement of fibers with many fibers traversing the plane of bilateral symmetry (Fig. 2d). From the latero-ventral sides of this posterior nerve net in the dorsal brain the two prominent branchial nerves emerge and project ventrally and posteriorly (Fig. 2a-c, f). Antibody staining against serotonin, a commonly found neurotransmitter in the animal kingdom, shows that serotonergic cells are scattered throughout the epidermis. However, a conspicuous concentration of serotonergic cells is found anterior to the fiber net just described: a concentration of serotonergic cells is present in the anterior portion of the dorsal brain (Fig. 2). These serotonergic cells also possess serotonergic fibers; the longer fibers emerging from serotonergic cells in the anterior brain project posteriorly (Fig. 2b-d). Some of these serotonergic cells seem to be bipolar with a longer and a shorter fiber emerging from the perikaryon (Fig. 2c’). Serotonergic immunoreactivity is also present along the posteriorly projecting nerves (Fig. 2). Specifically, serotonergic fibers run parallel to the fibers stained by

antibodies against acetylated α-tubulin in the branchial nerves. However, the serotonergic fibers diverge slightly from the branchial nerves just dorsal to the mesocoel pore where they run immediately along the posterior margin of this opening (Fig. 2f). In addition, serotonergic cells line the tentacles. The fibers of these serotonergic cells emerge from the brain and form a continuous line along the dorsal sides of the tentacles, running their entire length to the tips of the tentacles (Fig. 2e, f). In addition, serotonergic cells are found in the vicinity of the branchial nerve fibers and the mouth shield (Fig. 2).

Histological anatomy

Prominent parts of the nervous system along with general anatomical features can be detected in semi-thin sections stained with toluidine blue (Fig. 3). Nervous tissue in these preparations is always seen as a sheet basal in the epidermis. The sheet is light in coloration and of a granular appearance (Fig. 3). In several body regions thickenings of the nerve net are obvious, such as the dorsal brain (Fig. 3a), the ventral stalk (Fig. 3b), the branchial nerve posterior to the gill slits (Fig. 3c, d), and the lateral plexus (Fig. 3e). Less prominent nervous tissue can be seen connecting to the lateral dorsal brain and entering the tentacles (Fig. 3f). Cell bodies can rarely be ascribed confidently to the nervous tissue. Only in the ventral stalk nuclei are deeply embedded and completely surrounded by nervous tissue (Fig. 3b).

Ultrastructure of the nervous system

Low power electron micrographs are indicative alas not decisive for a clearer distinction between epidermal cells and nervous tissue in the brain (Fig. 4a, b). However, this method clearly reveals the deeply Fig. 4a, b). The neuropil layer in the

mid-sagittal brain is thickest in the posterior part where it ends rather abruptly at the border between mesosome and metasome (Fig. 4a). To the anterior, the neuropil layer becomes thinner and tapers into the general nerve net in the dorsal epidermis of the mouth shield. In this anterior region of the neuropil, the neurites are predominantly oriented in an anterior to posterior direction (Figs. 4a inset, 6a). This differs markedly and significantly from the orientation of nerve fibers in the central and posterior parts of the brain. In these latter parts there seems to be no clearly preferred orientation of the nerve fibers (Fig. 6b, c), an observation that is consistent with randomly oriented fibers but also with fibers that are mostly oriented transversally. The cells in the epidermal layer apical to the neuropil resemble general epidermal cells in other body regions. They bear a single apical cilium and are interconnected by apical cell junctions with neighboring cells. Occasionally glandular cells are interspersed (Fig. 4b) and it is probable that at least some of the neurites in the basal neuropil belong to somata of cells in the apical part of the epidermal layer. Approximately 15 µm anterior to the posterior end of the brain a conspicuous group of cells is situated between the apical epidermal layer and the basal neuropile (Fig. 4a). Theses cells appear lighter in electron microscopic aspect compared to the overlaying epidermal cells and are considerably larger (Fig. 4a inset).

The nerve in the ventral stalk can also be divided into a basal neuropil that appears as a deep longitudinal fold and an apical epidermal layer (Fig. 4c). The cells in the apical layer are markedly thin. Few cell somata are rarely encountered in the neuropil of the ventral stalk nerve (Fig. 4c).

The basiepithelial plexus in the epidermis is considerably thinner in the dorsal trunk compared to the ventral side of the trunk (Fig. 5a, b). While in the former the

thickness in sagittal sections measures merely 2 – 3 µm and consists of few neurites only (Fig. 5a), in the latter the plexus measures around 10 µm in thickness and is considerably more substantial (Fig. 5b). Figure 5a suggests that at least part of the plexus might receive input from primary sensory cells in the epidermis. The transmission electron micrographs also reveal that the thickness of the sheath of mesodermal epithelial muscle cells on the opposite side of the basal lamina is feeble in the dorsal trunk and more substantial in the ventral, corresponding to the thickness of the adjacent basiepidermal nerve nets. In general, the more substantial neuropils are closely associated with specific concentrations of musculature, such as the ring muscles around the mesocoel pore (Fig. 5c), or the longitudinal musculature in the stalk (Fig. 5f, g). Some of the epidermal nerve fibers come in especially close contact with the mesodermal musculature on the other side of the basal lamina. In many cases the distance between extensions of the nerve fibers and corresponding extensions of muscle cells measures clearly less than 0.1 µm (Fig. 5e-g). Occasionally the neurites that come in such close contact with the muscle cells contain small round vesicles (Fig. 5g). These vesicles have a diameter of approximately 20 nm. They might be of electron lucent content or contain an electron dense core and an electron lighter rim.

Discussion

The present study revealed details of the organization of the nervous system in the pterobranch *Cephalodiscus gracilis*. The dorsal brain in the mesosome contains a cluster of anterior serotonergic cells and posteriorly a dense network of neurites that predominantly run in transverse direction. From the posterior part of the brain a pair of prominent branchial nerves projects posteriorly where they arch around the dorsal side of the single pair of gill slits. Additional nerves containing serotonergic neurites run from the brain into each of the tentacles and anteriorly into the mouth shield. Statistical analysis demonstrates that neurite direction differs among brain regions. Serotonergic cells are in addition scattered throughout the epidermis. They are more numerous in the mouth shield and form a clear pattern in the tentacles, with serotonergic neurites running along the length of a tentacle and more or less regularly spaced serotonergic somata. Electron microscopy, in addition demonstrated the presence of synaptic vesicles in the brain of *C. gracilis*, similar to the earlier findings of Rehkämper et al. (1987) for *C. gracilis* and of Dilly (1975) and Rehkämper et al. (1987) for *Rhabdopleura compacta*.

The anatomy of the brain of the pterobranch *Cephalodiscus gracilis* thus is indicative of its function as an integrative center. Taking into account that stalked crinoids (Akasaka et al. 2005) and enteropneusts (Kaul and Stach 2010; Nomaksteinsky et al. 2009) possess anterior nerve centers and considering recent molecular phylogenies that exclude Xenoturbellida from Deuterostomia (Edgecombe et al. 2011; Hejnol et al. 2009), the demonstrated structure of the pterobranch brain supports the hypothesis that a centralized part of the nervous system was present in the last common ancestor of Deuterostomia as was recently also suggested by Burke (2011) alongside a

substantial part of the nervous system organized as an epithelial plexus. This argument in turn strengthens the hypothesis that a nerve center was present in the last common ancestor of the Bilateria (Arendt et al. 2008; Nomaksteinsky et al. 2009; Tomer et al. 2010).

However, the situation is more complex than the two contrasted hypotheses suggest. At least part of the conundrum stems from the linguistic difficulties in defining a central nervous system and the resulting problem in suggesting an accurate hypothesis of primary homology (Vogt et al. 2010). Holland defined a central nervous system "as a place where neurons (nerve cell bodies and neurites that arise from them) are considerably more concentrated, and interrelated in a more complex way, than elsewhere in the body" (Holland 2003), whereas Richter et al. (2010) did not define central nervous system yet defined the term "brain" as "the most prominent anterior condensation of neurons" (Richter et al. 2010). This latter purely structural definition fits the demonstrated anatomy of the brain of *Cephalodiscus gracilis* and is used in the present publication while it is acknowledged that Holland's more general definition of "central nervous system" would also apply but remains less straightforward. Nieuwenhuys (2002) uses the term "central nervous system" in chordates as that part of the nervous system that is "derived from the neural plate." Kaul and Stach (2010) have shown that the collar cord of the enteropneust *Saccoglossus kowalevskii* derives via neurulation from the dorsal neural plate and homologized neurulation in chordates and enteropneusts. Following previous authors (e.g. Bateson 1885; Bullock 1944; Kaul and Stach 2010; Knight-Jones 1952) we support this latter hypothesis of homology. Moreover we support homology of the enteropneust collar cord and the pterobranch brain based on their similarity in their dorsal position in the mesosome as has been previously suggested (Benito and Pardos

1997; Dilly 1975; Dilly et al. 1970). Based on gene expression profiling Tomer et al. (2010) suggested homology of specific areas in the brains of protostome annelids and vertebrates, i.e of annelid mushroom bodies and vertebrate pallium. Mushroom bodies are paired and defined as parts of a brain and "composed of dendrites and parallelly arranged axons made up of thousands of intrinsic neurons of the globuli cell type" (Richter et al. 2010). Using immunolabelling, we could not detect globuli cells in the brain of *C. gracilis*. Even when suitable methods are used, mushroom bodies are also not reported from the collar cords of enteropneusts (Kaul and Stach 2010; Nielsen and Hay-Schmidt 2007; Nomaksteinsky et al. 2009) or tunicates (Imai and Meinertzhagen 2007; Stach 2005) or cephalochordates (Meves 1973; Stach 2000; Wicht and Lacalli 2005). While cells with expression profiles similar to the ones documented for annelid mushroom bodies and vertebrate pallium (Tomer et al. 2010) might be present in other invertebrates, the anatomical comparisons weaken the hypothesis that homologous structures to mushroom bodies per se are present across the animal kingdom.

Because structural similarities are indicative of primary homologies (Bolker and Raff 1996; de Pinna 1991; Ereshefsky 2009; Hennig 1950; Patterson 1988), comparisons of the neuroanatomy of *C. gracilis* to nervous systems of other species are warranted. An anterior concentration of serotonergic cells in the dorsal brain in conjunction with a posterior net of neurites and posteriorly projecting neurites can be found in many deuterostome species. In chordates e.g., such an arrangement is found in tunicates (De Bernardi et al. 2006; Stach 2005), in cephalochordates (Candiani et al. 2001; Holland and Holland 1993), and in lampreys (Hay-Schmidt 2000). Moreover, this arrangement is in principle similar to the pattern of serotonergic immunoreactivity found in echinoderm larvae and enteropneust larvae (De Bernardi et al. 2006; Hay-Schmidt

2000). Note that these structural similarities lead to primary homology considerations between the chordate neural tube and the larval nervous systems of tunicates and so-called “lower” deuterostomes that have recently been also proposed based on considerations of similarities in gene pattern expression (Burke 2011). In this latter publication, it had been suggested that the chordate neural tube combines the larval and the adult components of the last common deuterostome ancestor consistent with our own interpretation of structural similarities presented above. It is noteworthy in this context that the long-held notion that the larval nervous system of ascidians degenerates during metamorphosis has recently been shown to be false (Horie et al. 2011) and that larval and adult nervous system are more continuous than previously thought.

In craniates the nerves of the peripheral nervous system associated with the pharyngeal slits show a specific arrangement. These so-called branchial nerves curve around the dorsal side of the pharyngeal slits and branch into an anteriorly directed pretrematic branch and a posttrematic branch (Jonz and Zaccone 2009; Kuratani et al. 1997; Mickoleit 2004). It is well established that especially the pretrematic branches of these branchial nerves possess serotonergic fibers (Dunel-Erb et al. 1982; Jonz and Zaccone 2009). Although the peripheral nervous system in cephalochordates shows clear similarities to the arrangement of branchial nerves found in craniates (Bone 1961; Holland and Holland 1993; Kuratani 2008; Yasui and Kaji 2008) precise homology statements remain difficult. In *Cephalodiscus gracilis* the most prominent nerves leaving the dorsal brain are also called branchial nerves in the present study. These curve dorsally around the single gill opening and the mesocoelic pore and contain serotonergic cell bodies and fibers. The main part of these branchial nerves is situated posterior to the gill opening, i.e. corresponding to the posttrematic branch of

craniates in position. A distinct pretrematic branch is not obvious, yet the ubiquitous plexus is present in the respective position as well as the widespread serotonergic cells. These similarities can be taken as evidence for primary homology of the branchial nerve of *C. gracilis* and branchial nerves in craniates a hypothesis that should be investigated further.

Acknowledgements

We gratefully acknowledge the financial support of the German research foundation (DFG grants: Sta 655/2-1&2) and the financial support of the Biological Institute of Ocean Sciences (Grants-in-Aid Program).

References

Akasaka K, Omori A, Amemiya S (2005) Primitive central nervous system of stalked crinoids (*M. rotundus*). Zool Sci 22:1389

Arendt D, Denes AS, Jekely G, Tessmar-Raible K (2008) The evolution of nervous system centralization. Phil Trans R Soc B 363:1523-1528

Arendt D, Nübler-Jung K (1999) Comparison of early nerve cord development in insects and vertebrates. Development 126:2309-2325

Ax P (2001) Das System der Metazoa: ein Lehrbuch der phylogenetischen Systematik. Spektrum Akademischer Verlag GmbH, Heidelberg, Berlin

Bateson W (1885) The later stages in the development of *Balanoglossus kowalevskyi*, with a suggestion on the affinities of the Enteropneusta. Quarterly journal of Microscopic Science 25:81

Benito J, Pardos F (1997) Hemichordata. In: Harrison FW, Ruppert EE (eds) Microscopic anatomy of invertebrates, vol 15. Wiley-Liss, New York, Chichester, Weinheim, Brisbane, Singapore, Toronto, pp 15-101

Bolker JA, Raff RA (1996) Developmental genetics and traditional homolgy. Bioessays 18:489-494

Bone Q (1961) The Organization of the Atrial Nervous System of Amphioxus (*Branchiostoma lanceolatum* (Pallas)). Philosophical Transactions of the Royal Society of London Series B, Biological Sciences 243:241-269

Bullock TH (1944) The giant nerve fiber system in balanoglossids. The Journal of Comparative Neurology 80:355-367

Burke RD (2011) Deuterostome neuroanatomy and the body plan paradox. Evolution & Development 13:110-115

Candiani S, Augello A, Oliveri D, Passalacqua M, Pennati R, De Bernardi F, Pestarino M (2001) Immunocytochemical localization of serotonin in embryos, larvae and adults of the lancelet, *Branchiostoma flordiae*. The Histochemical Journal 33:413-420

De Bernardi F, Pennati R, Candiani S, Zega G, Groppelli S, Pestarino M (2006) Serotonin in the morphogenesis of ascidian nervous system. Caryologia 59:375-379

de Pinna MCC (1991) Concepts and tests of homology in the cladistic paradigm. Cladistics 7:367-394

Dickinson WJ (1995) Molecules and morphology: where's the homology? Trends Genet 11:119-121

Dilly PN (1975) The pterobranch *Rhabdopleura compacta*: its nervous system and phylogenetic position. Symposium of the zoological Society of London 36:1-16

Dilly PN, Welsch U, Storch V (1970) The Structure of the nerve fibre layer and neurocord in the enteropneusts. Zeitschrift für Zellforschung 103:129-148

Dunel-Erb S, Bailly P, Laurent S (1982) Neuroepithelial cells in fish gill primary lamellae. J Appl Physiol 53:1342-1353

Edgecombe G, Giribet G, Dunn C, Hejnol A, Kristensen R, Neves R, Rouse G, Worsaae K, Sørensen M (2011) Higher-level metazoan relationships: recent progress and remaining questions. Organisms Diversity & Evolution 11:151-172

Ereshefsky M (2009) Homology: Integrating Phylogeny and Development. Biological Theory 4:225-229

Harzsch S (2007) The architecture of the nervous system provides important characters for phylogenetic reconstructions: Examples from the Arthropoda. Species, Phylogeny and Evolution 1:33-57

Harzsch S, Müller C, Rieger V, Perez Y, Sintoni S, Sardet C, Hansson B (2009) Fine structure of the ventral nerve centre and interspecific identification of individual neurons in the enigmatic Chaetognatha. Zoomorphology 128:53-73

Hay-Schmidt A (2000) The evolution of the serotonergic nervous system. Philosophical Transactions of the Royal society of London, B 267:1071-1079

Hejnol A, Obst M, Stamatakis A, Ott M, Rouse GW, Edgecombe GD, Martinez P, Baguna J, Bailly X, Jondelius U, Wiens M, Möller WEG, Seaver E, Wheeler WC, Martindale MQ, Giribet G, Dunn CW (2009) Assessing the root of bilaterian animals with scalable phylogenomic methods. Proceedings of the Royal Society B: Biological Sciences 276:4261-4270

Hennig W (1950) Grundzüge einer Theorie der phylogenetischen Systematik. Deutscher Zentralverlag, Berlin

Holland L (2009) Chordate roots of the vertebrate nervous system: expanding the molecular toolkit. Nat Rev Neurosci 10:736-746

Holland LZ, Holland ND, Gilland E (2008) Amphioxus and the evolution of head segmentation. Integr Comp Biol 48:630-646

Holland ND (2003) Early central nervous sytem evolution: an era of skin brains? Nature 4:1-11

Holland ND, Holland LZ (1993) Serotonin-containing cells in the nervous system and other tissues during ontogeny of a lancelet, *Branchiostoma floridae*. Acta Zoologica 74:195-204

Horie T, Shinki R, Ogura Y, Kusakabe TG, Satoh N, Sasakura Y (2011) Ependymal cells of chordate larvae are stem-like cells that form the adult nervous system. Nature 469:525-528

Imai JH, Meinertzhagen IA (2007) Neurons of the ascidian larval nervous system in *Ciona intestinalis*: I. Central nervous system. The Journal of Comparative Neurology 501:316-334

Jenner RA (2004) Towards a phylogeny of the Metazoa: evaluating alternative phylogenetic positions of Platyhelminthes, Nemertea, and Gnathostomulida, with a critical reappraisal of cladistic characters. Contributions to Zoology 73:3-163

Jonz MG, Zaccone G (2009) Nervous control of the gills. Acta Histochemica 111:207-216

Kaul S, Stach T (2010) Ontogeny of the collar cord: neurulation in the hemichordate *Saccolglossus kowalevskii*. J Morphol 271:1240-1259

Knight-Jones EW (1952) On the nervous system of *Saccoglossus cambrensis* (Enteropneusta). Philosophical Transactions of the Royal Society of London B 236:315-354

Kristensen RM (2002) An introduction to Loricifera, Cyliophora, and Micrognathozoa. Integr Comp Biol 42:641-651

Kugler J, Kerner P, Bouquet J-M, Jiang D, Di Gregorio A (2011) Evolutionary changes in the notochord genetic toolkit: a comparative analysis of notochord genes in the ascidian *Ciona* and the larvacean *Oikopleura*. BMC Evol Biol 11:21

Kuratani S (2008) Is the vertebrate head segmented? ----evolutionary and developmental considerations. Integr Comp Biol 48:647-657

Kuratani S, Ueki T, Aizawa S, Hirano S (1997) Peripheral development of cranial nerves in a cyclostome, *Lampetra japonica*: morphological distribution of nerve branches and the vertebrate body plan. The Journal of Comparative Neurology 384:483-500

Lacalli TC (2008) Basic features of the ancestral chordate brain: A protochordate perspective. Brain Res Bull 75:319-323

Lemaire P (2006) How many ways to make a chordate? Science 312:1145-1146

Lemaire P (2009) Unfolding a chordate developmental program, one cell at a time: Invariant cell lineages, short-range inductions and evolutionary plasticity in ascidians. Dev Biol 332:48-60

Loesel R, Heuer CM (2010) The mushroom bodies – prominent brain centres of arthropods and annelids with enigmatic evolutionary origin. Acta Zoologica 91:29-34

Lowe CJ, Terasaki M, Wu M, Freeman Jr. RM, Runft L, Kwan K, Haigo S, Aronowicz J, Lander E, Gruber C, Smith M, Kirschner M, Gerhart J (2006) Dorsoventral patterning in hemichordates: Insights into early chordate evolution. PLoS Biol 4:e291

Lowe CJ, Wu M, Salic A, Evans L, Lander E, Stange-Thomann N, Gruber CE, Gerhart J, Kirschner M (2003) Anteroposterior patterning in hemichordates and the origin of the chordate nervous system. Cell 113:853-865

Meves A (1973) Elektronenmikroskopische Untersuchungen über die Zytoarchitektur des Gehirns von *Branchiostoma lanceolatum*. Zeitschrift für Zellforschung 139:511-532

Mickoleit G (2004) Phylogenetische Systematik der Wirbeltiere. Verlag Dr. Friedrich Pfeil, München

Nielsen C (1999) Origin of the chordate central nervous system - and the origin of the chordates. Development, Genes and Evolution 209:198-205

Nielsen C (2001) Animal Evolution. Interrelationships of the living phyla. Oxford University Press, New York, Tokyo

Nielsen C, Hay-Schmidt A (2007) Development of the enteropneust *Ptychodera flava*: ciliary bands and nervous system. J Morphol 268:551-570

Nielsen C, Martinez P (2003) Patterns of gene expression: homology or homocracy? Development, genes and Evolution 213:149-154

Nieuwenhuys R (2002) Deuterostome brains: synopsis and commentary. Brain Res Bull 57:257-270

Nomaksteinsky M, Roettinger E, Dufour HD, Chettouh Z, Lowe CJ, Martindale MQ, Brunet J-F (2009) Centralization of the Deuterostome Nervous System Predates Chordates. Curr Biol 19:1264-1269

Patterson C (1988) Homology in classical and molecular biology. Mol Biol Evol 5:603-625

Pflüger HJ, Stevenson PA (2005) Evolutionary aspects of octopaminergic systems with emphasis on arthropods. Arthropod Structure & Development 34:379-396

Rehkämper G, Welsch U, Dilly PN (1987) Fine structure of the ganglion of *Cephalodiscus gracilis* (Pterobranchia, Hemichordata). The Journal of Comparative Neurology 259:308-315

Richter S (2005) Homologies in phylogenetic analyses - concept and tests. Theory in Biosciences 124:105-120

Richter S, Loesel R, Purschke G, Schmidt-Rhaesa A, Scholtz G, Stach T, Vogt L, Wanninger A, Brenneis G, Döring C, Faller S, Fritsch M, Grobe P, Heuer CM,

Kaul S, Møller OS, Müller CHG, Rieger V, Rothe BH, Stegner MEJ, Harzsch S (2010) Invertebrate neurophylogeny: suggested terms and definitions for a neuroanatomical glossary. Frontiers in Zoology 7:29

Satoh N (2008) An aboral-dorsalization hypothesis for chordate origin. Genesis 46:614-622

Schepotieff A (1907) Die Pterobranchier. Zoologische Jahrbücher Abteilung für Anatomie 23:463-534, Tafeln 425-433

Stach T (2000) Microscopic anatomy of developmental stages of *Branchiostoma lanceolatum* (Cephalochordata, Chordata). Bonn Zool Monogr 47:1-111

Stach T (2005) Comparison of the serotonergic nervous system among Tunicata: implications for its evolution within Chordata. Organisms, Diversity and Evolution 5:15-24

Swalla BJ (2006) Building divergent body plans with similar genetic pathways. Heredity 97:235-243

Swalla BJ, Smith AB (2008) Deciphering deuterostome phylogeny: molecular, morphological and palaeontological perspectives. Philosophical Transactions of the Royal Society of London B 363:1557-1568

Tomer R, Denes AS, Tessmar-Raible K, Arendt D (2010) Profiling by image registration reveals common origin of annelid mushroom bodies and vertebrate pallium. Cell 142:800-809

Vogt L, Bartolomaeus T, Giribet G (2010) The linguistic problem of morphology: structure versus homology and the standardization of morphological data. Cladistics 26:301-325

Wanninger A, Fuchs J, Haszprunar G (2007) Anatomy of the serotonergic nervous system of an entoproct creeping-type larva and its phylogenetic implications. Invertebr Biol 126:268-278

Wicht H, Lacalli TC (2005) The nervous system of amphioxus: structure, development, and evolutionary significance. Canadian Journal of Zoology 83:122-150

Yasui K, Kaji T (2008) The lancelet and ammocoete Mouths. Zool Sci 25:1012-1019

Captions

Figure 1 - General anatomy of the nervous system of the pterobranch *Cephalodiscus gracilis*

A – Scanning electron micrograph. Note the dorsal tentacle crown, the ventral mouth shield, and the posterior stalk. B – Semi-schematic representation of the anatomy of *C. gracilis*, showing the arrangement of major components of the nervous system in yellow. C – Light micrograph of a sagittal section. D – Computer based 3D-reconstruction of the major components of the nervous system, based on complete serial sections.

apn – anterior projecting nerves, bnl – left branchial nerve, br – brain, gl – glomerulus, gs – gill slit, in – intestine, lil/r – left/right lip, lp – lateral plexus, ms – mouth shield, pc – pericard, prc – protocoel, ph – pharynx, te – tentacles, mscl/re – left/right mesocoel, mscp – pore of mesocoel, st – stalk, tn – tentacle nerve, tr – trunk, vsn – ventral stalk nerve.

Figure 2 - Confocal laser scanning micrographs of immunohistochemical staining against serotonin (green), acetylated α-tubulin (red), and DNA (blue)

A – Lateral view of an entire animal showing the position of the brain at the base of the tentacles and the posterior projecting branchial nerve. B – Higher magnification of the brain and left branchial nerve seen in A. C – Dorsal aspect of another specimen depicting the brain, single serotonergic fibers in the tentacles, and both paired branchial nerves. C’ – Inset: single serotonergic neuron with two fibres. Note also button-like swellings in the longer fibre and in the perykaryon. D – Higher magnification of the brain in dorsal aspect, revealing the anterior position of

numerous serotonergic cells with posteriorly projecting axons (arrows) and a posterior nerve net with fibres crossing the midline (double arrowheads). E – Slightly oblique posterior view of mesosome with tentacles. In this aspect it becomes evident that a serotonergic nerve runs along each tentacle on the dorsal side (arrowheads). F – Slightly oblique dorso-lateral aspect of brain, serotonergic fibres in the tentacles (single arrowheads), and branchial nerves. Note the serotonergic fibres that accompany the left branchial nerve (double arrowheads).

bnr/l – right/left branchial nerve, br – brain, in – intestine, mscpl – pore of left mesocoel, ms – mouth shield, nn – nerve net, te – tentacles,

.

Figure 3 - Selected light micrographs of the complete series of sections that was the basis of the digital 3D-reconstruction.

A – Sagittal section showing the dorsal brain. B – Cross section of the stalk, depicting the prominent ventral nerve. C – Parasagittal section showing the left mesocoel pore and the left gill slit. D – Higher magnification of C depicting the left branchial nerve passing just dorsal of the gill slit. E – Parasagittal section showing the left lateral plexus at the base of the left lip. F – Section through the base of the posteriormost left tentacle showing the tentacle nerve projecting into it.

bnl – left branchial nerve, br – brain, dbv – dorsal blood vessel in the stalk, ep(te) – epidermis (of tentacle) ex – exterior, gl – glomerulus, gs – gill slit, in – intestine, lil/r – left/right lip, lmu – longitudinal muscles in the stalk, lpl – left lateral plexus, ms – mouth shield, mu – muscle, prc – protocoel, pc – pericardium, ph – pharynx, te – tentacles, mscl/re – left/right mesocoel, mtcl/re – left/right metacoel, mscp – pore of

mesocoel, st – stalk, tn – tentacle nerve, tr – trunk, vbv – ventral blood vessel in the stalk, vsn – ventral stalk nerve

Figure 4 - Low power transmission electron micrographs of the brain and ventral stalk nerve.

A – Sagittal section of the brain, anterior is to the left. Note the basiepithelial organization. Yellow: neuropil region of the brain. Green: giant cells at the dorsal anterior region of the brain. Left inset: higher magnification of the neuropil at the anterior end of the brain; note the predominant antero-posterior orientation of the sectioned fibres. Right inset: compare the outline of one of the giant cells (white dotted line) with the outline of one of the overlying epidermis cells (black dotted line). B – Parasagittal section through the brain. Note the basiepithelial organization, the glandular cells in the epidermis, and the prominent blood vessel immediately beneath the brain. C – The ventral stalk nerve is also basiepithelial in organization, though perykarya are found in the middle of the ventral stalk nerve as well.

bv – blood vessel, ci – cilia, ecm – extracellular matrix, gc – giant cell, glc – gland cell, m, lmu – longitudinal muscle in the stalk sc – mesocoel, ne – neuropil, nu – nucleus, pc – pericard, prc – protocoel

Figure 5 - Transmission electron micrographs of several regions of the nervous system.

A – Longitudinal section through a tentacle showing longitudinal nerve on the dorsal side. B – Ventral epidermis with basiepithelial neuropil closely apposed to the strong ventral longitudinal muscles. C – Branchial nerve in the vicinity of the strong mesocoelic musculature inserting in the tough extracellular matrix. D – Branchial

nerve close to the myoepithelial musculature of the metacoel, just dorsal to the intestine. E – Extensions of the ventral longitudinal musculature and apposed basiepithelial ventral nerve fibres. Note the thin extracellular matrix separating the two tissues. F & G – Probable neuromuscular connection between the longitudinal muscle in the stalk and the ventral stalk nerve. Note the two types of vesicles present in the extension of the nerve cells (enlarged in G).

aj – apical junction, bn – branchial nerve, co – collagen, ecm – extracellular matrix, epbr – epidermis of gill slit, msc – mesocoel, mu(mtc) – muscle cell (of the metacoel), mv – microvilli, neu – neurites, nu – nucleus.

Figure 6 - Statistical presentation of direction of fibers in different brain regions.

A – Anterior brain. Most fibres are anterior-posterior in orientation. B & C – No clearly preferred orientation of nerve fibres can be seen in the central brain (B) and the posterior brain (C).

Figure 7 - Semi-schematic 3D-representation of the anatomy of *C. gracilis*, showing the arrangement of major components of the nervous system in yellow, with major results from the immunohistochemical investigation added in green (serotonin) and red (acetylated α-tubulin).

an – anus, anp – anterior projecting nerves, bnl – left branchial nerve, br – brain, in – intestine, lp – lateral plexus, mo – mouth, ms – mouth shield, ph – pharynx, prc – protocoel, st – stalk, sto – stomach, te – tentacle, tr – trunk, vsn – ventral stalk nerve.

Additional file 1 – 3D-animation movie of the nervous system of the pterobranch *Cephalodiscus gracilis*.

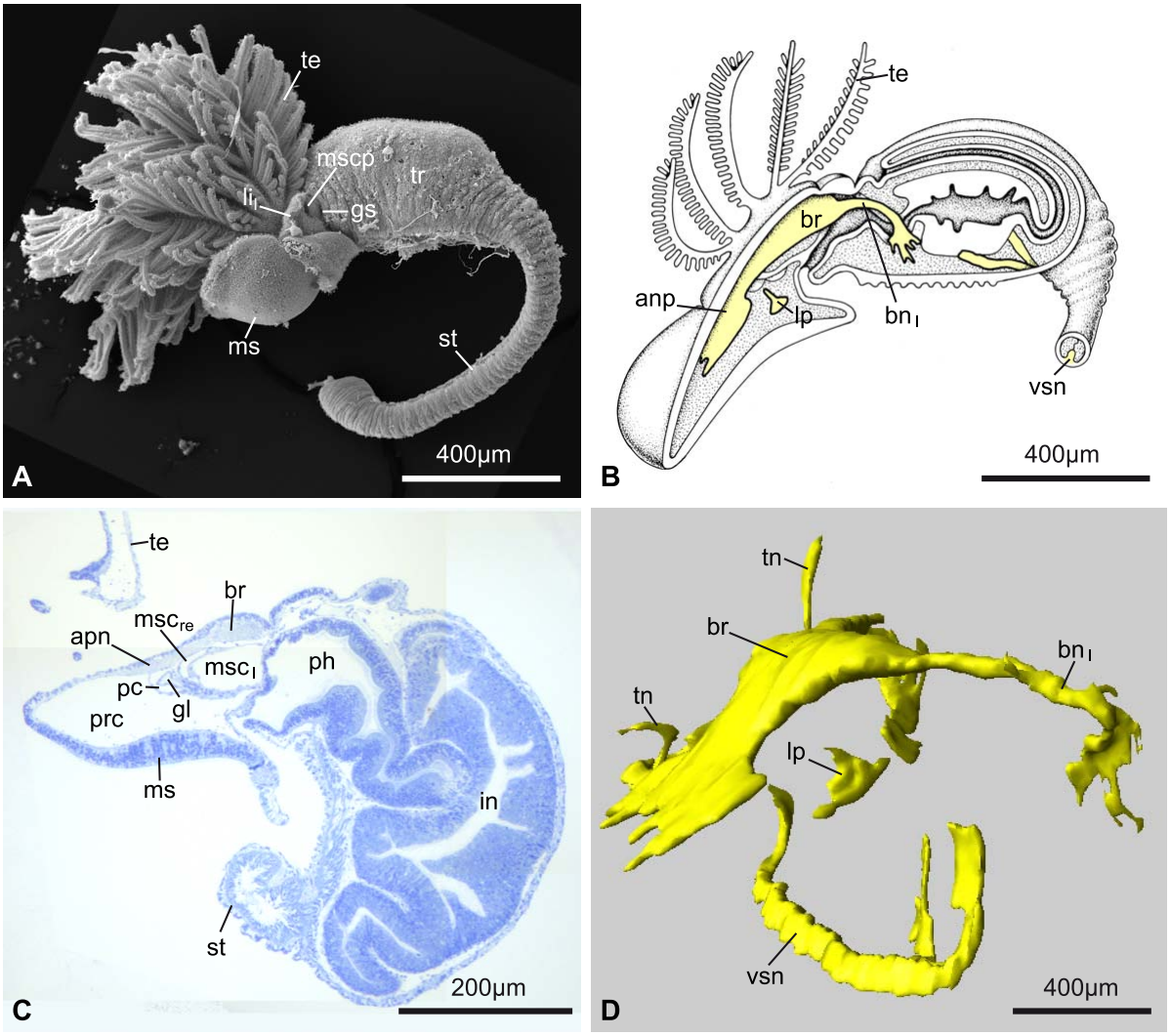
te
mscp
tr
li
gs
ms
st
400µm
A
te
br
anp
lp
bn l
vsn
400µm
B
te
br
msc re
apn
msc l
ph
pc
gl
prc
ms
in
st
200µm
C
tn
br
bn l
tn
lp
vsn
400µm
D

Figure 1

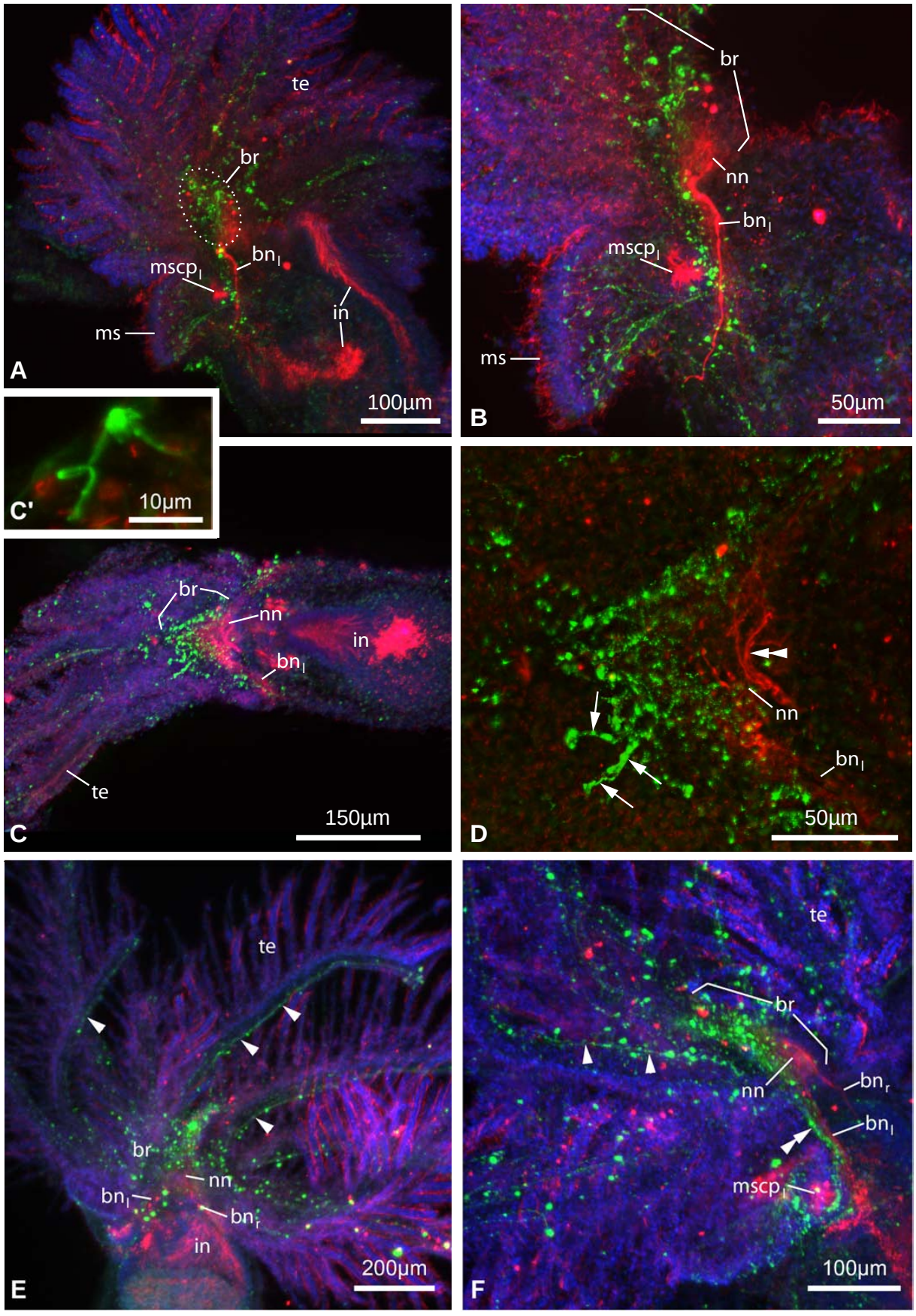
te
br
mscp$_l$
bn$_l$
in
ms
A
100µm
br
nn
bn$_l$
mscp$_l$
ms
B
50µm
C'
10µm
br
nn
in
bn$_l$
te
C
150µm
nn
bn$_l$
D
50µm
te
br
nn
bn$_l$
bn$_r$
in
E
200µm
te
br
nn
bn$_r$
bn$_l$
mscp$_l$
F
100µm

Figure 2

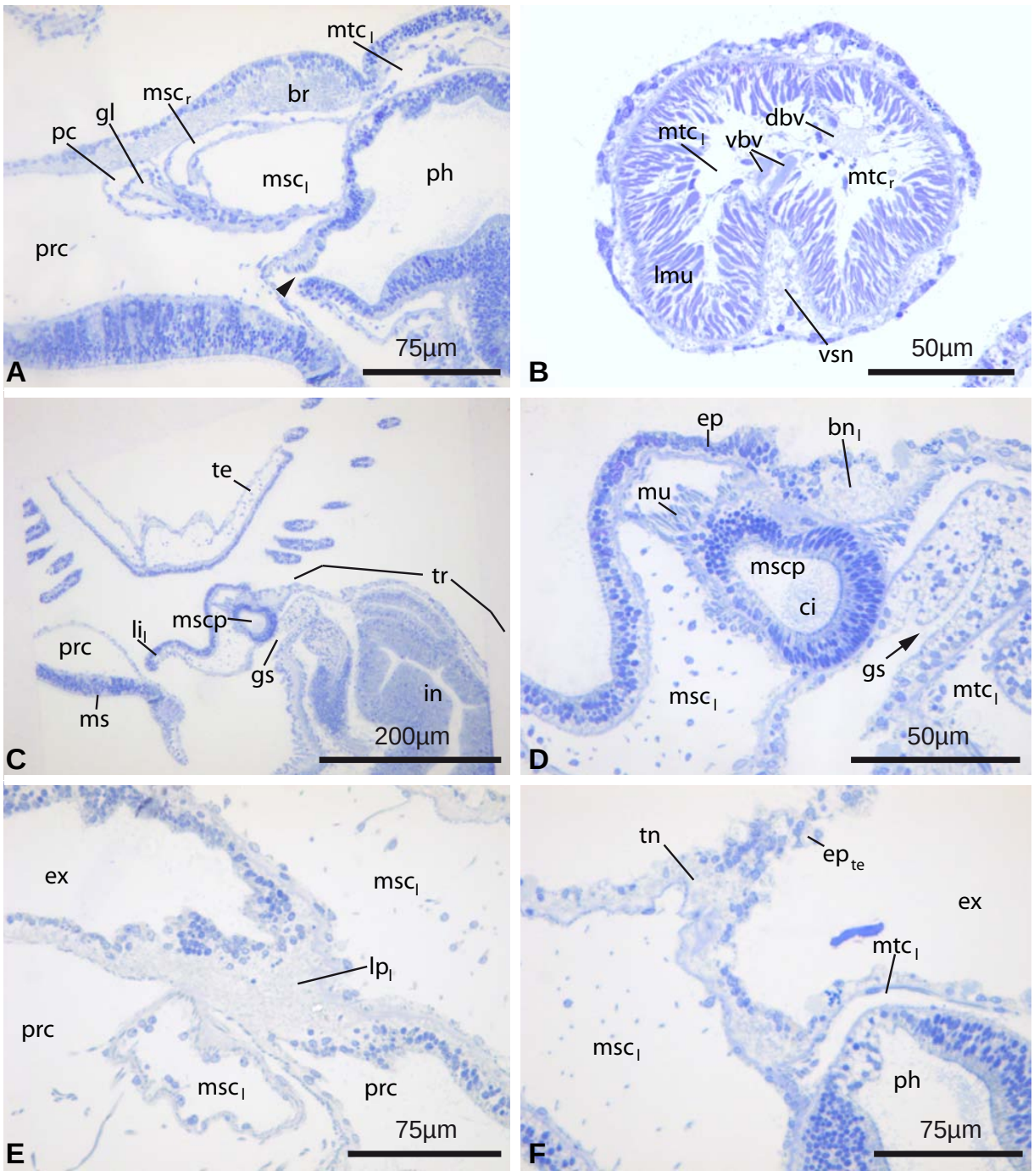
mtc$_l$
msc$_r$
br
gl
pc
msc$_l$
ph
prc
75µm
A
mtc$_l$
dbv
vbv
mtc$_r$
lmu
vsn
50µm
B
te
tr
li$_l$
mscp
prc
gs
in
ms
200µm
C
ep
bn$_l$
mu
mscp
ci
gs
msc$_l$
mtc$_l$
50µm
D
ex
msc$_l$
lp$_l$
prc
msc$_l$
prc
75µm
E
tn
ep$_{te}$
ex
mtc$_l$
msc$_l$
ph
75µm
F

Figure 3

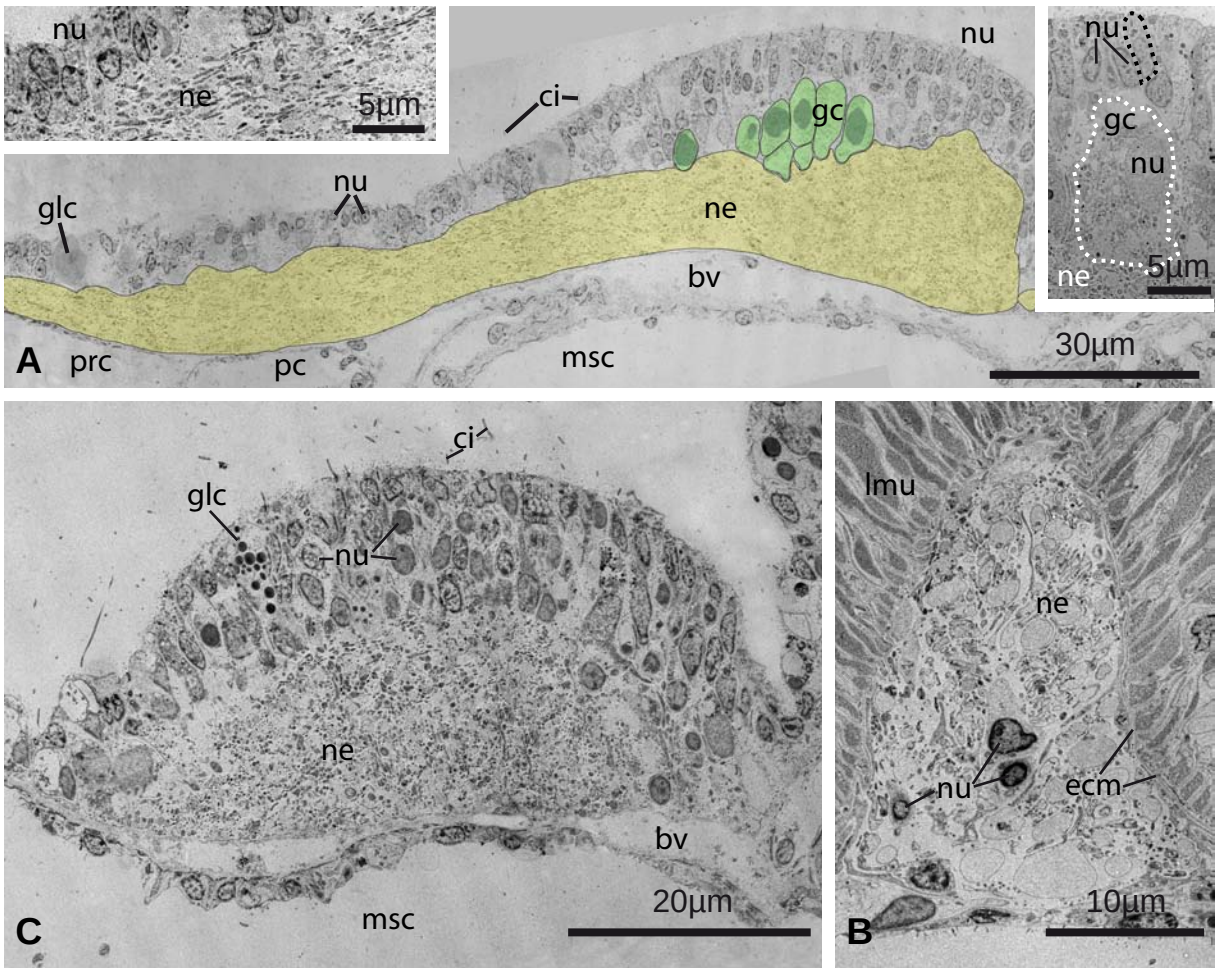
nu
ne
5µm
ci
nu
gc
nu
gc
nu
glc
nu
ne
bv
ne
5µm
A
prc
pc
msc
30µm
ci
glc
nu
lmu
ne
ne
nu
ecm
bv
20µm
10µm
C
msc
B

Figure 4

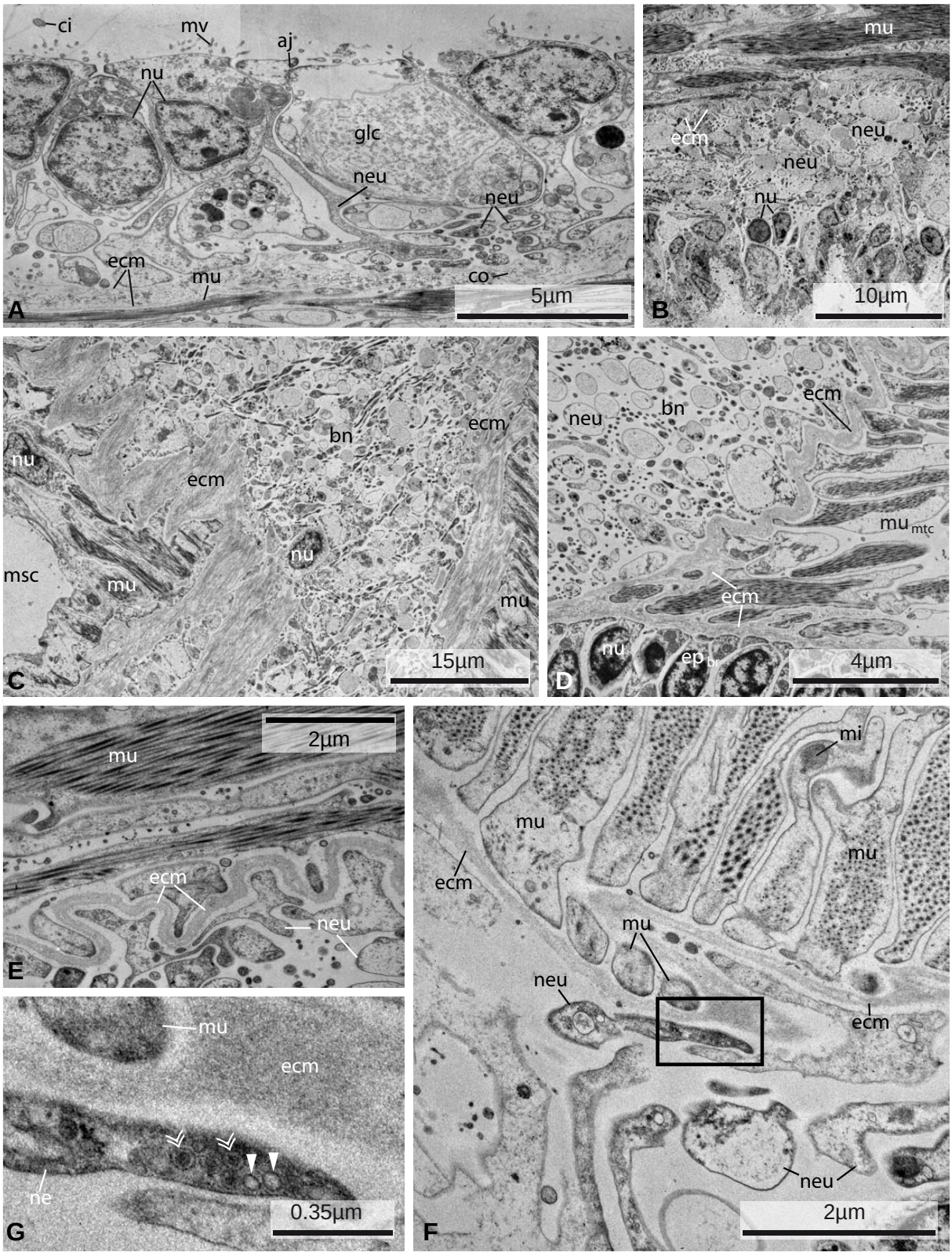
ci
mv
aj
nu
glc
neu
neu
ecm
mu
co
5µm
A
mu
ecm
neu
neu
nu
10µm
B
nu
ecm
bn
ecm
msc
mu
nu
mu
15µm
C
neu
bn
ecm
mu mtc
ecm
nu
epbr
4µm
D
2µm
mu
ecm
neu
E
mu
ecm
ne
0.35µm
G
mi
mu
mu
ecm
mu
neu
ecm
neu
2µm
F

Figure 5

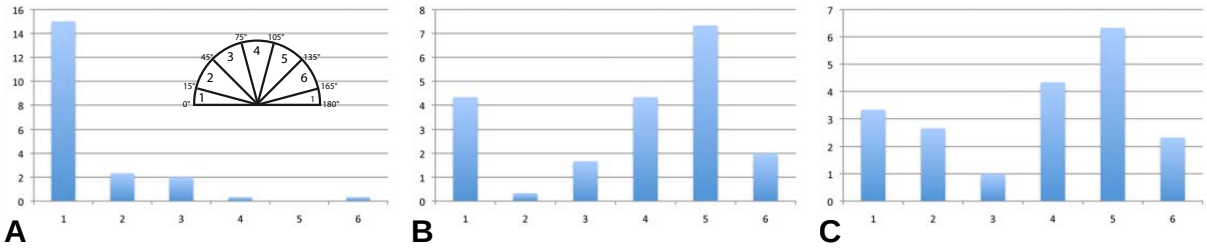

Figure 6

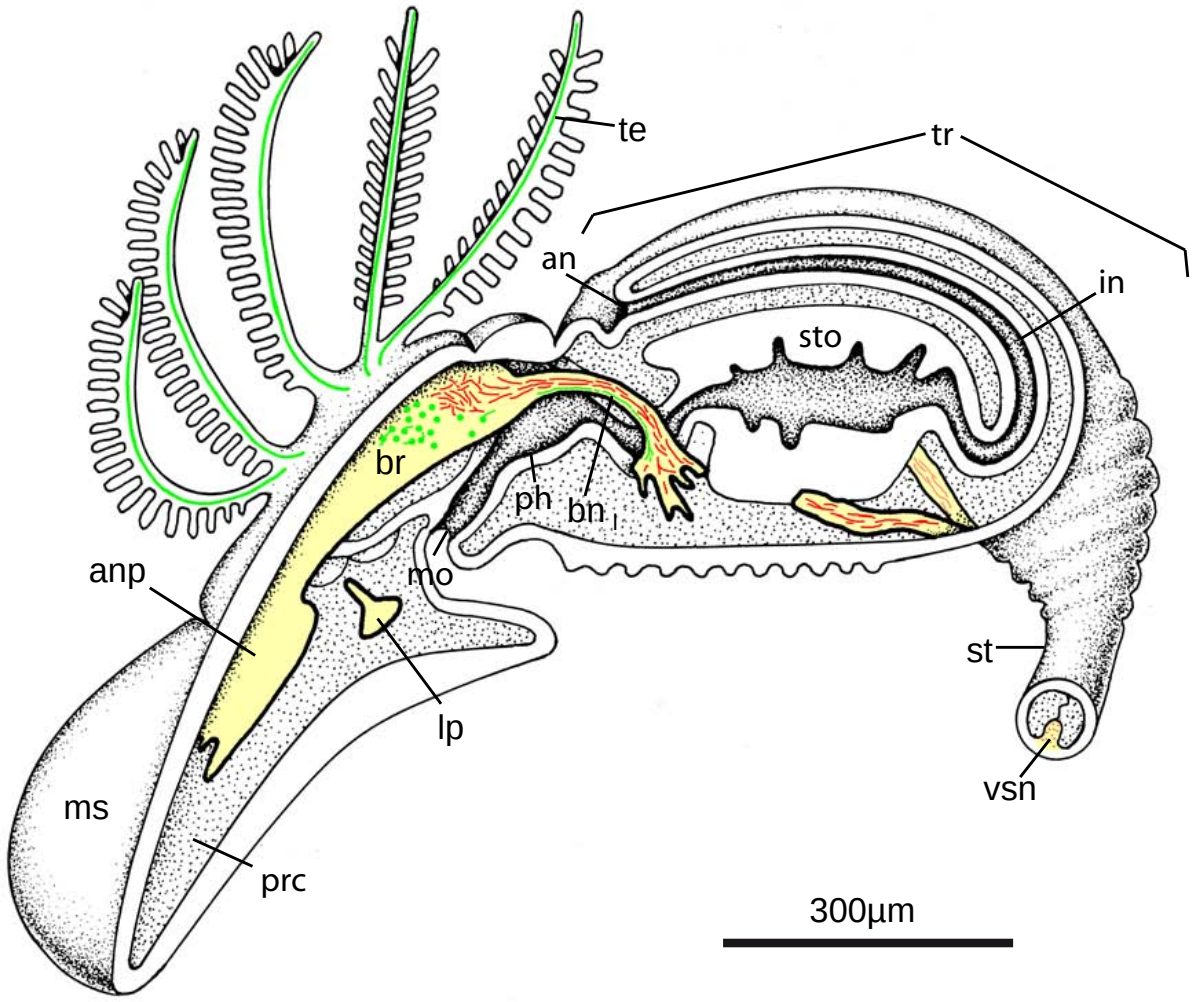

Figure 7

6. Coelom formation and developmental LR asymmetries in *Saccoglossus*

6.1 Contribution to this paper

Project conception: S K-S 90%; performance of practical work: S K-S 80%;
writing of manuscript: S K-S 90%.

6.2 Manuscript

Kaul-Strehlow S, Stach T. Ultrastructural investigations of the coelom formation and early development of the gill slits in *Saccoglossus kowalevskii* (Enteropneusta: Deuterostomia).

The development of the mesoderm in the hemichordate *Saccoglossus kowalevskii*: Left-Right asymmetries in a non-chordate deuterostome

Sabrina Kaul-Strehlow[1*] and Thomas Günther Stach[1]
[1]Institut für Zoologie, Freie Universität Berlin, Königin-Luise-Str. 1-3, 14195 Berlin, Germany
*Corresponding author. E-mail: skaul@zoosyst-berlin.de

Abstract

Chordates are known by a number of characteristic traits, e.g. notochord, neural tube, pharyngeal gill slits, post-anal tail, possession of endostyle, or characteristic left-right (*LR*) *asymmetries* in the organization of certain structures. However, the evolutionary origin of each of the aforementioned features is still far from being understood, when it comes to find potentially homologous structures in early deuterostomes. In particular, enteropneust hemichordates that share some of these chordate features (stomochord, collar cord, pharyngeal gill slits) may hold a key position in unravelling early chordate evolution. The origin of the third germ layer and its special formation including a coelomic cavity has traditionally been given high importance in phylogenetic analyses. In deuterostomes, the third germ layer derives from the endoderm by a process called enterocoely. The formation of the coelomic cavities through a *single* outpocketing pinching off from the apical end of the endoderm which then gives off mesocoela and metacoela on each side, has been observed in many echinoids and asteroids and is often regarded as being typical for deuterostomes. However, our data show that in enteropneusts all main coelomic cavities (single protocoel, paired mesocoela and metacoela) derive as *separate* outpocketings from the endoderm via enterocoely. This condition is recapitulated in the larva of amphioxus and can be observed in crinoid echinoderms in a similar way. Therefore, coelom formation from separated pockets, rather than from a single apical pocket is suggested as the ancestral type of coelom formation in Deuterostomia. Furthermore, we documented a left-dominated development of the gill pores and skeletal rods in *Saccoglossus* as has been reported from amphioxus in a slightly different way. Phylogenetic implications for the Deuterostomia in regard to *LR asymmetries* are discussed.

Introduction

Investigations aiming to reveal the evolution of the Metazoa are unquestionably one of the most important fields of systematic zoologists and their fascination can even be dated back to the time Darwin's "The origin of species" was published (1859).

More than three quarter of all known Bilateria belong to the major taxon Protostomia, e.g. nematods, molluscs, annelids or arthropods (Brusca & Brusca 1990, Westheide & Rieger 2007). Most of the remaining animals, including humans as members of the Vertebrata, are placed into the group Deuterostomia, namely the Echinodermata, Hemichordata and Chordata (Nielsen 2001). The evolution of the Deuterostomia and in particular that of the highly complex organized chordates from a more simple, bilaterian invertebrate ancestor remain unclear in many points (Nielsen 2009). All extant members of Chordata are characterized by a number of characteristic traits, e.g. notochord, neural tube, pharyngeal gill slits, post-anal tail, possession of endostyle/thyroid, or characteristic left-right (*LR*) *asymmetries* in the organization of certain structures (Benito & Pardos 1997, Boorman & Shimeld 2002, Lemaire et al. 2008, Stach 2008). For instance, distinct asymmetries yet can be seen in the developing head and gill slits in the larva of cephalochordates (Conklin 1932, Hatschek 1881, Stach 1996; 2000). However, the evolutionary origin of each of the aforementioned features is still far from understood, when it comes to find potentially homologous structures in early deuterostomes.

Since the end of the 19th century, scientists have been eager in proposing and discussing several conflicting scenarios concerning chordate origins, of which few have survived to the present (for review see Gerhart et al. 2005). In particular, Hemichordata, as a potential sister group to Chordata is thought to hold a key position in unravelling early chordate evolution (Ax 2001, Maisey 1986, Schaeffer 1987). There are two groups within the exclusively marine hemichordates. Pterobranchs are consistently small, sessile, and colonial animals, which develop tentacles for filter-feeding at their middle body region, i.e. the mesosoma (Anderson 1907, Schepotieff 1907). In contrast, enteropneusts are solitary and wormlike animals ranging in size from 2 – 250 cm (Spengel 1893). Even though body organization and life habits differ substantially within the two groups, Hemichordata is well supported as a monophyletic group by the presence of the character complex of the stomochord-pericardium-glomerulus within the anterior body region, i.e. the prosoma (Dohle 2004). However, until today it is not clear which of the body organizations is the more ancient one. Classical hypotheses of early deuterostome evolution postulate a pterobranch-like ancestor (Ax 2001, Garstang 1928, Nielsen 2001, Romer 1967), whereas molecular analyses of 18S rDNA sequences of recent years have shown that pterobranchs may be a sister group to one of the enteropneust families, namely the Harimaniidae and therefore have evolved within the Enteropneusta (Cameron et al. 2000, Cannon et al. 2009, Halanych 1995). Thus, a vermicular enteropneust-like ancestor for the Hemichordata could be postulated. Moreover, the assumption that an enteropneust-like body plan might be plesiomorphic for Hemichordata

is further supported by similarities of certain structures in hemichordates (collar cord, gill slits and stomochord) with some of the above mentioned chordate features. Indeed, these similarities have been described and recognized almost 150 years ago by Bateson (1885), who was the first to put hemichordates into a close relationship with chordates. In contrast, most of the recent molecular analyses and moreover some combined analyses support a sister group relationship between Hemichordata and Echinodermata, together comprising the Ambulacraria (Bourlat et al. 2006, Castresana et al. 1998, Halanych 1995, Cameron 2000, 2005, Zrzavy et al. 1998). The name Ambulacraria can be referred to Metschnikoff (1881), a morphologist who emphasized resemblances between the tornaria larva of enteropneusts and the dipleurula larva of echinoderms, more precisely the hypothetical larval form of a inferred stem-echinoderm (Dohle 2004, Nielsen 2001). If hemichordates are indeed more closely related to echinoderms than to chordates any homologous features present in hemichordates and chordates must have been present in the last common ancestor of all deuterostomes (Gerhart et al. 2005, Lowe et al. 2006).

The origin of the third germ layer and its special formation including a coelomic cavity has traditionally been given high importance in phylogenetic analyses (Hyman 1959, Nielsen 2001, Telford 2004). The suggestion of homology of the third germ layer across the animal kingdom can be traced back to the early studies of Hertwig and Hertwig (1881) and Mastermann (1898). In principle, two modes of coelom formation can be distinguished and have been associated with one of the main animal groups: schizocoely in protostomes and enterocoely in deuterostomes (Technau & Scholz 2003). Although this classification is applicable in many cases, exceptions have been reported as well (e.g. see Kaul-Strehlow & Stach 2011).

The formation of coelomic cavities (pro-, meso-, and metacoel) in enteropneusts, one of the part groups of Hemichordata, has been studied in detail several times (Bateson 1884, Morgan 1891, 1894, Spengel 1893, Davis 1908, Stiasny 1914). Despite the fact, that enteropneusts compose a group of phenotypically quite homogenous animals, early researchers reported at least five different modes of coelom formation, which have since been depicted throughout textbooks or treatises (van der Horst 1939, Hyman 1959, Nielsen 2001). However, occasionally the interpretations drawn from the original light microscopical data were based on a very limited set of stages (see also comments in Cameron 2005, Nielsen 2001). Moreover, in determining germ layer affiliation of early embryonic tissues, it is of crucial importance to identify and trace the extracellular matrix (*ecm*) separating tissues accurately, as it forms a basal lamina on which epithelial cells rest on (Bartolomaeus 1993, Bartolomaeus et al. 2009, Stach 2000, 2009, Kaul-Strehlow & Stach 2011). The thickness of such *ecm* in marine invertebrate embryos is often below the resolution distance of classical light microscopy (< 0.2 µm), a potential explanation for the different results of the classical comparative studies. A re-examination of coelom formation in hemichordates with modern techniques using electron microscopy is lacking until today, as the latest detailed, morphological studies on the ontogeny of enteropneusts were conducted in the 1950s (Colwin & Colwin 1953).

The aim of the present study is to fill this gap. We investigated densely sampled successive ontogenetic stages of the direct-developing enteropneust *Saccoglossus kowalevskii* using SEM, TEM, and histology. The detailed analysis of complete serial sections in combination with computer-aided 3D-reconstructions of all major organ systems enables the exemplarily illustration of profound description of the development of an enteropneust.

Our data show, that all of the five main coelomic cavities form from the endoderm by the way of enterocoely. Moreover, the mesocoela and metacoela are given off as separated coelomic pouches from the middle and posterior regions of the endoderm, respectively. By comparing these results with those reported from other hemichordates and deuterostomes, we hypothesize the ground pattern of coelom formation in enteropneusts. Subsequently, by evaluation of current phylogenetic hypotheses, the likely ancient condition of coelom formation in the last common ancestor of hemichordates, ambulacrarians and probably even of deuterostomes is reconstructed.

In addition, this is the first study that reveals developmental *LR asymmetries* of the gill slits in an enteropneust. A comparison with characteristic *LR asymmetries* in chordates is presented and possible phylogenetic implications of a loss of symmetry during morphogenesis are discussed.

Materials and methods

Adult specimens of *Saccoglossus kowalevskii* (Agassiz 1873) were collected from intertidal areas near Woods Hole (Massachusetts, USA) in September 2007. Animals were brought to the laboratory, separated according to sex, and kept individually in finger bowls. Animals were kept at 18 °C on a seawater-table and inspected frequently. When eggs were spawned they were mixed with active sperm isolated from a ripe male individual and diluted in seawater. These procedures are described in more detail in Lowe (2004). Fertilization envelopes were ruptured using fine forceps and appropriate embryonic stages were collected using Pasteur pipettes. Embryos were relaxed in a mix of 7% $MgCl_2$ and sea water (1:1) for 5-10 minutes prior to processing for transmission and scanning electron microscopy (TEM/SEM).

For TEM most of the relaxation agent was removed and replace with ice-cold primary fixative containing 2.5% glutaraldehyde in 0.2 M sodium cacodylate buffer (pH 7.2), adjusted to an osmolarity of approximately 800 mosm with the addition of NaCl. Primary fixation was stopped after 45 minutes with three buffer rinses for 10, 15, and 20 minutes. Primary fixation was followed by 30 minutes of postfixation with 2% OsO_4 in sodium cacodylate buffer. Postfixation was stopped with three buffer rinses (15, 30, 30 minutes) followed by two rinses with ddH_2O (15, 30 minutes). After dehydration through a graded series of ethanol specimens were embedded in Araldite for TEM and light microscopy. For SEM specimens were critical point dried in a CPD 030 (Balzers Union, Liechtenstein). Dried specimens were sputter coated with gold in a SCD 040 (Balzers Union, Liechtenstein) and viewed with a Fei Quantum 200 scanning electron microscope at 15 kV (FEI Co. Netherlands)

Complete longitudinal and transverse serial sections in 0.5 µm thickness for light microscopy of nine specimens from five stages (36 h, 56 h, 96 h, 132 h and 432 h post fertilization (pf)) were sectioned on a Leica Ultracut S. Complete transverse and one longitudinal series of sections in thickness of about 60 nm for TEM were cut from eight specimens from five stages (36 h, 56 h, 96 h, 132 h and 432 h pf). An additional single specimen from stage 432 h pf was serially sectioned alternating between semi-thin sections (0.5 µm) and ultrathin sections (60 nm). Semi-thin sections were stained with toluidin blue. Ultrathin sections were stained with 2% uranylacetate and 2.5% lead citrate in an automatic stainer (NanoWlm Technologie GmbH, Göttingen). Light microscopic images were recorded with a digital camera (Olympus BX-UCB) mounted on an OlympusBX51 compound microscope. TEM pictures were documented with a Philips CM120 BioTWIN electron microscope at 60 kV on Ditabis Digital Imaging Plates were read by a Ditabis Micron IP-Scanner. Images were aligned using Imod align Software on a Linux computer. Based on the resulting stack of images 3D-models of the anatomy of all organ systems were created in Amira 3.0 software (Mercury Computer Systems, Berlin).

Results

Early blastula stage

The fertilized eggs of *Saccoglossus kowalevskii* develop into an early blastula stage measuring about 400 µm in height and 430 µm in breadth at the age of 8 h post fertilization (pf) (Fig. 1A, D). The early blastula exhibits a somewhat irregular spherical shape, slightly punched in at the vegetal pole. A shallow notch at one side characterizes the vegetal pole of the embryo, indicating the position of the prospective blastopore (Fig. 1A). Under the scanning electron microscope the individual cells comprising the early blastula can clearly be distinguished from each other. On some cell surfaces partial constrictions indicate ongoing cleavage processes (Fig. 1A inset). The cells at this developmental stage are more or less of elongated cuboid shape, measuring about 20 µm in diameter and 30 µm in height ranging from the surface facing the blastocoel inside the embryo to the outer surface (Fig. 1D). The outer cell surface is covered with evenly distributed short microvilli. Furthermore, about 6 µm of the space underneath the apical cell surface is occupied by an area comprising occluding cell junctions. In particular, these cell junctions form bridges connecting neighbouring cells (Fig. 1D).

Early gastrula stage

During the next few hours the so-called early or flattened gastrula is formed by repetitive cleavages of the cells (Fig. 1B). The beginning of gastrulation is indicated by the invagination of the blastomere cells in the centre of the flattened vegetative pole, forming the opening of the blastopore. After 24 h pf, the early gastrula is cup-shaped and measures 300 µm in height and 340 µm in width (Fig. 1B). Moreover, the cells now have a different shape they are highly columnar measuring 60 µm in length and barely 8 µm in width (Fig. 1E). They are tall and form a smooth outer as well as inner blastocoel-facing surface. A close-up of the outer cell surface shows that the majority of the cells have developed a single cilium between the dense microvilli. In the region of the prospective telotroch noticeably longer cilia are present (Fig. 1B inset). At this stage of development the embryos are constituted of one single layer of cells enclosing an inner lumen namely, the blastocoel.

Gastrula stage

At an age between 30 and 36 h pf most embryos develop an elongated, ovoid shape and measure about 300 µm in length (Fig. 1C). One of the most important larval characters is the conspicuous telotroch. The telotroch is constituted by multiciliated cells encircling the animals approximately 50 µm anterior to the blastopore. The remaining cells of the ectoderm are monociliated (Fig. 1C). A SEM micrograph of a dissected animal reveals the diploblastic organization of the embryos at this stage of development (Fig. 1F). The invaginated endoderm tightly adjoins the ectoderm, no space is left between the two germ layers, thus

obliterating the blastocoel almost completely. The ectoderm consists of a highly columnar epithelium. The shape of the cells is somewhat irregular. Sometimes, cells exhibit slender elongations giving the whole epithelium an almost pseudostratified appearance (Fig. 1F). The ectodermal cells measure about 30 µm in height. Their bulged surfaces indicate a cytoplasm rich in vesicles. At this stage of development, the majority of these vesicles are likely to contain granules of yolk. The endodermal cell layer likewise contains a monolayered epithelium measuring about 40 µm in height. The cells have a columnar shape, bordering a central lumen along their apical cell surface, the lumen of the archenteron. The apical cell surfaces of the endodermal cells are unevenly covered with short microvilli. Moreover, each endodermal cell is equipped with a single cilium which protrudes into the lumen of the archenteron (Fig. 1F).

1st groove stage

Gross morphology

The embryos at the 1st groove stage are of elongated shape measuring 450 µm in length, with a more rounded anterior end and a more flattened posterior end (Fig. 2A-P, 3D, E). The conspicuous telotroch surrounding the embryo separates the posterior perianal field from the larger anterior part of the animal. The telotroch is constituted of multiciliated cells (Fig. 3E). This developing stage is named after a shallow circular groove that is visible from the exterior ca. 200 µm behind the anterior pole (Fig 2, 3D). This groove characterizes the boundary between the prospective proboscis and collar region. Later on, it constricts deeply to separate the proboscis from the remaining body. SEM of dissected embryos and serial sections reveal the internal anatomy.

The endoderm extends to the posterior end of each embryo and is separated from the ectoderm by means of a basement membrane, except the blastoporus region (supplementary (S) fig. S1D). Here, ectodermal and endodermal tissues come in direct contact to each other. The endodermal lumen is a flattened tube, measuring hardly more than 2 µm in height, but still up to 50 µm in width in the prospective collar region (Fig. 2I, J). These lateral protrusions of the endodermal wall are the *anlagen* of the pouches of the prospective mesocoela.

The anterior portion of the endodermal tissue will give rise to the anteriormost mesodermal cavity, i.e. the protocoel (Fig. 2A-D, M-P, 3D). In most of the examined embryos at this stage, the protocoelic cavity is still continuous with the lumen of the endoderm (Fig. 3A), although lateral invaginations of the basement membrane begin to constrict the protocoel from the remaining endoderm (Fig. S1F, G). In the 3D reconstruction of a slightly further developed embryo the protocoel is completely separated from the remaining endoderm, as it forms the ontogenetically first completely separated coelomic cavity.

In contrast, the prospective meso- and metacoela form lateral pouches in the middle and posterior regions of the endoderm, respectively (see Fig. 2A-D and M-P for coloured pri-

mordal mesodermal cells). Both mesodermal *anlagen* constitute left and right parts which later on surround the endoderm.

Fine structure of the endoderm

The endoderm consists of a highly columnar monociliated epithelium which encloses a slit-like central lumen, the archenteron (Fig. 3A, C, E, F). The central lumen extends from the anterior region, where it connects to the protocoelic cavity, to the posterior region, where it bifurcates both dorsally and ventrally (Fig. 2K, L). At the anterior margin of the endoderm, the protruding axonemata of the cilia of the endodermal cells project into the protocoelic cavity that is still continuous with the endodermal lumen at this 1st groove stage (Fig. 3A). The endodermal cells measure about 20 µm in height and border the luminal side with narrow elongations about 3 µm in breadth (Fig. 3E, F, S1D, E). The apical surface of each endodermal cell is equipped with numerous slender microvilli measuring 1 µm in height and 100 nm in width. The microvilli are evenly distributed and encircle a single cilium to form a collar-like arrangement (Fig. 3C inset). The axoneme of each cilium shows a regular 9x2+2 microtubular pattern in cross sections, which is common for motile cilia. The cilia are anchored into the apical cytoplasm by one striated rootlet running basally into the cell body (Fig. 3C inset). Neighbouring cells are interconnected apically by adhering junctions (Fig. 3C). The apical cytoplasm is often filled with many electron-opaque vesicles of various diameters measuring between 400 nm and 950 nm in diameter (Fig. 3C). The high number of vesicles indicates a secretory and modifying function as expected for endodermal tissue. Moreover, different granules are present within the cytoplasm, giving it a moderately electron-dense appearance. The nucleus has a central position and contains a spherical and electron-dense nucleolus (Fig. S1D). Mitochondria are numerous and located in the distal half of the cell between the cell surface and the nucleus. Few yolk granules are found in the apical cell portion. In contrast, yolk granules of various diameters represent the predominating type of organelles in the central and basal compartments of the cytoplasm (Fig. 3D, F, S1D, F). The high amount of yolk within all endodermal cells reflects the developmental stage of these embryos. At their bases, the endodermal cells attach to a basement membrane, which separates endoderm from ectoderm.

Fine structure of the protocoel

Almost the complete protocoel is packed with rather undifferentiated protocoelic cells, except for a limited central fluid filled space, the prospective protocoelic cavity (Fig. 3A, B). The shape of these cells is less columnar, compared to those of the endodermal cells. The protocoelic epithelium consists of stalked goblet-shaped cells up to 80 µm long, with a spherical somatic part projecting into the lumen of the protocoel (Fig. 3A, B, S1A, C). A narrow and elongated neck region connects the somatic part to the more voluminous basal portion that is attached to the basement membrane by hemidesmosomes. The nucleus is generally located within the goblet-shaped region of the cell. The cytoplasm contains numer-

ous spherical and electron-dense yolk granules, as well as other organelles. The protocoelic cells posses a single cilium at their apical cell surface. The remaining surface is smooth, no microvilli are present.

Fine structure of the meso- and metacoel

Light microscopic sections show a slightly darker staining in those areas, where the collar and trunk mesoderm will differentiate (Fig. 3D). Scanning electron micrographs show the prospective trunk mesoderm, i.e. the metacoel developing as a third germ layer between the ectoderm and endoderm (Fig. 3E, F inset). The trunk mesoderm consists of one to two layers of more or less cuboid cells measuring about 12 µm in length and width. The surface of the mesodermal cells is smooth and comparable to those of the endodermal cells, but it remains unclear with SEM if cilia are developed at this stage.

Early kink stage

Gross morphology

Embryos at this developmental stage show a proboscis that is more flattened at the anterior end and is separated by a deep constriction from the rest of the body, the collar and trunk region (Fig. 4A-H, 5A). The animals measure about 450 µm in total length. The trunk region is elongated measuring up to 300 µm in length, and shows a slightly ventral kink.

The endoderm is present as a simple, blind-ending structure extending from the anterior collar region to the posterior end of the trunk. No anus is opened yet (Fig. 4I-L, 5A). However, the ventromedian mouth opening has developed to connect the anterior endoderm with the outer environment. The mouth opening is located exactly within the circular groove that separates the proboscis from the collar region (Fig. 4K, L). The epithelium of the endoderm is about 45 µm high and surrounds the narrow slit-like lumen (Fig. 4I-L, 5A, S2A). This lumen is flattened dorso-ventrally and follows a straight course through the embryo. Following the kink of the animal, it is slightly bent within the posterior trunk region. The endodermal wall shows a pair of lateral outpockets visible just before the posterior margin of the collar region (Fig. 4I and J, 5A). These are the former connections to the mesocoelic pouches, which derive from the archenteron via enterocoely. Beside the lateral outpocketings, the endodermal wall shows a shallow longitudinal depression at the ventral midline within the collar region (Fig. 4J-L). Moreover, the lumen of the gut sends a 20 µm short projection towards the anterodorsal region, representing the *anlage* of the stomochord (Fig, 4K and L).

The proboscis region is completely dominated by the anterior body cavity, the protocoel (Fig. 4A-D, M-P, 5A). At the lateral and dorsal sides the protocoel extends slightly posteriorly contacting the mesocoela at the margin of the collar region (Fig. 4A,B,M,N). The 3D reconstruction shows a small, more or less triangulate mass within the ectoderm, dorsally above the posterior end of the protocoel (see also Kaul-Strehlow & Stach 2011, Fig. 2A,

3A). This is the *anlage* of the pericardium, a contractile fluid-filled coelomic cavity. For more details see Kaul-Strehlow & Stach (2011).

The paired mesocoelic and metacoelic pouches have expanded and extended in all directions to adjoin each other in anterior to posterior direction and to encircle the median endoderm (Fig. 4A-D, M-P). All coelomic sacs are separated from the endoderm by means of a thin sheath of *ecm* (Fig. 5A, E, S2E). The middle pair of mesoderm, the prospective mesocoela extend about 100 µm in length and demarcate the position of the collar region. The paired metacoel is restricted to the trunk region and encircles the posterior endoderm. The left and right cavities extend over about 280 µm in total length and are separated dorsally as well as ventrally by mesenteries.

Fine structure of the endoderm

The anterior end of the endoderm is flattened and protrudes shortly into the protocoel (Fig. 4I-L, 5A). The endoderm is a highly columnar epithelium that appears to be pseudostratified in ultrathin cross sections. The endodermal cells measure about 65 µm in height but only 3.5 µm in width (Fig. 5D, S2A) and border a central ellipsoid-shaped lumen located in the centre. Each cell is equipped with a single cilium and moreover numerous short microvilli measuring about 1 µm in height. Between microvilli numerous vesicles are seen apically in longitudinal sections. These vesicles are filled with different content (Fig. 5D). The cilium shows a typical 9x2+2 microtubular arrangement and is anchored in the apical cytoplasm via a vertical striated rootlet. Neighbouring cells are interconnected by adhering junctions. The slightly elongated nucleus is central in position (Fig. S2) and contains an electron-dense, spherical nucleolus. Numerous yolk granules varying between 0.5 to 3 µm in diameter dominate the cytoplasm of endodermal cells. In general, the endodermal cells appear quite undifferentiated at the early kink stage. The conspicuous and abundant clear vesicles observed in the 1st groove stage (see Fig. 3C) are not present anymore (Fig. 5D, S2). While endodermal cells are exclusively monociliated, the ectodermal epithelium consists of multiciliated supporting cells and different monociliated glandular cells. Those endodermal cells lining the former connection to the mesocoelic pouches are likewise monociliated cells equipped with numerous microvilli across the cell surface (Fig. 5C, inset). The cilia are at least 5 µm long and anchored into the cytoplasm by two striated rootlets. The first rootlet remains short and runs horizontally, while the second one projects, slightly obliquely in vertical direction. The accessory centriole is attached to the vertical rootlet by means of a bundle of filaments (Fig. 5C inset).

Fine structure of the protocoel

The protocoelic lining is composed of monociliated myoepithelial cells, which can be classified into two types, according to the different amount and the arrangement of myofilaments. A sagittal section of the proboscis shows that the cells positioned laterally in the protocoel have developed into long, slender cells, which span the protocoelic cavity completely in anterior-

posterior direction (Fig. 5B, S2B). These cells have a minimum length of 50 µm by measure barely 2 µm in width. They are connected to the basement membrane anteriorly as well as posteriorly by hemidesmosomes. The protocoelic lining cells are interconnected among each other by adhering junctions that are commonly found close to more voluminous basal part of the cells (Fig. 5B, S2B). Most of the cytoplasm of these cells is filled with myofilaments accompanied by numerous mitochondria. Myofilaments are orientated in longitudinal direction. The nucleus is of elongated shape and is located aside the myofilaments within the narrow elongated part of the cells. These slender longitudinal epitheliomuscle cells alternate with a second type of cells which contains basal myofilaments that are circularly arranged (Fig. S2B). The shape of these cells is less elongated. Instead, these cells appear more compact and ellipstic when examined in sagittal sections. These cells have a more electron-dense cytoplasm. The nucleus is located almost basally or is found at least in the basal portion of the cells. Besides the obligate presence of yolk granules, the cytoplasm contains several weakly electron-dense vesicles of various diameters. A sagittal section reveals that here the cells are less differentiated (Fig. 5A). These cells retain the club- or goblet-shaped profile already described for the 1st groove stage. There may be individual bundles of circularly arranged myofilaments present in the very basal part of the cytoplasm.

Fine structure of the meso- and metacoel

Ultrastructural investigations show that the mesodermal tissue is composed of two layers (Fig. 5E-H). This applies to the mesocoelic mesoderm as well as for the metacoelic mesoderm. There is no difference in ultrastructure between the coelothelia bordering both coelomic compartments. However, cross sections demonstrate that both cell layers rest on different basement membranes (Fig. 5G, inset, F-G, S2E). The distal cells beneath the ectoderm display a cubical to columnar shape, measuring 11 µm in height and between 3 to 7 µm in width (Fig. 5E, inset). The cytoplasm is electron light and contains several yolk granules the larger ones of which are more osmiophilic. Some mitochondria are observed throughout the cytoplasm. The nucleus is more or less spherical measuring 5 µm in diameter and is restricted to the apical part of the cells (Fig. 5G). Myofilaments are present in the very basal portion of the cells. These filaments are about 15 nm in diameter and longitudinally arranged in all cells in cross sections (Fig. 5G). The proximal layer of cells is resting on a very thin sheath of *extracellular matrix* (*ecm*) that separates the mesoderm from the endoderm (Fig. 5E, inset). At some points this sheath becomes so narrow that it is discontinuous in the electron micrographs (Fig. 5F). The cells of this layer consist of much more flattened cells, measuring only 2.5 µm in height but at least 13 µm in breadth. The cytoplasm is similar to the cytoplasm of the distal cells in most aspects. Distinctive characters are more flattened nuclei and the myofilaments, which are circularly arranged (Fig. 5F).

Both cell layers show signs of epithelialization and surround a virtual lumen between them (Fig. S2D). Following serial sections, single cilia can be found at the apical cell surfaces, whose axonemata protrude into the virtual lumen (Fig. 5E, S2D). Apical cell junctions and

spot desmosomes are scarcely found and poorly developed. However, apical cell junctions are restricted to connect neighbouring cells of the same cell layer, but are never present between proximal and distal cells.

Late kink stage

Gross morphology

The embryos at 96 h pf measure about 470 µm in total length and can be divided into three body regions, the anterior proboscis region, the middle collar region, and the kinked trunk region (Fig.6A-H, 7A). The proboscis is slightly elongated and tapers at the anterior end. It measures about 140 µm in length and is separated from the collar region by a circular constriction.

The endoderm is of somewhat bunchy shape and well surrounded by the paired collar and trunk coeloms. The endoderm is connected to the exterior by means of a mouth opening (Fig.6B, C). The position of the mouth opening shifted from ventral to anteroventral and is now located deeply within the circular constriction. Although the lumen of the endoderm is still compressed at this stage, specific regions of the prospective digestive tract can be distinguished due to conspicuous constrictions of the endodermal wall. Within the buccal cavity, a short diverticulum is protruding anterodorsally into the protocoel measuring about 40 µm in total length (Fig. 6K, L, 7B). This diverticulum constitutes the *anlage* of the stomochord and possesses a central narrow lumen that is continuous with the lumen of the buccal cavity. The buccal cavity is continuing into the pharynx region posteriorly. At the late kink stage, the *anlagen* of the first pair of gill pores is distinguishable as tubular dorsolateral outgrows of the pharyngeal wall (Fig. 6I, J, 7A). These outgrows are still blindly closed at the distal ends, where the endodermal tissue is directly adjoining the ectodermal layer. Careful analysis of the complete serial sections and the 3D-reconstruction reveal that the right and left *anlage* of the gill pores are slightly asymmetrical. The areas of attachment of endoderm and epidermis are circular on both sides, but the area on the left side is bigger (Fig. 6C, D, O, P). The pharyngeal region ends after about 120 µm by a slight annular constriction just behind the *anlagen* of the gill pores and continues into the intestine. The intestine is the sac-like posterior part of the digestive tract, situated in the kinked trunk region of the embryo. The intestinal lining is very high, just leaving a flattened narrow lumen (Fig. 7A). The intestine is not subdivided further and ends blindly as there is no anus opened yet.

The shape of the protocoel mirrors that of the external of the proboscis. It tapers anteriorly and is extended posteriorly to border the paired mesocoelic cavities (Fig. 6A-D, M-P). The pericardial sac is suspended dorsally in the posteriormost region of the protocoel. It is pear-shaped measuring 25 µm in width and 30 µm in height and projects into the protocoelic cavity (Fig. 7B). The pericardial sac is attached dorsally to the epidermis and adjoined ventrally by the stomochord.

The paired mesocoela surround the anterior digestive tract completely omitting only the ventral mouth area (Fig. 6A-D, M-P). The left and right mesocoela adjoin in the ventral and dorsal midline and are separated by longitudinal mesenteries. Moreover, each of the mesocoela is extended anteriorly by sending lateral extensions into the basis of the proboscis (Fig. 6O, P). The trunk region is occupied by the paired metacoelic cavities ensheathing the gill region and intestine from the left and right side (Fig. 6A-D, M-P). The left and right coeloms adjoin each other in the ventral and dorsal midline, but stay separated by mesenteries.
The main changes compared to the early kink stage concern the ongoing development of the pericardial complex and the *anlagen* of the gill pores. The following description of the fine structure will therefore particularly focus to them.

Fine structure of the endoderm

All endodermal cells are still comparably undifferentiated and constitute a pseudostratified monociliated epithelium similar to the one found in the early kink stage. More interesting are the cells lining the lateral outgrowings of the pharyngeal wall, namely the *anlagen* of the gill pores. These ducts of the gill pores are tubular and ellipstic in cross sections. The cells lining the still blind terminal ending of the duct are monociliated cells though, the cytoplasm of individual cells contain several centrioles indicating ciliogenesis.

Fine structure of the protocoel

The cells lining the protocoel can be divided into two different types of monociliated epithelial cells according to differences in form and function. The first type of cells is lining the pericardial sac and is differentiated into podocytes (Fig. 7C). These bulbed-shaped cells may be slightly elongated protruding about 7 µm into the protocoelic cavity. The cytoplasm contains several vesicles of yolk and a central nucleus, somewhat irregular of shape. Moreover, most of the abundant mitochondria are placed closely to the basal myofilaments (Fig. 7C). Such myofilaments are also well developed within the fine pedicels arising from the podocytes. The majority of myofilaments are longitudinally arranged. The podocytes rest on a basement membrane beneath which a prominent haemal sinus is present (for more details see Kaul-Strehlow & Stach 2011).

The second type of epithelial cells comprises well developed myoepithelial cells that are interconnected by apical adherence junctions (Fig. 7E). They form either a distinct outer circular muscle layer or individual longitudinal muscle strands spanning the lateral and ventral portions of the protocoel. The centre of the protocoel on the other hand is occupied by the fluid-filled coelomic cavity. The basal portion of the circular muscle cells are flattened and elongated in circular direction and attached to the basement membrane via hemidesmosomes. Several mitochondria positioned next to the basal circular myofilaments are typically found in this portion. The cytoplasm is of medium electron density in electron micrographs. The basal portion of these cells is connected to a goblet-shaped perikaryon via a slender elongated neck region (Fig. 7E, F). The perikaryon projects deeply into the

protocoelic cavity and contains vesicles of yolk. Furthermore, organelles such as rough ER and a golgi apparatus are present. The latter is located close to the basal structures of the single cilium that emerges from the soma. The longitudinal muscle cells on the contrary show only limited connection areas to the basement membrane and are located interspersed between the circular muscle cells (Fig. 7E). Some cells span the protocoelic cavity laterally and are connected to a basement membrane on both ends, whereas others protrude into the cavity with a goblet-shaped soma (Fig. 7F). The cytoplasm appears electron light and is primary filled with myofilaments running in longitudinal direction. Numerous mitochondria are commonly found accompanying the myofilaments. Other organelles such as the rER, nucleus or vesicles of yolk are restricted to the areas without myofilaments, namely the perikaryon or the basal portions.

Fine structure of the mesocoel and metacoel

As stated above, the mesocoelic and metacoelic cavities do not show further differentiations in their ultrastructure, compared to the early kink stage. Both are secondary body cavities lined completely by monociliated squamous epithelia (Fig. 7G). The cells rest on a basal lamina and the cytoplasm is filled with numerous yolk granules. Most of the cells are elongated in anterior to posterior direction, measuring between 8 µm and 16 µm in length.

1 gill slit stage

Gross morphology

The embryos of this stage are about 510 µm long. The dorsal epidermis of the collar region shows a longitudinal depression, the neural groove where the neurulation of the collar cord proceeds (Fig. 8A-H, 9A). For more details see also Kaul & Stach (2010, Figs. 4 and 5). The posterior part of the collar cord is already invaginated underneath the epidermis and forms a hollow tube, whereas the anterior part is still an open groove (see Kaul & Stach 2010, Fig. 5A-C). At this developmental stage the 1st pair of gill pores is present just behind the collar region. The pores open asynchronously, namely first on the left side (Fig. 8A, C, D). The trunk region posterior to the gill pores is kinked and elongated ventrally to an extend of 140 µm.

The endoderm comprises the digestive tract and is subdivided into three different regions. The developing stomochord measures about 80 µm in length and projects anteriorly into the protocoel (Fig. 8K, L, S3C, D). Its central lumen is continuous with that of the buccal cavity. The buccal cavity lies within the collar region and opens to the exterior through the mouth on the ventral side (Fig. 8K, L, 9A). The entire lumen of the digestive tract is enlarged and dilated from the time the 1st pair of gill pores opened. The buccal cavity continues into the pharynx region that is situated within the anterior trunk region, just behind the collar. Here, one pair of lateral outgrows are developed to form the 1st pair of gill pores. The endodermal tissue is directly connected to the epidermis and constitutes an opened circular-shaped

gill pore on the left side only. The corresponding right side is still closed (Fig. 8C, D). The pharynx region ends shortly behind the gills and continues into the intestine posteriorly. This area is discernible by an annular constriction (Fig. 8I-L, 9A). Pharynx and intestine are joined by the oesophagus, a short and small tubular connection that is running in the right half of the body in relation to the dorsal midline. The intestine is a somewhat sac-like structure and about 130 µm long. The prospective hindgut region can be distinguished by a shallow circular constriction about 60 µm from its posterior closed ending. There is no anus connecting the hindgut to the exterior.

The proboscis is occupied by the protocoel and is lined by a muscular epithelium composing the proboscis musculature (Fig. 9A). The pericardial coelom is suspended dorsally in the posteriormost region above the stomochord and measures about 32 µm in width and breadth (Fig. S3F). It is attached posteriodorsally to the epidermis and projects into the protocoel anteriorly together with the adjoining stomochord.

The paired mesocoel fills the collar region (Fig. 8A-D, M-P, 9A). The left and right mesocoela encircle the buccal cavity and are bordered anteriorly by the protocoel and posteriorly by the metacoel by means of vertical septa. Both coelomic cavities are separated in the dorsal and ventral midline by longitudinal mesenteries. The metacoel fills the trunk region completely. It is a paired structure as well and ensheaths the pharynx by surrounding the gill pores, the intestine, and the hindgut regions (Fig. 8A-D, M-P, 9A). All coelomic cavities at this stage are sac-like structures with no coelomopores present.

Fine structure of the endoderm

The entire digestive tract is composed of a pseudostratified, monociliated epithelium that is covered by numerous short and slender (2µm length, 60 nm diameter) microvilli at the apical cell surfaces (Fig. 9B and inset, S3D). Albeit the enormous enlargement of the lumen of the endoderm compared to the late kink stage, the endodermal cells are still comparably undifferentiated and no special cell types as e.g. glandular cells are found. However, the organization of the apical cell surface, predominantly the ciliation, differs in certain endodermal regions and will be described in more detail in the following.

Close to the mouth opening at the ventrolateral side few individual multiciliated cells are interspersed between the monociliated endodermal cells containing a very electron light cytoplasm compared with the neighbouring cells (Fig. S3E). These cells contain several basal complexes in accordance with the increased number of cilia. As mentioned above, the *anlage* of the stomochord is visible as a rod-like extension of the anterior epithelium lining the buccal cavity (Fig. S3C, D). It is completely surrounded by extracellular matrix and appears oval in cross section (Fig. S3A, B). The epithelial cells are equipped with one cilium and several microvilli at the apical cell surface. Furthermore, neighbouring cells are interconnected by adherence junctions. However, the cells comprising the *anlage* of the stomochord are not further differentiated.

In the posterior pharynx region the 1st pair of gill pores is developed (Fig. 8A, B, and 9A). The duct region leading to the gill pore opening is almost slit-like measuring 25 µm in lenght and 8 µm in breadth (Fig. 9C, S3C). The lining cells contain a conspicuously high number of centrioles within the cytoplasm of the cells (Fig. 9C, E and inset). Furthermore, numerous mitochondria are placed aside the centrioles within the cytoplasm. The increased number of centrioles together with associated basal structures is a clear indication for continued immense ciliogenesis in these cells as the cells will develop into heavily ciliated cells. The future substantial ciliation of the gill duct is needed for the maintenance of water.

The intestine region is composed of columnar and monociliated cells, whose microvilli differ from those present on the cells lining the buccal cavity and pharyngeal region. Here, the entire apical cell surface is enlarged to form 1.5 µm short, but 160 nm thick microvilli (Fig. 9D). The cilia are anchored to the cytoplasm by two striated rootlets. The cells contain the common set of organelles and several granules of yolk placed basally within the cells. Adjacent cells are interconnected by apical adherence junctions (Fig. 9D).

Fine structure of the protocoel

The cells that constitute the outer circular and inner longitudinal muscle layer show the same ultrastructural features as the myoepithelial cells described for the late kink stage. We could not detect any further differentiations or changes in the shape or arrangement of the cells and will therefore focus on the changes occurring in the development of the proboscis pore and the podocytes. On the left side of the posteriormost region a short tubular outgrowth of the protocoel, the prospective proboscis pore duct, is visible. The duct is not connected to the exterior yet, and the cells lining this duct are comparably undifferentiated. In contrast to the myoepithelial cells forming the proboscis musculature, the cells lining the duct do not contain substantial bundles of myofilaments (Fig. S3G).

The protocoelic cells lining the pericardial sac from the protocoelic side rest on a basement membrane which covers a prominent blood vessel situated between basement membranes (Fig. S3F, H). There, the protocoelic cells have developed into podocytes, while still containing numerous yolk granules. The apical surfaces of the podocyte cells bear a single cilium anchored to the cell by a basal body and one striated rootlet fibre. The pedicels of neighbouring podocytes form fenestrations between them (Fig. S3H). Bundles of myofilaments can be found in the basal portions of the podocytes as well as in larger pedicels. The myofilaments are exclusively arranged in transverse direction and therefore correspond to the findings in the late kink stage.

Fine structure of the mesocoel and metacoel

Both, mesocoel as well as metacoel are exclusively lined by a squamous and monociliated epithelium (Fig. 9F, G). The cells are interconnected by adherence junctions and rest on a basal lamina (Fig. 9H). The area containing the nucleus usually bulges into the coelomic cavity. Furthermore, the cells taper laterally and send flattened elongations to their neigh-

bouring cells. Myofilaments can be found within the basal portion of the epithelial lining cells (Fig. 9H inset) and are more distinct in areas where a blood vessel is present within the *ecm* these cells rest on. Obviously, the myofilaments are supposed to perform contractile function for maintaining blood flow.

2 gill slit stage

Gross morphology

These juveniles are freely crawling over the substratum and their overall appearance resembles those of the adults in many aspects, except for the reduced number of gill pores and the post-anal tail (Fig. 10A-D, 11A, B, 12A). The small acorn worm is about 800 µm long. The body is separated into a proboscis measuring 330 µm in length that is followed by two epidermal rings demarcating the collar region connecting to a wormlike trunk. The proboscis is connected to the collar region by a narrow, dorsal stalk. At the anterior trunk region two pairs of gill pores are visible dorsolaterally (Fig. 11A, B). A post-anal tail, 180 µm short, is developed ventrally at the posterior end of the trunk (Fig. 10C, D). This post-anal tail is a unique character of the juvenile stage of harrimaniid enteropneusts and will be reduced later during development. It is a creeping organ without detailed morphological similarities to the chordate tail (see also Stach & Kaul 2011). The condensed portions of the nervous system, a dorsal and a ventral cord, are developed as two basiepidermal, longitudinal neurite bundles (Fig. 10E-H, 11D, F). A ubiquitous nerve net is present basiepidermally, but not shown in the 3D-reconstructions (for details see Kaul & Stach 2010). The anterior part of the dorsal neurite bundle is broadened to form the so-called proboscis stem at the base of the proboscis (Fig. 11B, H). The dorsal cord runs in the dorsal midline all the way posterior terminating just prior to the anus opening at the trunk region (Fig. 11D). The dorsal cord is internalized within the collar region to form the collar cord. The ventral cord runs longitudinally at the ventral midline within the trunk region, it is not extending into the post-anal tail and also absent from the collar region (Fig. 10G, H). The ventral cord is more extensive compared to the dorsal cord and accompanies the substantial ventral trunk musculature that is formed by the myoepithelial lining cells of the paired metacoela (Fig. 11F).

The proboscis is occupied by the protocoel that is almost completely filled by circular and longitudinal muscle strands (Fig. 10M-P, 11H, 12A, 13B). The protocoel is connected to the exterior by a small proboscis pore, which is located posterodorsal on the left side at the base of the proboscis (Fig. 11E, H). This coelomopore is part of the metanephridial excretory system together with the heart-kidney complex that is suspended medially in the posteriormost region of the protocoel (Fig. 10M-P, 11C, H, 12A). The heart-kidney is composed of the pericardium, the supportive stomochord and the glomerulus that spans the anterior tip of the pericardium and stomochord (Fig. 11C). The pericardium forms a tubular sac measuring 60 µm in length and 15 µm in breadth. It is placed dorsally above the stomochord and encloses a dilated blood space, the heart sinus, which is located within the *ecm* between

the pericardium and stomochord (Fig. 11H, 13E). The heart sinus bifurcates anteriorly into two anteriolateral vessels connecting to the glomerulus (Fig. 11F). The glomerulus extends posteriorly to cover the lateral and ventral areas of the stomochord as well. It is about 30 µm long and 35 µm wide and corresponds to the filtrational part of the excretory system.
The stomochord is a rod-like protrusion emerging from the roof of the buccal cavity (Fig. 10I-L, 11C), and its vacuolated cells surround a central lumen and their function is supporting the heart-glomerulus complex. Within the proboscis stalk, the stomochord is reinforced ventrally by the proboscis skeleton. The y-shaped skeleton bifurcates posteriorly when entering the collar by sending one curved branch to each side of the buccal cavity (Fig. 10E-L). Further skeletal elements are developed in terms of rods of the gill bars within the pharyngeal region (Fig. 10G, H, K, L). The skeletal rods are crescent-shaped and taper at both ends, where they are continuous with the *ecm* of the pharynx. Three skeletal rods are discernable at this stage of development, two on the left side whereas only one is found on the right side (Fig. 11E). This uneven number of gill bars further documents the asymmetric development of the gill pores already observed in earlier stages. Furthermore, the two gill pores on the right side are not separated yet by means of a mesodermal gill bar which will then develop later together with the skeletal rod (Fig. 11A, B). In fact, the gills are developed as simple tubular ducts with no further subdivision. The pharyngeal region containing the gill pores is about 180 µm long and enlarges anteriorly into the buccal cavity where the anteroventral mouth is located (Fig. 12A). The pharynx is connected posteriorly to the intestine by means of a 70 µm short and right-curved oesophagus (Fig. 10I, J, 11E). The oesophagus is barely 20 µm in diameter, but opens into the considerably wider lumen of the intestine. The intestine is 190 µm long and kinked ventrally at the transition to the hindgut. This transition can be recognized by a shallow circular constriction (Fig. 10I-L, 11D, F). The hindgut region ends after 100 µm and terminates into an anus opening dorsally in respect to the post-anal tail.

The paired mesocoelic cavities occupy the collar region (Fig. 10M-P, 11A, B). Furthermore, two elongations projecting anteriorly flank the stomochord laterally about 60 µm into the protocoel (Fig. 11C). These elongations are filled with longitudinal muscle strands (Fig. 12A), which obviously support the thin proboscis stalk and move the entire proboscis. The remaining coelomic cavity is fluid-filled and lined by flattened epithelial cells. Left and right coeloms are separated bilaterally by a mesentery by which the collar cord is surrounded as well (11G, see also Kaul & Stach 2010 Fig. 6C, G, and H). At the posterior end of the collar region the coelomic cavities are blindly closed and bordered by the posteriorly metacoela by means of vertical septa. There is no coelomoduct or coelomopore developed yet, as described for the adult acorn worm (Benito & Pardos 1997). The paired metacoela surround the pharyngeal region, intestine and hindgut completely and continue ventrally with sac-like elongations into the post-anal tail (Fig. 10M-P, 11D, F). The metacoela are pierced by the pharyngeal tissue that forms the gill pores at the anterior region of the trunk

(Fig. 11A, B). The metacoelic cavities are lined by two different types of cells. The dorsal and dorsolateral portions are occupied by flattened epithelial cells, whereas the ventral and ventrolateral areas are lined by the aforementioned substantial longitudinal muscle strands (Fig. 11 F). Left and right metacoela are separated by mesenteries that keep the digestive tract in place.

Fine structure of the endoderm

The anterior pharynx region, the buccal cavity is constituted of different epithelial cell types. The lateral and ventral portions are lined almost exclusively by highly vacuolated cells (Fig. 12C). The single, clear and large vacuole may be of hydrostatic function to stabilize the shape of the mouth cavity. The nucleus is either displaced to the very basal part within the cytoplasm or it is delaminated together with the remaining organelles to the apical cytoplasm, because of the voluminous vacuole. Furthermore, the cells are equipped with one cilium and numerous microvilli at the apical cell surface. The roof of the buccal cavity in contrast, is lined by epithelial cells whose cytoplasm is electron dark is densely packed (Fig. 12B). No vacuoles are present in these cells. These non-specialized cells are accompanied by mucous gland cells. The gland cells are filled with electron-lucent secretory product packed in cisternae. Some neurites are present between the basal parts of the cells (Fig. 12B).

The stomochord is lined by a monolayered epithelium, which is highly columnar and composed of vacuolated cells (Fig. 12D). The cells are interconnected by adherence junctions and have slender microvilli and a single cilium, protruding into the medial lumen. The single, large, membrane-bound vacuole is filled with flocculent precipitate and occupies most of the cytoplasm. The nucleus and other cell organelles are confined to the remaining peripheral cytoplasm.

The proximal region of the duct of the gills is composed of columnar cells which are extremely densely ciliated (Fig. 12 E and inset). Each cell bears numerous cilia at its apical cell surface of which each is anchored by one vertical rootlet into the cytoplasm (Fig. 12 E inset). Several mitochondria are always placed close to the basal structures of the cilia. The cell surface is furthermore covered evenly by 1.3 µm short and 45 nm slender microvilli. In contrast, the distal duct region is built up by mostly monociliated cells. Nevertheless, the cell surface is covered by microvilli as well. Following the duct more and more to the exterior, the cells are connected to supporting epidermal cells and different glandular cells (Fig. 12 E).

The lumen of the intestine is voluminous and lined by a single layer of epithelial cells (Fig. 12F). The shape of the cells ranges from more or less cuboid to columnar, measuring about 17 µm in height. The cells are interconnected by apical adherence junctions and anchored basally to a basement membrane. A single cilium is always developed, although cells bearing several cilia are present as well. The nucleus is usually placed basally within the cytoplasm.

Furthermore, the cytoplasm contains a high number of mitochondria and lysosomes. Microvilli are covering the apical cell surface evenly.

In addition, another type of intestinal cells can be distinguished, as the cytoplasm contains distended amounts of rough endoplasmatic reticulum, filling almost the entire cell (Fig. 12H). Additionally, several electron dark granules, which resemble zymogen granules typically found in pancreatic exocrine cells in vertebrates, are present in some of these cells (Fig. 12G). This type of cell is found predominantly in the anterior portion of the intestine close to the opening of the oesophagus.

Fine structure of the protocoel

The major part of the protocoelic lining cells is differentiated into myoepithelial cells that build up the proboscis musculature (Fig. 11H, 13B). Cells with circularly arranged myofilaments and cells containing longitudinal myofilaments are present (Fig. 13B). Longitudinal muscle cells invade and span the coelomic space to attach to the basement membrane of the opposite wall. The circular muscle cells in contrast, form an outer layer of muscles. The majority of the cytoplasm of the cells is filled with myofilaments.

The duct of the proboscis pore is constituted of a proximal and a distal duct region, lined by different cell types, respectively. The proximal duct is composed of monociliated columnar to cuboid cells, which are interconnected by apical junctions (Fig. 13A). Seemingly no microvilli are developed at the surface and the nucleus is positioned centrally. The basal portion of these cells contains a considerable amount of myofilaments which are arranged circularly surrounding the duct. Therefore, the proximal duct region is equipped to function as a sphincter (Fig. 13A). The transition to the cells forming the distal duct region is quite distinctive as these cells posses numerous microvilli (Fig. 13F). Moreover, the cells are monociliated and the shape is more or less cuboid or flattened. The nucleus is placed basally and there are no myofilaments present in the cells lining the distal duct region. At the very distal end of the duct the cells are connected to common supportive epidermal cells, which are usually equipped with several cilia at the cell surface. Because myofilaments are restricted to the proximal duct region it it likely that this part of the duct is derived from the coelothelium of the protocoel. In contrast, the distal region of the duct is composed of cells without myofilaments but equipped with microvilli and probably derived from the ectoderm.

The fine structure of the heart-glomerulus complex has been described in detail in Kaul & Stach 2011 and is only summarized here. The pericardial cell which line the heart sinus are monociliated epithelial cells containing thick and thin myofilaments in their basal portions (Fig. 13E). These bundles of myofilaments show repetitive striation in longitudinal sections (see Kaul-Strehlow & Stach Fig. 6b). The glomerulus comprises a highly folded and dilated blood space within the matrix and is lined by podocytes at the protocoelic side. Each monociliated podocyte gives rise to numerous pedicels (Fig. 13C). The pedicels may

contain myofilaments and furthermore form fenestrations between them ranging from 50 nm to 150 nm.

Fine structure of the mesocoel

The mesocoelic lining is composed of a monolayered and monociliated myoepithelium. The somatic cell layer, namely the somatopleura is constituted of cells possessing a somewhat irregular shape (Fig. 13G). The cells may be up to 8 µm in height and bulge into the coelomic cavity. The cytoplasm appears to be empty except for the nucleus, several mitochondria and myofilaments, which may be positioned either basally or apically within the cytoplasm. However, all myofilaments within the somatic cell layer are orientated longitudinally (Fig. 13G). The visceral cell layer, the visceropleura, in contrast, is composed of an extremely flattened myoepithelium, measuring barely 0.6 µm in height (Fig. 13G inset). In these cells, the myofilaments are exclusively arranged in circular direction.

Fine structure of the metacoel

The cells lining the metacoelic cavity are similarly differentiated, forming a monolayered myoepithelium. On the ventral side, the somatic metacoelic lining forms the substantial longitudinal musculature (Fig. 13H). The cells are comparably large containing enormous bundles of myofilaments within the basal part of the cells. The myofilaments are connected to the basement membrane via numerous adhesion plaques (Fig. 13H inset). The apical part of the cells is bulb-shaped and protrudes into the coelomic cavity containing the nucleus. Neighbouring cells are interconnected by apical adherence junctions. The visceropleura in the metacoel is also developed as an extremely flattened epithelium (Fig. 13D). Only the area containing the nucleus is bulging into the coelomic cavity. Close to the nucleus a cilium is present (Fig. 13D).

Discussion

Coelom formation

Traditionally, the origin of the third germ layer, the mesoderm in its specific form as a coelomic cavity has been given high significance for phylogenetic considerations of metazoan relationships (Lüter 2000, Nielsen 2001, Kaul-Strehlow & Stach 2011). In principle, two main modes of coelom formation can be distinguished in the two major groups of bilaterian animals: schizocoely in protostomes and enterocoely in deuterostomes (Technau & Scholz 2003). A precise definition of both terms was given by Lüter (2000) and will be applied in this discussion. Following Lüter's definition, schizocoely is characterized by the development of coelomic cavities and coelomic epithelium from a solid mass of mesodermal cells that is not derived from the endoderm or archenteron. In contrast, if coelomic cavities and epithelia originate from the endoderm, then coelom formation is called enterocoely. Not that the mesodermal tissue does not have to pinch off as pouches from the endoderm, instead a central lumen can be acquired secondarily (Lüter 2000).

In the present study we investigated the origin of the mesoderm, particularly the formation of the paired mesocoela and metacoela, in the direct-developing enteropneust *Saccoglossus kowalevskii*. Our data show that all of the five main coelomic cavities (single protocoel, paired mesocoela and metacoela) derive as separate outpocketings from the endoderm via enterocoely. The anterior, single protocoel is separated by a basement membrane from the archenteron as the ontogenetic first coelomic cavity. Later on, the paired mesocoela and metacoela pinch off from the lateral endodermal wall in the middle and posterior body regions, respectively. The lumen within the paired coelomic outpocketings and within the connection to the archenteron is reduced to a very narrow slit during the entire formation process and not visible under the light microscope. However, the continuity between the epithelia of the mesodermal outpocketings and the endoderm could be traced accurately by the resolution of the electron microscope. Furthermore, the mesodermal pouches are not developed as voluminous outpocketings projecting into the blastocoel as described in some echinoderm larvae (Hyman 1959), because the embryonic blastocoel is reduced almost completely in direct-developing enteropneusts.

In the literature, about five different types of coelom formation in enteropneusts have been suggested and can be found in various text books (e.g. Nielsen 2001, van der Horst 1939, Westheide & Rieger 2007) and are shown in Fig. 14a-e. These five types of coelom formation have been transferred into schematic drawings by Korschelt & Heider (1936) and have since been adopted with minor changes. By compiling and schematising the various types some inaccuracies occurred seemingly leading to partial misinterpretations.

Type I

The origin of the mesocoela and metacoela from separated outpocketings of the endodermal wall as documented in this study confirms the early observations of Bateson (1884, 1885)

who first studied and described coelom formation in an enteropneust, *S. kowalevskii* (Fig. 14a). Nevertheless, Bateson's described mode of coelom formation for enteropneusts was doubted by Spengel (1893) and Morgan (1894), and was eventually challenged by a competing documentation proposed by Davis (1908).

Type II

Davis concluded, his observations made on another direct-developer, *Saccoglossus pusillus*, would substantially coincide with those made by Bateson, the only essential difference being that Bateson drew a definite line separating the anterior from the middle body cavity (Davis 1908, p. 212). Davis (1908) believed that Bateson must have failed to notice the connection between the anterior and other body cavities. According to Davis, the mesocoela and metacoela form by posterior growth and subsequent separation of the protocoel (Fig. 14b). The definite course of this certain line, the extracellular matrix could be determined in the current study, thus confirming Bateson's observations on coelom formation in enteropneusts (Fig. 14a).

Type III

Another scheme displays coelom formation of the mesocoela and metacoela from separated, paired but *solid* masses of cells emerging at the enodermal wall (Fig. 14c). However, by reviewing the original literature by Morgan (1891) reporting his study of a tornaria from New England, this author states to the contrary: "In origin the third body cavities (metacoela) are undoubtedly to be regarded as gut pouches or enterocoels,...(p. 414)". Concerning the formation of the mesocoela Morgan is uncertain, since the mesocoela do not clearly arise as pouches from the endoderm but Morgan could also not exclude such a formation (Morgan 1891, p. 413). Probably, Morgan's use of the term *solid* brought some confusion into this discussion, because at the time this term was also used for closely adjoining layers of epithelia (Stiasny 1914), whereas nowadays *solid* is applied exclusively to describe compact masses of cells (Bartolomaeus 1993). See also: "Es bilden sich zwei solide Epithelplatten als Verlängerung der Epithelien des Enddarms,..." (Stiasny 1914, p.68). Today we differentiate between *solid* masses of cells, which are composed of mesenchymatic cells and epithelia which are composed of epithelial cells (Bartolomaeus 1993).

Type IV

In further studies on the tornaria of *Balanoglossus clavigerus* Bourne (1889), Spengel (1893), and Stiasny (1914) describe coelom formation of the mesocoela and metacoela from a single *anlage* on each side that later subdivides (Fig. 14d). By critical reviewing the original literature it becomes clear that actually only the origin of the mesocoela could be traced convincingly by the authors, whereas the origin of the metacoela remained either completely unknown (Rao 1953, Stiasny 1914) or was described rather vague (Bourne 1889, Spengel 1893). Concerning a common origin of the mesocoela and metacoela, Spengel wrote (1893, p. 430): „Allerdings wäre es noch möglich, dass aus den beschriebenen Anlagen nicht die

beiden Cölompaare hervorgingen, sondern nur die hintern, die Rumpfcölome, und das Morgan für die vordern vielleicht doch recht hätte."

Type V

Another type of coelom formation (Fig. 14e) was observed in tentaculated tornaria larvae of an unknown ptychoderid species by Spengel (1893) and Morgan (1894). These observations are the origin of schemes where multiple, mesenchymatic clusters of cells accumulating in the blastocoel give rise to the mesocoela and metacoela. Spengel, however, did not feel confident about the origin of the coelomic cavities, because the stages he observed were already too far developed. Even though, he noticed that the placement of the clusters of cells so distantly away from the endodermal gut was peculiar and may have reflected an artefact caused during fixation (Spengel 1893, p. 433). Even more interesting is Morgan's statement of caution before he describes coelom formation at all: „It is by no means an easy matter to determine with accuracy the origin of an embryonic organ, and in the present case, owing to the comparatively small number of embryos at the critical period, I have had no little difficulty in getting positive evidence on the point." (Morgan 1894, p. 31). A mesenchymatic origin of the mesocoela and metacoela and moreover the origin of the mesenchymatic cells themselves in enteropneusts is currently not convincingly documented and re-examination using modern electron microscopy is warranted. Since all previous mentioned types of coelom formation in enteropneusts at least assume an origin from the endodermal tissue, and furthermore enterocoely is a characteristic mode of coelom formation for other deuterostomes as well (Nielsen 2001, Technau & Scholz 2003), a possibly mesenchymatic or non-endodermal origin, if demonstrated one day, is likely to be regarded as a derived condition for ptychoderid enteropneusts.

After critical reviewing of the original literature and by providing new data from this study we would like to summarize the previous discussion as follows (Tab. 1). Type I and II described for direct-developing enteropneusts were actually competing descriptions by which type I (Fig. 14a) could be demonstrated to be essentially correct on the ultrastructural level (Fig. 14b). Ergo, the mesocoela and metacoela develop as separated, epithelial outpocketings from the middle and posterior gut regions (Fig. 14f). Types III, IV, V have been described to occur in enteropneusts that develop through a tornaria larva. A review of the original literature could show that the illustration of type III (Fig. 14c) is a misinterpretation thereof, as Morgan (1891) emphasized the origin of the mesocoela and metacoela from endodermal outpocketings or enterocoels rather than from *solid* masses of cells as reported and displayed in diverse text books. The presumed common origin of the mesocoela and metacoela as stated for type IV (Fig. 14d) has neither been documented convincingly by Bourne (1889), Spengel (1893), Stiasny (1914) nor Rao (1953) as the authors admit in their own papers. With more certainty though, the authors observed the origin of the mesocoela as outpocketings from the endodermal wall that in turn corresponds exactly to the conclusions Morgan has already made (1891).

At this point we would like to conclude that regarding coelom formation observed in tornaria larvae, the development as separated enterocoela from the middle and posterior gut regions (Fig. 14g) is reasonably precisely and convincingly documented and coincides with our findings. Type V (Fig. 14e) should be re-examined with modern techniques as the origin of the mesenchymatic cells has not been documented.

The majority of enteropneust species belong to one of the three main families (Harrimaniidae, Spengelidae and Ptychoderidae), although relationships among enteropneusts are controversially debated (Cameron 2005, Cannon 2009). The previously compiled results dealt with enteropneusts covering all of the three major families (*S. kowalevskii* und *S. pusillus*: Harriminiidae, *Glandiceps* sp.: Spengelidae and *Balanoglossus* spp.: Ptychoderidae), and if type I (Fig. 14f, g) of coelom formation is also present in other deuterostomes, then it is likely that type I constitutes the ancestral mode of coelom formation for enteropneusts. As a consequence, type V should be regarded as a derived condition within enteropneusts. However, types II, III, IV and V of coelom formation have to be re-investigated by using modern morphological techniques in order to falsify or validate those modes with certainty.

Coelom formation in other deuterostomes

Unfortunately, the situation in pterobranchs is barely investigated. The only ultrastructural work of Lester (1988) shows the elongated larva of *Rhabdopleura normani* with isolated and paired strands of mesocoela and metacoela on both sides of the endoderm. Lester could not document the origin of the mesoderm though, the described condition in *R. normani* resembles the early kink stage in *S. kowalevskii* (this study) and a similar origin of the mesocoela and metacoela is not unlikely. The development of the genus *Cephalodiscus* is still unknown.

Some of the oldest and most extensive studies on the development of deuterostomes are present from members of the Echinodermata (Gemmill 1912, 1914, Hörstadius 1973, MacBride 1896, 1903, von Ubisch 1913). In many echinoids and asteroids it has been reported that a single, voluminous sac pinches off from the anterior end of the endoderm or archenteron, which then gives off paired axo-, hydro- and somatocoel (pro-, meso- and metacoel in enteropneusts) on each side (for reviews see Hyman 1955, Nielsen 2001). This echinoid-type is often regarded as typical for deuterostomes, although studies show differences between groups. For instance, in crinoids, coelom formation is described from separated pockets that derive from the anterior, middle and posterior endodermal regions (Nielsen 2001, Holland 1991). Given the difference, that right axocoel and hydrocoel are reduced in crinoids, this description shows similarities to the enteropneust-type of coelom formation (cf. Fig 14f, g and Nielsen 2001, Fig. 43.2). However, a putative ancestral type of coelom formation in echinoderms remains ambiguous at present, although similarities between coelom formation in enteropneusts and crinoids may be inherited from the last common ancestor of echinoderms and enteropneusts.

During the development of amphioxus, multiple pairs of coelomic sacs are formed successively from the endoderm by enterocoely (Conklin 1932, Stach 2000). The fate of the coelomic sacs, especial the anterior ones, is much more complex than in early deuterostomes yet the early larva of amphioxus passes trough a stage (or one may even say that amphioxus recapitulates a stage) where only three coelomic sacs are developed, thus highly resembling the condition found in enteropneusts (see Stach 2002, Fig. 3).

Conclusion

A constitutive feature uniting deuterostomes is the formation of coelomic cavities from the endoderm by enterocoely (Ax 2001, Hyman 1951, Nielsen 2001). The body is tripartite and thus subdivided into three body regions each with its own coelom: protocoel, mesocoel and metacoel. Regarding the precise mode of coelom formation, the aforementioned echinoid-type is emphasized as ancestral for deuterostomes. One of the reasons for this may be the lack of information concerning coelom formation in enteropneusts. The previous discussion could show, however, that coelom formation from separated pockets from different regions of the endoderm occurs in enteropneusts. Furthermore, this condition is recapitulated in the larva of amphioxus and can be observed in crinoids in a similar way. This leads us to conclude that coelom formation from separated pockets (enteropneust-type, Fig. 14f, g), rather than from a single anterior pocket (echinoid-type) is likely to represent the ancestral type of coelom formation in Deuterostomia.

*Left-right asymmetries in **Saccoglossus***

All members of the Chordata are characterized by a number of specific features, whereby *left-right (LR) asymmetries* might be regarded as a more subtle one (Boorman & Shimeld 2002, Gerhart el al. 2005, Nielsen 2001). In mammals visceral organs as liver or stomach are developed asymmetrically and the heart is generally placed to the left body half (Brown & Wolpert 1990, Levin 2005, Palmer 2004, Patten 1922). In adult ascidians and members of the larvaceans in the taxon Tunicata the digestive tract is folded asymmetrically (Burighel & Cloney 1997). Furthermore, a part of the course of the gut in adult amphioxus is asymmetric as well. Here, the transition between branchial sac and midgut is shifted to the left-handed side due to the position of the hepatic caecum (Conklin 1932, Hatschek 1881, Ruppert 1997). Nevertheless, the possibly most conspicuous *LR asymmetries* are present in the larva of amphioxus during development. First mentionable is the mouth opening that penetrates the left larval side while the first row of gill slits successively arises along the ventral midline (Hatschek 1881, Ruppert 1997, Willey 1891, for review see Jefferies 1986, Jefferies et al. 1996). These gill slits phylogenetically correspond to the left gill slits of tunicates and vertebrates (Conklin 1932, Willey 1894, Jefferies et al. 1996) and eventually shift to the left body half whereas the right row of gill slits develop later on during metamorphosis.

In the present study we observed different *LR asymmetries* in *S. kowalevskii*, for instance the proboscis pore that connects the protocoel to the exterior on the left side. A correspond-

ing structure in echinoderms is present in form of the axohydrocoel that opens externally through the madreporic porus (Hyman 1955, Nielsen 2001). Specific similarities between these pori as part of the excretory complex (axial complex in echinoderms and pericard-glomerulus complex in hemichordates) have been intensely studied (Nielsen 2001, Ruppert & Balser 1986, Stach 2002) and homology of both complexes is generally accepted. However the homology of the protocoel and porus of echinoderms and hemichordates to chordates is less clear. Based on the anterior position, homology with Hatschek's left diverticulum or Hatschek's pit is traditionally suggested (Goodrich 1917, Franz 1927, Nielsen 2001), whereas according to similarities in structure, ontogenetic position, and excretory function, homology with Hatschek's nephridium is emphasized by Stach (2002).

Besides the asymmetric proboscis pore in *S. kowalevskii* that has been known for a long time (Bateson 1884, Spengel 1893), the present work demonstrates the left-dominated development of gill slits in enteropneusts. Our data show that the 1st gill slit opens on the left side, while the corresponding right slit lacks behind. Moreover, during the following juvenile stage the asymmetric development is clearly visible by an unequal number of skeletal rods on each side, two on the left, just one developed on the right. In adult enteropneusts, including *S. kowalevskii*, the gill slits are consistently developed bilaterially symmetric (Benito & Pardos 1997, Cameron 2000, Hyman 1959, van der Horst 1939), thus, the observed asymmetry is only present during development. Although comprehensive studies on the development of enteropneusts are available in the literature (Bateson 1884, Burdon-Jones 1952, Colwin & Colwin 1953, Morgan 1891, 1894, Spengel 1893, Davis 1908, Stiasny 1914) an asymmetric development of gill slits in enteropneusts has not been documented before. This may be due to technical limitations before the invention and availability of electron microscopes and computer-aided 3D-reconstructing techniques. In fact the thickness of classical histological section ranges from 5 µm to 10 µm, far too coarse to determine diminutive structures as the incipient gill slits in enteropneusts. Nowadays, advanced morphological methods allow increasing precision significantly. Additionally, by using resin as embedding medium a practically undeformed sectioning and reconstruction of the animal is possible and subtle asymmetries such as the development of gill slits can be traced accurately. Perhaps, because evo-devo studies usually operate likewise on a low light microscopic level, gill slit development on the base of gene expression studies has been described symmetrically (Lowe et al. 2003, Ogasawara 1999, Gillis 2011).

Our data show, that particularly developmental *LR asymmetries* can be found not only within chordates but also occur in enteropneusts. Our knowledge of the development of close related pterobranchs is still incomplete and most of it relies upon interpretations drawn from limited number of ontogenetic stages (Nielsen 2001). However, a quite informative work on the development can be found in Dilly's (1973) paper on *Rhabdopleura*, although this genus does not develop gill pores. A more promising comparison could be obtained by studying *Cephalodiscus*, but the development of *Cephalodiscus* is unfortunately completely unknown

(Nielsen 2001). On the other hand, asymmetric structures, namely the oral lamella, position of the gonopore, and the gonads in adult pterobranchs which were described by Schepotieff (1907) have recently been doubted by Sato & Holland (2008) and remain controversial.

In members of the Echinodermata that also belong to the Deuterostomia, we find almost the entire adult body organized asymmetrically in favour of the left side (Gemmill 1914, Hörstadius 1973, MacBride 1903, for review see Hyman 1955). The bilaterially organized larva enters an asymmetric stage early during development by forming the rudiment of the juvenile at the left side of the larva (Morgan 1891, von Ubisch 1913). From this fact we can conclude that left-dominated asymmetries described for chordates are present in enteropneusts and echinoderms as well.

Whereas asymmetries in echinoderms and vertebrates have plausible functional or evolutionary explanations, there is currently no such explanation accepted for the bizarre asymmetries of cephalochordate larvae (Ruppert 1997). The phylogenetic relationships of deuterostome phyla is still controversially debated, although the majority of phylogenetic analyses that include molecular data suggest that the sister group of the Chordata may be the Ambulacraria, a group consisting of Echinodermata and Hemichordata (Bourlat et al. 2006, Cameron 2005, Cannon et al. 2009, Castresana et al. 1998, Zrzavy et al. 1998). An alternative phylogenetic hypothesis particularly considering *LR asymmetries* in deuterostome taxa has been emphasized by Jefferies' (1968) theory of the calcichordates. Jefferies assumes that the Echinodermata represent the sister group to Chordata, together comprising the Dexiotheca. This group derived from a pterobranch-like ancestor that laid down on the right body half on the substratum. By reducing the right body side appropriately, animals with a left-dominated side evolved and are present in recent echinoderms. During evolution that has led to the chordate lineage, these asymmetries have gradually been transformed back into bilateral symmetries resulting in modern chordates. According to Jefferies (1968, 1986), evidence supporting his theory can be found in different calcichordate fossils. Therefore, the conspicuous *LR asymmetries* present during the development of the larva of amphioxus can be explained as Haeckelian recapitulations (Jefferies et al. 1996). However, the developmental *LR asymmetries* found in an enteropneust hemichordate, a non-Dexiotheca (sensu Jefferies), can not be declared by the calcichordate-theory.

Other authors (Jollie 1982, Nielsen 2001, Peterson 1995, Smith 2008) reject the calcichordate-theory, because they interpret the so-called calcichordate fossils as members of the echinoderm stem-group. Maybe the most important problem with this theory is that most of the fossils that supposedly represent stem groups of the chordate lineage are from Ordovician, whereas earliest vertebrate fossils are known already from Early Cambrian (Shu et al. 1999). Following Smith (2008), early members of the echinoderm stem-group (stylophoran and solutes) might have possessed gill slits, although drawing inferences from fossils alone should be treated with certain caution. Smith, who does not know about developmental asymmetries in enteropneust hemichordates, assumes such *LR asymmetries*

as evolutionary novelties of the last common ancestor of the Pan-Echinodermata (Smith 2008). The previous discussion however, showed that left-dominated asymmetries during development occur in hemichordates as well and thus are present in all major deuterostome groups, Echinodermata, Hemichordata and Chordata. Moreover, the similarities in left-dominated development of the gill slits in *S. kowalevskii* and amphioxus lead us to suggest a closer relationship of hemichordates and chordates. Regardless of whether a grouping of Ambulacraria or Pharyngotremata (Hemichordata + Chordata, sensu Schaeffer 1987) is taken as a basis, is seems likely that at least to some extent *LR-asymmetries* have been present in the last common ancestor of Deuterostomia.

References

Ax P (2001) Das System der Metazoa III. Ein Lehrbuch der phylogenetischen Systematik. Spektrum Akademischer Verlag, Heidelberg.

Anderson K (1907) Die Pterobranchier der schwedischen Südpolar-Expedition 1901-1903. Wiss Ergeb schwed Südpolarexpedition 5:1-122.

Bartolomaeus T (1993) Die Leibeshöhlenverhältnisse und Verwandtschaftsbeziehungen der Spiralia. Fachbereich Biologie. Georg-August-Universität Göttingen, Göttingen, pp 301.

Bartolomaeus T, Quast B, Koch M (2009) Nephridial development and body cavity formation in *Artemia salina* (Crustacea: Branchiopoda): no evidence for any transitory coelom. Zoomorphology 128: 247-262.

Bateson W (1884) The early stages of the development of *Balanoglossus* (sp. incert.). Q J Microsc Sci, NS 24: 208-236, pls 18-21.

Bateson W (1885) The later stages in the development of *Balanoglossus kowalevskii,* with a suggestion on the affinities of the Enteropneusta. Q J Microsc Sci 25: 81-128.

Benito J, Pardos F (1997) Hemichordata. In: Harrison FW, Ruppert EE (eds) Microscopic anatomy of invertebrates, vol 15. Wiley-Liss, New York, Chichester, Weinheim, Brisbane, Singapore, Toronto, pp 15-101.

Boorman CJ, Shimeld SM (2002) The evolution of left-right asymmetries in chordates. BioEssays 24: 1004-1011.

Bourlat SJ, Juliusdottir T, Lowe CJ, Freeman R, Aronowicz J, Kirschner M, Lander ES, Thorndyke M, Nakano H, Kohn AB, Heyland A, Moroz LL, Copley RR and Telford MJ (2006) Deuterostome phylogeny reveals monophyletic chordates and the new phylum Xenoturbellida. Nature, 444: 85–88.

Bourne GC (1889) On a Tornaria found in British seas. Journ Mar Biol Assoc (2), 1: 63-68, pls 7-8.

Burighel P, Cloney RA (1997) Urochordata: Ascidiacea. In: Harrison FW, Ruppert EE (eds) Microscopic anatomy of invertebrates, vol 15. Wiley-Liss, New York, Chichester, Weinheim, Brisbane, Singapore, Toronto, pp 221-347.

Brown NA, Wollpert L (1990) The development of handedness in left/right asymmetry. Development 109: 1-9.

Brusca RC, and Brusca G J (1990) Invertebrates. Sinauer Associates, Sunderland, MA.

Burdon-Jones C (1952) Development and biology of the larva of *Saccoglossus horsti* (Enteropneusta). Phil Trans R Soc B 236: 553-590.

Cameron CB (2005) A phylogeny of the hemichordates based on morphological characters. Canadian Journal of Zoology 83:196-215

Cameron CB, Garey JR, Swalla BJ (2000) Evolution of the chordate body plan: new insights from phylogenetic analyses of deuterostome phyla. Proc Natl Acad Sci USA 97: 4469-4474.

Cannon JT, Rychel AL, Eccleston H, Halanych KM (2009) Molecular phylogeny of hemichordata, with updated status of deep-sea enteropneusts. Mol Phylogenet Evol 52: 17-24.

Castresana J, Feldmaier-Fuchs G, Yokobori S, Satoh N, Paabo S (1998) The mitochondrial genome of the hemichordate *Balanoglossus carnosus* and the evolution of deuterostome mitochondria. Genetics 150: 1115–1123.

Colwin Al, Colwin LH (1953) The normal embryology of *Saccoglossus kowalevskii*. J Morphol 92: 401-453.

Conklin EG (1932) The embryology of *Amphioxus*. J Morphol 54: 69-118.

Darwin C (1859) On the Origin of Species by Means of Natural Selection. John Murray, London.

Davis BM (1908) The early life history of *Dolichoglossus pusillus* Ritter. Univ Calf Publs Zool 4: 187-226, pls 4-8.

Dilly PN (1973) The larva of *Rhabdopleura compacta* (Hemichordata). Mar Biol 18: 69-86.

Dohle W (2004) Die Verwandtschaftsbeziehungen der Großgruppen der Deuterostomier: Alternative Hypothesen und ihre Begründungen. Sber Ges Naturf Freunde Berlin 43: 123-162.

Franz V (1927) Morphologie der Akranier. Zeitschr ges Anat 27: 464-692.

Garstang W (1928) The morphology of the Tunicata and its bearing on the phylogeny of the Chordata. Q J Microsc Sci 72: 51-187.

Gemmill JF (1912) The development of the star fish *Solaster endeca* Forbes. Trans Zool Soc Lond 20: 1-71.

Gemmill JF (1914) The development and certain points in the adult structure of the starfish *Asterias rubens*, L. Phil Trans R Soc B 205: 213-294.

Gerhart J, Lowe C, Kirschner M. 2005. Hemichordates and the origin of chordates. Curr Opin Genet Dev 15:461–467.

Gillis JA, Fritzenwanker JH, Lowe CJ (2011) A stem-deuterostome vertebrate pharyngeal transcriptional network. Proc R Soc Lon B doi:10.1098/rspb.2011.0599.

Goodrich ES (1917) 'Proboscis pores' in craniate vertebrates, a suggestion concerning the premandibular somites and hypophysis. Q J Microsc Sc 62: 539–553.

Halanych KM (1995) The phylogenetic position of the pterobranch hemichordates based on 18S rDNA sequence data. Mol Phylogenet Evol 4: 72-76.

Hatschek B (1881) Studien über die Entwicklung des *Amphioxus*. Arb Zool Inst Univ Wien 4: 1-88, pls 1-9.

Hertwig O, Hertwig R (1881) Die Coelomtheorie. Versuch einer Erklärung des mittleren Keimblattes. Gustav Fischer Verlag, Jena.

Hörstadius S (1973) Experimental Embryology of Echinoderms. Clarendon Press, Oxford.

Holland ND (1991) Echinodermata: Crinoidea. In AC Giese, JS Pearse and VB Pearse (eds): Reproduction of marine Invertebrates, Vol. 6: 247-299. Boxwood Press, Pacific Groove, CA.

Hyman LH (1955) The Invertebrates, Vol.4: Echinodermata. McGraw-Hill, New York.

Hyman LH (1959) The Invertebrates, Vol.5: Smaller coelomate groups. McGraw-Hill Book Company, Inc., New York.

Jefferies RPS (1968) The subphylum Calcichordata (Jefferies 1967) – primitive fossil chordates with echinoderm affinities. Bull Brit Mus 16: 243-339.

Jefferies RPS (1986) The ancestry of the vertebrates. British Museum & Cambridge University Press, London and Cambridge.

Jefferies RPS, Brown NA, Daley PEJ (1996) The early Phylogeny of Chordates and Echinoderms and the Origin of Chordate Left-Right Asymmetry and Bilateral Symmetry. A Zool 77: 101-122.

Jollie M (1982) What are the 'calcichordata'? And the larger question of the origin of chordates. Zool J Lin Soc 75: 167-188.

Kaul S, Stach T (2010) Ontogeny of the collar cord: Neurulation in the hemichordate *Saccoglossus kowalevskii*. J Morph 271: 1240-1259.

Kaul-Strehlow S, Stach T (2011) The pericardium in the deuterostome *Saccoglossus kowalevskii* (Enteropneusta) develops from the ectoderm via schizocoely. Zoomorphology 130: 107-120.

Korschelt E, Heider K (1936) Lehrbuch der vergleichenden Entwicklungsgeschichte der wirbellosen Thiere. Gustav Fischer Verlag, Jena.

Lemaire P, Smith WC, Nishida H (2008) Ascidians and the Plasticity of the Chordate Developmental Program. Curr Biol 18: 620-631.

Levin M (2005) Left-right asymmetrie in embryonic development: a comprehensive review. Mechan Dev 122: 3-25.

Lester SM (1988) Ultrastructure of adult gonads and development and structure of the larva of *Rhabdopleura normani* (Hemichordata: Pterobranchia). AZool 69: 95-109.

Lowe CJ, Terasaki M, Wu M, Freeman RM, Runft L, Kwan K, Haigo S, Aronowicz J, Lander E, Gruber C, Smith M, Kirschner M, Gerhart J (2006) Dorsoventral patterning in hemichordates: insights into early chordate evolution. PLoS Biol 4: e291.

Lowe C, Tagawa K, Humphreys T, Kirschner M, Gerhart J (2004) Hemichordate embryos: Procurement, culture, and basic methods. Methods Cell Biol 74:171–194.

Lowe CJ, Wu M, Salic A, Evans L, Lander E, Stange-Thomann N, Gruber CE, Gerhart J, Kirschner M. (2003) Anteroposterior patterning in hemichordates and the origin of the chordate nervous system. Cell 113: 853–865.

Lüter C (2000) The origin of the coelom in Brachiopoda and its phylogenetic significance. Zoomorphology 120: 15-28.

MacBride EW (1896) The development of *Asterina gibbosa*. Q J Microsc Sci 38: 339-411.

MacBride EW (1903) The development of *Echinus esculentus* together with some points of the development of *E. miliaris* and *E. acutus*. Philos Trans R Soc Lond B 195:285–327.

Maisey JG (1986) Heads and tails: A chordate phylogeny. Cladistics 2: 201:256.

Masterman AT (1898) On the theory of archimeric segmentation and its bearing upon the phyletic classification of the Coelomata. Proc R Soc Edinb 22: 270-310.

Metschnikoff E (1881) Über die systematische Stellung von *Balanoglossus*. Zool Anz 4: 139-157.

Morgan TH (1891) The growth and metamorphosis of Tornaria. J Morphol 5:407-458

Morgan TH (1894) The development of *Balanoglossus*. J Morphol 9: 1–86.

Nielsen C (2001) Animal Evolution. Interrelationships of the Living Phyla. New York: Oxford University Press.

Nielsen C (2009) How did Indirect Development With Planktotrophic Larvae Evolve? Biol. Bull. vol. 216, 3: 203-215.

Ogasawara M, Wada H, Peters H, Satoh N (1999) Developmental expression of Pax1/9 genes in urochordate and hemichordate gills: insight into function and evolution of the pharyngeal epithelium. Development 126: 2539-2550.

Palmer AR (2004) Symmetry Breaking and the Evolution of Development. Science 306: 828-833.

Patten BM (1922) Formation of the cardiac loop in the chick. Am J Anat 30: 373–397.

Peterson KJ (1995) A phylogenetic test of the calcichordate scenario. Lethaia 28: 25-38.

Peterson KJ, Eernisse DJ (2001) Animal phylogeny and the ancestry of bilaterians: inferences from morphology and 18S rDNA sequences. Evolution & Development 3:170-205.

Rao KP (1953) The development of *Glandiceps* (Enteropneusta; Spengelidae). J Morphol 93: 1-17.

Romer AS (1967) Major steps in vertebrate evolution. Science 158: 1629-1637.

Ruppert EE (1997) Cephalochordata (Acrania). In: Harrison FW, Ruppert EE (eds) Microscopic anatomy of invertebrates, vol 15. Wiley-Liss, New York, Chichester, Weinheim, Brisbane, Singapore, Toronto, pp 349-504.

Ruppert EE (2005) Key characters uniting hemichordates and chordates: Homologies or homoplasies? Can J Zool 83: 8–23.

Ruppert EE, Balser EJ (1986) Nephridia in the larvae of hemichordates and echinoderms. Biol Bull 171: 188-196.

Schaeffer B (1987) Deuterostome monophyly and phylogeny. Evol Biol 21: 179-235.

Schepotieff A (1907) Die Pterobranchier. Anatomische und histologische Untersuchungen über *Rhabdopleura normani* Allman und *Cephalodiscus dodecalophus* M'int. 1. Teil. *Rhabdopleura normani*. 1. Abschnitt. Die Anatomie von *Rhabdopleura*. Zool. Jahrb. Anat. 23: 463-534.

Shu D-G, Luo H-L, Conway Morris S, Zhang X-L, Hu S-X, Chen L, Han J, Zhu M, Li Y, Chen L-Z (1999) Lower Cambrian vertebrates from south China. Nature 402: 42–46.

Smith AB (2008) Deuterostomes in a twist: the origins of radical new body plan. Evol Dev 10: 493-503.

Spengel JW 1893 Die Enteropneusten des Golfes von Neapel und der angrenzenden Meeres-Abschnitte. Fauna und Flora des Golfes von Neapel. Vol. 18. Engelmann, Leipzig.

Stach T (1996) On the preoral pit of the larval amphioxus (*Branchiostoma lanceolatum*). Annales des Sciences naturelles, Zoologie, Paris 17: 129-134.

Stach T (2000) Microscopic anatomy of developmental stages of *Branchiostoma lanceolatum* (Cephalochordata, Chordata). Bonn Zool Monogr 47: 1-111.

Stach T (2002) Minireview: On the homology of the protocoel in Cephalochordata and 'lower' Deuterostomia. A Zool 83: 25-31.

Stach T (2008) Chordate phylogeny and evolution: A not so simple three-taxon problem. J Zool 276: 117–141.

Stach T (2009) Anatomy of the trunk mesoderm in tunicates: homology considerations and phylogenetic interpretation. Zoomorphology 128: 97-109.

Stach T, Kaul S (2011) The postanal tail of the enteropneust *Saccoglossus kowalevskii* is a ciliarly creeping organ without distinct similarities to the chordate tail. A Zool 92: 150-160.

Stiasny G (1914) Studium über die Entwicklung des *Balanoglossus clavigerus* Delle Chiaje. II. Darstellung der weiteren Entwicklung bis zur Metamorphose. Mitt zool Stat Neapel 22: 255-290.

Swalla BJ, Smith AB (2008) Deciphering deuterostome phylogeny: molecular, morphological and palaeontological perspectives. Phil Trans R Soc B 363: 1557-1568.

Technau U, Scholz CB (2003) Origin and evolution of endoderm and mesoderm. Int J Dev Biol 47: 531-539.

Telford MJ (2004) Animal phylogeny: back to the Coelomata? Curr Biol 14: 274-276.

van der Horst CJ (1939) Hemichordata. In: Bronns Klassen und Ordnungen des Tierreichs. 4. Band, 4. Abteilung, 2. Buch, Teil 2. Akademische Verlagsgesellschaft mbH, Leipzig.

von Ubisch L (1913) Die Entwicklung von *Strongylocentrotus lividus* (*Echinus microtuberculatus*, *Arbacia pustulosa*). Z Wiss Zool 106: 409-448, pls 405-407.

Westheide W, Rieger R (2007) Spezielle Zoologie, Vol. 1: Einzeller und wirbellose Tiere. 2. Auflage. Elsevier GmbH, Spektrum Akademischer Verlag, Heidelberg.

Willey A (1891) The later larval development of *Amphioxus*. Q J Microsc Sci 32: 183-234, pls 13-15.

Willey A (1894) Amphioxus and the Ancestry of Vertebrates. Macmillan, New York.

Zrzavy J, Mihulka S, Kepka P, Bezdek A, Tietz D (1998) Phylogeny of the Metazoa based on morphological and 18S ribosomal DNA evidence. Cladistics 14: 249-185.

Figure captions

Fig. 1: Scanning electron micrographs showing different early embryological stages of *Saccoglossus kowalevskii*. A The 8 hour post fertilization (h pf) blastula shows a prominent depression at the vegetal pole (*vp*). Inset shows blastomeres at higher magnification (high mag). Partial constrictions demonstrate ongoing cleavage (*arrowhead*). **B** The flattened gatrula (24 h pf) shows the invagination of the archenteron at the blastoporus region (*bp*). Inset: a single cilium (*ci*) is developed on each cell's surface. **C** Around 30 h pf gastrulation is completed. Embryos display an elongated shape. The multiciliated telotroch (*tt*) is developed about 50 µm from the blastopore. **D** The cells of the blastula stage are of cuboid shape, and covered apically with microvilli (*mv*). The cells are interconnected by occluding cell junctions (*ocj*). **E** The cells of the gastrula are highly prismatic enclosing the blastocoel (*bc*). **F** The blastocoel is reduced by the endodermal germ layer almost completely. Endodermal cells (*edc*) are columnar, bordering the lumen of the archenteron (*ar*) with their apical cell surface. Long cilia protrude into the lumen. Ectodermal cells (*ecc*) exhibit a columnar shape, with sometimes very narrow elongated parts, conveying a pseudostratified appearance. *ap* animal pole, *pf* perianal field.

Fig. 2: 3D reconstruction of the embryo of *Saccoglossus kowalevskii* at 36 h pf. Rows from left to right: dorsal, ventral, left, and right view. Columns from top to bottom: The merge row (**A-D**) shows the embryo with all reconstructed structures. Ectoderm row (**E-H**) shows external shape of embryo, telotroch not shown. Endoderm row (**I-L**) reveals the transparent endodermal tissue (*light green*) and the position of the endodermal lumen (*yellowish green*). Mesoderm row (**M-P**) shows the position of the anterior protocoel (*blue*) and the primordal meso- (*pink*) and metacoelic (*red*) tissue. Click image in online version to activate 3D model.

Fig. 3: Histology and fine structure of the embryo of *Saccoglossus kowalevskii* at 36 h pf. A - C, Electron micrographs. D Semithin sagittal sections. E-F Scanning electron micrographs. **A** The lumen of the archenteron (*ar*) is still continuous with the anterior primordal protocoel (*ppc*). **B** The apical cell processes of the primordal protocoelic cells (*pcc*) are goblet-shaped and their basal portion is resting on ecm (*arrowheads*) separating the protocoel from the ectoderm (*ec*). **C** The epithelial endodermal cells (*edc*) are filled with several vesicles (*vs*) apically. Inset: Each cilium is connected to the cytoplasm by an anchoring complex. **D** Sagittal sections of two specimens. At the onset of mesoderm formation, the endoderm (*ed*) shows two shallow constrictions (*arrowheads*) mirroring the embryo's future tripartite body organization. The lower embryo is slightly older indicated by the completely separated protocoel (*pc*). The primordal mesoderm (*pmd*) starts to establish laterally, at the middle and posterior regions of the endoderm. The extracellular matrix (*ecm*) is indicated by the dotted line. **E-F** Sagittally dissected embryo showing the internal organization of the posterior end

(note the position of the telotroch (*tt*)). Ectoderm and endoderm have close contact to each other. A third layer of cells, the primordal mesoderm, reaches between ecto- and endoderm. *ac* accessory centriole, *bb* basal body, *ecc* ectodermal cell, *ci* cilium, *cr* ciliary rootlet, *mi* mitochondrion, *mv* microvilli, *nn* nerve net, *yo* yolk, *za* zonula adherence.

Fig. 4: 3D reconstruction of the embryo of *Saccoglossus kowalevskii* at early kink stage (~ 56 h pf). Rows from left to right: dorsal, ventral, left and right view. Columns from up to down: The merge row (**A-D**) shows the embryo with all reconstructed structures. Epidermis row (**E-H**) shows the external shape of embryo. The telotroch is not shown. Endoderm row (**I-L**) reveals the transparent endodermal tissue (*light green*) and the straight course of the endodermal lumen (*yellowish green*). Lateral outpockets (*double arrowheads*) in the collar region illustrate the connections to the pockets that constitute the mesocoela. Mesoderm row (**M-P**) shows the position of the anterior protocoel (*blue*) and the paired meso- (*pink*) and metacoelic (*red*) compartments. The *anlage* of the pericardium (*purple*) emerges in the posteriormost region of the proboscis (*pr*) within the ectoderm. Click image in online version to activate 3D model. *co* collar, *mo* mouth opening, *stA* anlage of the stomochord, *tr* trunk.

Fig. 5: Histology and fine structure of the early kink stage of *Saccoglossus kowalevskii*. A Semithin sagittal section showing the inner organization of the embryo. The lateral outpocket of the endodermal wall constitutes the rudiment of the earlier connection to the mesocoela. Fine structure of the tubular connection is shown in C. **B** The longitudinal epitheliomuscle cells (*lec*) of the protocoel (*pc*) are rich in myofilaments (*myo*) and mitochondria (*mi*). Neighbouring cells are interconnected by zonulae adherences (*za*). **C** The cells comprising the former connection to the mesocoela are monociliated and resemble those of the endodermal lining. Inset: Each cilium (*ci*) is anchored to the cytoplasm by a short horizontal rootlet and a second vertical rootlet. **D** The endodermal cells (*edc*) are columnar and monociliated. They are covered by numerous bulbus microvilli (*mv*) and several yolk granules (*yo*) are present within the cytoplasm. **E** Cross section of the mesocoelic mesoderm composed of two layers. The proximal mesothelium (*pms*) is made up of flattened cells, while the distal mesothelium (*dms*) contains more cuboid and voluminous cells. Note the course of the ecm (*arrowheads*). **F** The proximal flattened cells contain basal myofilaments in a circular arrangement. There is a virtual lumen present between both cell layers as indicated by interspersed cilia (see S2D for high mag). **G** The distal cells contain basal myofilaments in a longitudinal arrangement. **H** SEM of a dissected embryo showing the same area as seen in E. The mesodermal is composed of a distal and proximal layer of cells. *ac* accessory centriole, *cr* ciliary rootlet, *ec* ecdoderm, *ecc* ectodermal cell, *ed* endoderm, *lu* lumen, *ms* mesocoel, *msc* mesodermal cell, *mt* metacoel, *nu* nucleus, *vs* vesicles.

Fig. 6: 3D-reconstruction of the embryo of *Saccoglossus kowalevskii* at early kink stage (~ 96 h pf). Rows from left to right: dorsal, ventral, left and right view. Columns from up to down: The merge row (**A-D**) shows the embryo with all reconstructed structures. Note the asymmetric development of the anlagen of the gill pores (*double arrowheads*) in C and D and O and P. Epidermis row (**E-H**) shows the external shape of embryo. The telotroch is not shown. Endoderm row (**I-L**) reveals the transparent endodermal tissue (*light green*) revealing the subdivision into an anterior pharynx and posterior intestine region. The anlagen of the gill pores (*gpA*) can easily be discerned. The *anlage* of the stomochord (*stA*) is protruding shortly into the protocoel. Mesoderm row (**M-P**) shows the position of the anterior protocoel (*blue*) and the paired meso- (*pink*) and metacoelic (*red*) compartments. The pericardium (*purple*) is bulb-shaped and protruding into the protocoelic cavity. Click image in online version to activate 3D model. *co* collar, *mo* mouth opening, *stA* anlage of the stomochord, *tr* trunk.

Fig. 7: Histology and fine structure of the late kink stage in *Saccoglossus kowalevskii* (~ 96 h pf). A sagittal section showing the internal organization. The *anlagen* of the 1st gill pores (*gpA*) are visible. The meso- (*ms*) and metacoelic (*mt*) cavities enlarge to form central lumina. **B** The pericardium (*pd*) is surrounded by a basement membrane (*arrowheads*) and furthermore bulb-shaped by protruding into the protocoelic cavity (*pc*). **C** The protocoelic cells lining the pericardium are differentiated into podocytes (*po*) resting on prominent blood sinus (*bs*) nested underneath the basement membrane (*bm*). **D** The elliptic *anlage* of the gill pore is constituted by monociliated cells though, the cytoplasm of individual cells contain several centrioles (*ct*) indicating ciliogenesis. **E** The majority of the protocoelic cells are differentiated into myoepithelial cells. Inner longitudinal muscle cells alternate with circular muscle cells as indicated by the arrangement of myofilaments (*myo*). **F** SEM of a dissected embryo revealing the goblet-shape of the apical cell processes of the protocoelic cells. **G** The meso- and metacoelic lining cells constitute a sqamous epithelium holding a single cilium (*ci*) at the cell surface. *dms* distal mesodermal cell, *ed* endoderm, *ep* epidermis, *gpc* gill pore cell, *mi* mitochondrion, *nn* nerve net, *nu* nucleus, *pdc* pericardial cell, *pe* pedicels, *pms* proximal mesodermal cell, *pph* primordal pharynx, *stA* anlage of the stomochord, *yo* yolk, *za* zonula adherence.

Fig. 8: 3D-reconstruction of the embryo of *Saccoglossus kowalevskii* at 1 gill slit stage (~ 132 h pf). Rows from left to right: dorsal, ventral, left and right view. Columns from up to down: The merge row (**A-D**) shows the embryo with all reconstructed structures. The first gill pore (*gp*) is opened on the left side whereas the right side is still closed. Epidermis row (**E-H**) shows the external shape of embryo. The telotroch is not shown. The collar cord (*cc*) is invaginated by a process similar to chordate neurulation. Endoderm row (**I-L**) shows the transparent endodermal tissue (*light green*) revealing the right-curved course of the

oesophagus (*oe*). Only the left gill pore is opened. The still short stomochord (*st*) is protruding into the protocoel. At the posterior end of the digestive tract a hindgut region (*hg*) can be distinguished. Mesoderm row (**M-P**) shows the position of the anterior protocoel (*blue*) and the paired meso- (*pink*) and metacoelic (*red*) compartments. The pericardium (*purple*) is protruding into the protocoelic cavity. Click image in online version to activate 3D model. *i* intestine, *mo* mouth opening, *ph* pharynx.

Fig. 9: Histology and fine structure of the 1 gill slit stage of *Saccoglossus kowalevskii* (~ 132 h pf). A Slightly oblique sagittal section displaying the opening of the mouth (*mo*) and the left gill pore (*gp*). **B** Pharyngeal lining cells. Inset: The slender microvilli (*mv*) produce a glycokalyx (*gx*) covering the cells. **C** Duct of the gill pore. Cilia (*ci*) and microvilli are projecting into the lumen of the duct. **D** High mag of the apical cell surfaces of the cells lining the intestinal region. The entire surface area is enlarged to form microvilli. E The cells lining the duct of the gill pores are interconnected by zonulae adherences (*za*). The apical cytoplasm contains numerous centrioles (*ct*). Inset: The duct lining cells are developing into multicilated cells. **F** The proximal (*pmt*) and distal (*dmt*) cells of the metacoel constitute flattened epithelial cells. **G** Epithelial cells constituting the mesocoelic lining. **H** Cross section of the mesocoelic lining cells (*msc*). Blood vessels (*bv*) are situated between the basement membranes (*arrowheads, bm*). Inset: The mesocoelic cells contain myofilaments (*myo*) within the very basal portions of the cytoplasm. P *ac* accessory centriole, *cr* ciliary rootlet, *ep* epidermis, *i* intestine, *lu* lumen, mi mitochondrion, *ms* mesocoel, *mt* metacoel, *nn* nerve net, *nu* nucleus, *pc* protocoel, *ph* pharynx, *yo* yolk.

Fig. 10: 3D-reconstruction of the juvenile of *Saccoglossus kowalevskii* at 2 gill slit stage (~ 432 h pf). Rows from left to right: dorsal, ventral, left and right view. Columns from up to down: The merge row (**A-D**) shows the juvenile with all reconstructed structures. Note the characteristic post-anal tail (*pat*). Epidermis row (**E-H**) shows the external shape of juvenile, condensed nervous structures and the skeletal elements. There is only one skeletal rod (*skr*) developed on the right side yet, whereas two are already present on the left side. Endoderm row (**I-L**): The stomochord (*st*) is projecting into the protocoel and supported ventrally by the proboscis skeleton (*sk*). The oesophagus (*oe*) is positioned asymmetrically on the right body half of the juvenile. The anus (*an*) is opened at the posterior end of the hindgut region (*hg*). Mesoderm row (**M-P**) shows the position of the anterior protocoel (*blue*) and the paired meso- (*pink*) and metacoelic (*red*) compartments. The glomerulus (*gl*) is visible covering the anterior tip of the stomochord. Click image in online version to activate 3D model. *cc* collar cord, *dns* dorsal nerve cord, *gp* gill pore, *i* intestine, *pd* pericardium, *ph* pharynx, *ps* proboscis stem, *vnc* ventral nerve cord.

Fig. 11: Detail images of the juvenile of *Saccoglossus kowalevskii* at 2 gill slit stage (~ 432 h pf). A-E 3D-reconstruction, F-H histological sections. A, B Detail images showing the left and right sides of the collar and anterior trunk region. Note the asymmetric development of the gill pores (*gp*). **C** The pericardium (*pd*) is overlying the heart sinus (*hs*), which is in turn connected to the glomerulus (*gl*) by a pair of lateral vessels (*lv*). Note, the dorsal vessel which supplies the heart sinus from posterior is not shown. **D** View from posterior, the right meso- and metacoel are hidden. The dorsal nerve cord (*dnc*) terminates just before the anus (*an*). The metacoel is extended into the post-anal tail (*pat*). **E** Dorsal view focussed on the pharyngeal region (*ph*). The skeletal rods (*skr*) develop asymmetrically and ar of unequal number. The proboscis pore (*pp)* opens dorsally on the left side of the base of the proboscis. **F** Cross section of the trunk region. The ventrolateral metacoelic cells constitute the substantial longitudinal muscles (lm*)* of the trunk. **G** Cross section of the collar region. The collar cord (*cc*) runs within the dorsal mesentery. **H** Longitudinal section showing the position of the proboscis pore, stomochord, pericardium and heart sinus. The majority of the protocoelic cavity (*pc*) is filled with longitudinal muscles. Anterior is to the left. *ep* epidermis, *hg* hindgut, *mc* mouth cavity, *ms* mesocoel, *mt* metacoel, *oe* oesophagus, *ps* proboscis stem, *sk* proboscis skeleton, *st* stomochord, *vnc* ventral nerve cord.

Fig. 12: Histology and fine structure of the juvenile of *Saccoglossus kowalevskii* at the 2 gill slit stage (~ 432 h pf). A Histological section, B-H Transmission electron micrographs. A Sagittal section showing internal structures. The proboscis stalk is flanked by elongations of the mesocoelic cavity, which are filled with longitudinal muscle strands (*lm*) completely. **B** Cells lining the roof of the mouth cavity. Glandular mucus cells (*glc*) are interspersed. **C** Vacuolated cells lining the ventrolateral regions of the anterior pharynx. **D** The stomochord is oval in cross sections and its vacuolated cells surround a central lumen (*lu*). **E** Horizontal section of the gill pore (*gp*). The proximal duct of the gill pore is extremely high ciliated. Inset: high mag of the cilia (*ci*) and their associated basal structures. **F** The intestinal lining is composed of columnar cells. **G**, **H** special intestinal cells containing zymogen-like granules (*zg*) or distended amount of rough endoplasmatic reticulum (*dER*). *cr* ciliary rootlet, *epc* epidermal cell, *hg* hindgut, *mo* mouth opening, *mi* mitochondrion, *ms* mesocoel, *mt* metacoel, *muc* mucus cell, *mv* microvilli, *ne* neurites, *nu* nucleus, *pc* protocoel, ph pharynx, *skr* skeletal rod, *va* vacuole, *vs* vesicles, *za* zonula adherence.

Fig. 13: Fine structure of the juvenile of *Saccoglossus kowalevskii* at 2 gill slit stage (~ 432 hpf). A Cells lining the proximal duct of the proboscis pore. These cells have developed circular myofilaments (*myo*). B Longitudinal section showing the musculature of the protocoel. Outer circular muscles cells alternate with inner longitudinal muscle cells. **C** Podocytes (*po*) resting on the basement membrane (*bm*) covering the glomerular sinus (*gls*). Pedicels (*pe*) form fenestrations between them. **D** SEM showing the highly flattened

metacoelic cells resting on the intestinal region. The area containing the nucleus is protruding into the coelomic cavity. **E** Cross section of the pericardial cells (*pdc*) covering the heart sinus (*hs*). Basal myofilaments are orientated in longitudinal direction. F Cells lining the distal duct of the proboscis pore. These cells are flattened and highly microvillar (*mv*). **G** Cross section of the mesocoelic lining cells (*msc*). Myofilaments of the somatic lining are longitudinally arranged. Inset: in contrast, myofilaments of the visceral lining cells are orientated in circular direction. **H** The somatic lining of the metacoel is hyperdeveloped to form the substantial longitudinal strands of the ventral musculature within the trunk region. Inset: numerous adhesion plaques (adj) anchor the myofilaments to the extracellular matrix (*ecm*). *ac* accessory centriole, *ci* cilium, *cr* ciliary rootlet, *cmyo* circular myofilaments, *lmyo* longitudinal myofilaments, *ms* mesocoel, *mt* metacoel, *ne* neurites, *nu* nucleus, *phc* pharyngeal cell, *za* zonula adherence.

Fig. 14: Coelom formation in Enteropneusta. a – e Schematic drawings of different types of coelom formation compiled from text books (Korschelt & Heider 1936, Nielsen 2001, van der Horst 1939). **f** New scheme of type I for direct-developing enteropneusts, confirmed by ultrastructural investigations (present study). **g** Recommended new scheme for indirect-developing (tornaria larva) enteropneusts. For a more detailed explanation see text and table 1.

Table 1: Summary of characteristics of the five types of coelom formation described for enteropneusts according to literature. For a more detailed explanation see text and figure 14.

Fig. S1: Internal organization of the late gastrula of *Saccoglossus kowalevskii* (~ 36 h pf). A Low mag of the enoderm (*ed*) showing the slit-like central lumen. **B** Sagittal section displaying the area shown in A. **C** Low mag of the anterior endodermal region, i.e. the primordal protocoel (*ppc*). **D** Low mag of the posterior endoderm. The columnar cells are attached to the basement membrane (*arrowheads*). In the area of the former blastopore, no basement membrane is present (in the mid at the bottom of the image). **E** High mag of the apical cell surface of the endoderm. **F** The primordal protocoel is beginning to constrict from the endoderm by means of a sheath of ecm. **G** High mag of the blind ending of the ecm that separates the prospective protocoel from the endoderm incompletely. *ar* archenteron, *ci* cilium, *ec* ectoderm, *ecc* ectodermal cell, *edc* endodermal cell, *mi* mitochondrion, *mv* microvilli, *nn* nerve net, *pcc* protocoelic cell, *vs* vesicles, *yo* yolk.

Fig. S2: Electron micrograph of the early kink stage of *Saccoglossus kowalevskii*. A Low mag of cross section of the endodermal tissue. The endodermal cells (*edc*) are highly columnar and filled with numerous granules of yolk (*yo*). **B** The protocoelic lining cells

(*pcc*) are differentiated into myoepitelial cells. Longitudinal muscle cells span the protocoel (*pc*) and are connected basally to the basement membrane (*arrowheads*). Additional cells contain basal myofilaments (*myo*) which are orientated circularly. **C** Low mag of the endoderm showing the position of the former connection to the mesocoel outpocking (see 5C for high mag). **D** High mag of a cilium (*ci*) present within the two layers of mesocoelic mesoderm indicating the slit-like lumen (*lu*). **E** Longitudinal section, ventral is down, median is up, anterior to the right.The mesodermal outpocketings are separated from the neighbouring tissues by besement membranes. *ec* ectoderm, *ed* endoderm, *msc* mesocoelic cell, *mi* mitochondrion, *mv* microvilli, *za* zonula adherence.

Fig. S3: Internal organization of the 1 gill slit stage of *Saccoglossus kowalevskii* (~ 132 h pf). A, B, D-H transmission electron micrographs. C Image of histological sagittal section. A Cross section of the developing stomochord (*st*). The single layer of stomochordal cells (*stc*) surround a central lumen (*lu*), and rest basally on a sheath of ecm (*arrowheads*). **B** The stomochordal cells are monociliated and interconnected by zonulae adherences (*za*). **C** The stomochord protrudes into the protocoel anteriorly (*pc*). The lumen of the stomochord is continuous with the buccal cavity. **D** Sagittal section illustrating the position of the duct of the gill pore (*gp*). **E** Multiciliated cells interspersed between the otherwise monociliated cells lining the buccal cavity. **F** The pericardium (*pd*) is surrounded by a sheath of ecm and contains a central cavity. **G** The *anlage* of the duct of the proboscis pore (*ppA*) is composed of rather undifferentiated cells at this stage. **H** Podocytes (*po*) are lining the pericardium from the protocoelic side and furthermore rest on a prominent blood sinus (*bs*). *bb* basal body, *bm* basement membrane, *ci* cilium, *ep* epidermis, *mi* mitochondrion, *fe* fenestrations between pedicels, *ms* mesocoel, *mv* microvilli, *myo* myofilaments, *nn* nerve net, *pdc* pericardial cell, *ph* pharynx.

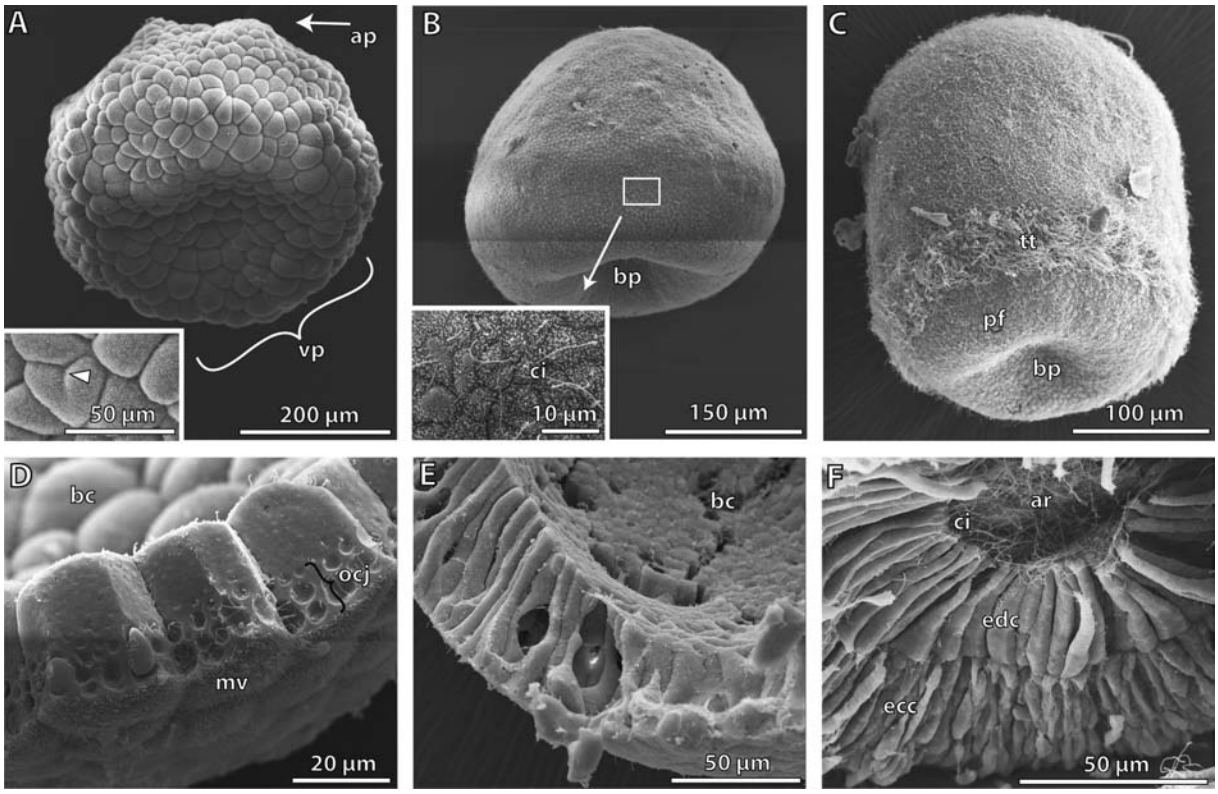
A
ap
vp
50 µm
200 µm
B
bp
ci
10 µm
150 µm
C
tt
pf
bp
100 µm
D
bc
ocj
mv
20 µm
E
bc
50 µm
F
ar
ci
edc
ecc
50 µm

Figure 1

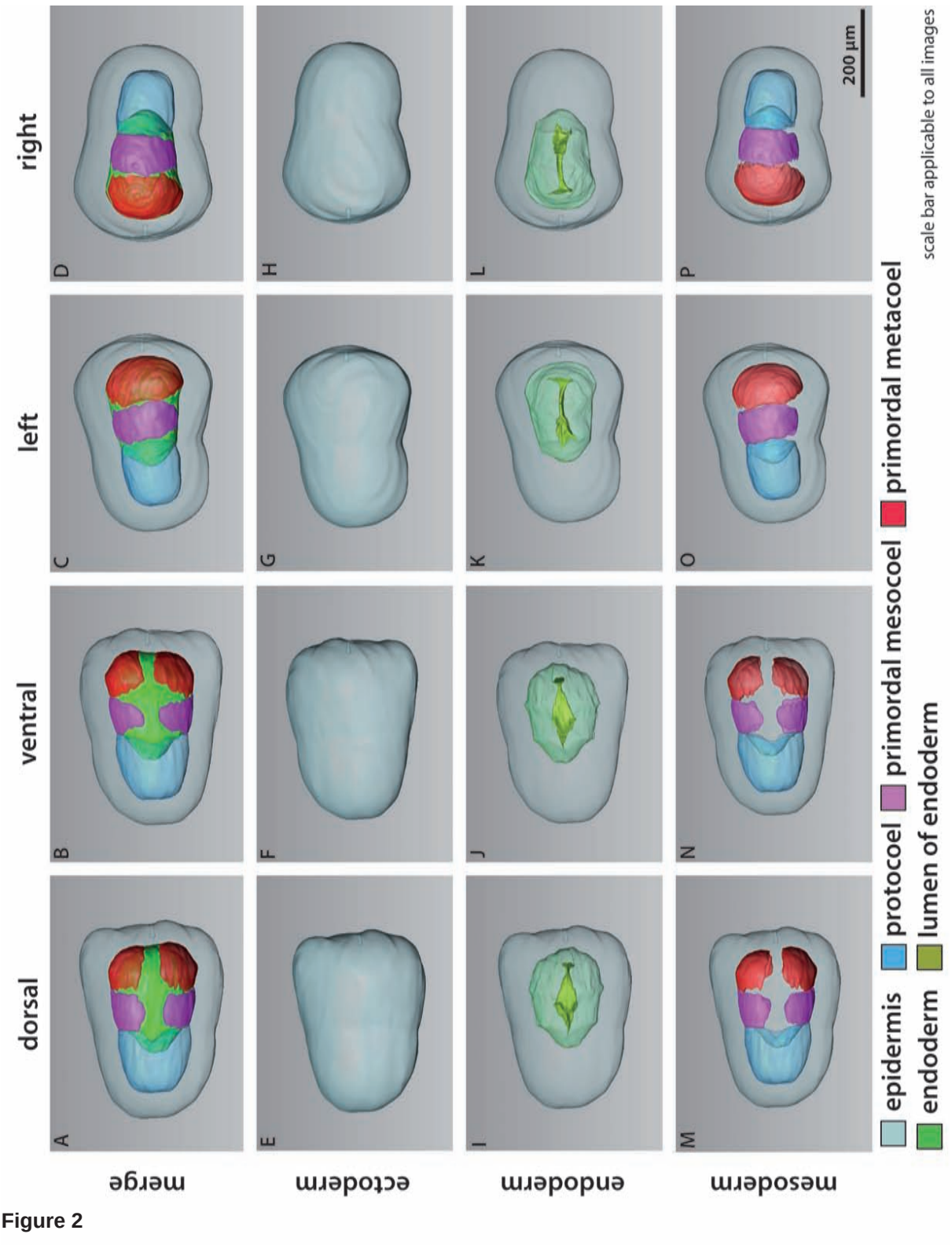
dorsal
ventral
left
right
merge
ectoderm
endoderm
mesoderm
A
B
C
D
E
F
G
H
I
J
K
L
M
N
O
P
200 µm
scale bar applicable to all images
epidermis
protocoel
primordal mesocoel
primordal metacoel
endoderm
lumen of endoderm

Figure 2

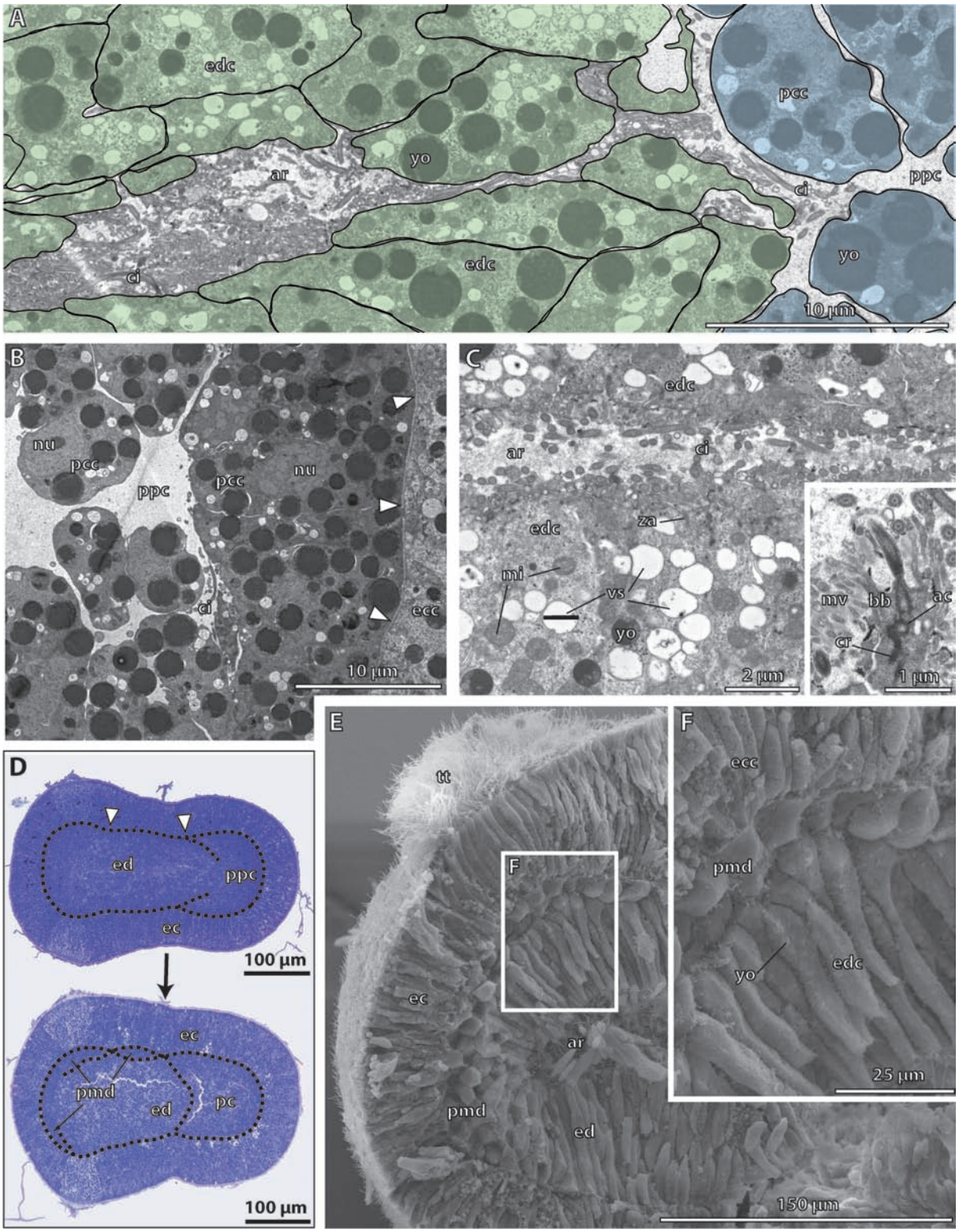
A
edc
pcc
yo
ar
ci
ppc
ci
edc
yo
10 µm
B
nu
pcc
ppc
pcc
nu
ci
ecc
10 µm
C
edc
ar
ci
edc
za
mi
vs
yo
2 µm
mv
bb
ac
cr
1 µm
D
ed
ppc
ec
100 µm
ec
pmd
ed
pc
100 µm
E
tt
F
ec
ar
pmd
ed
150 µm
F
ecc
pmd
yo
edc
25 µm

Figure 3

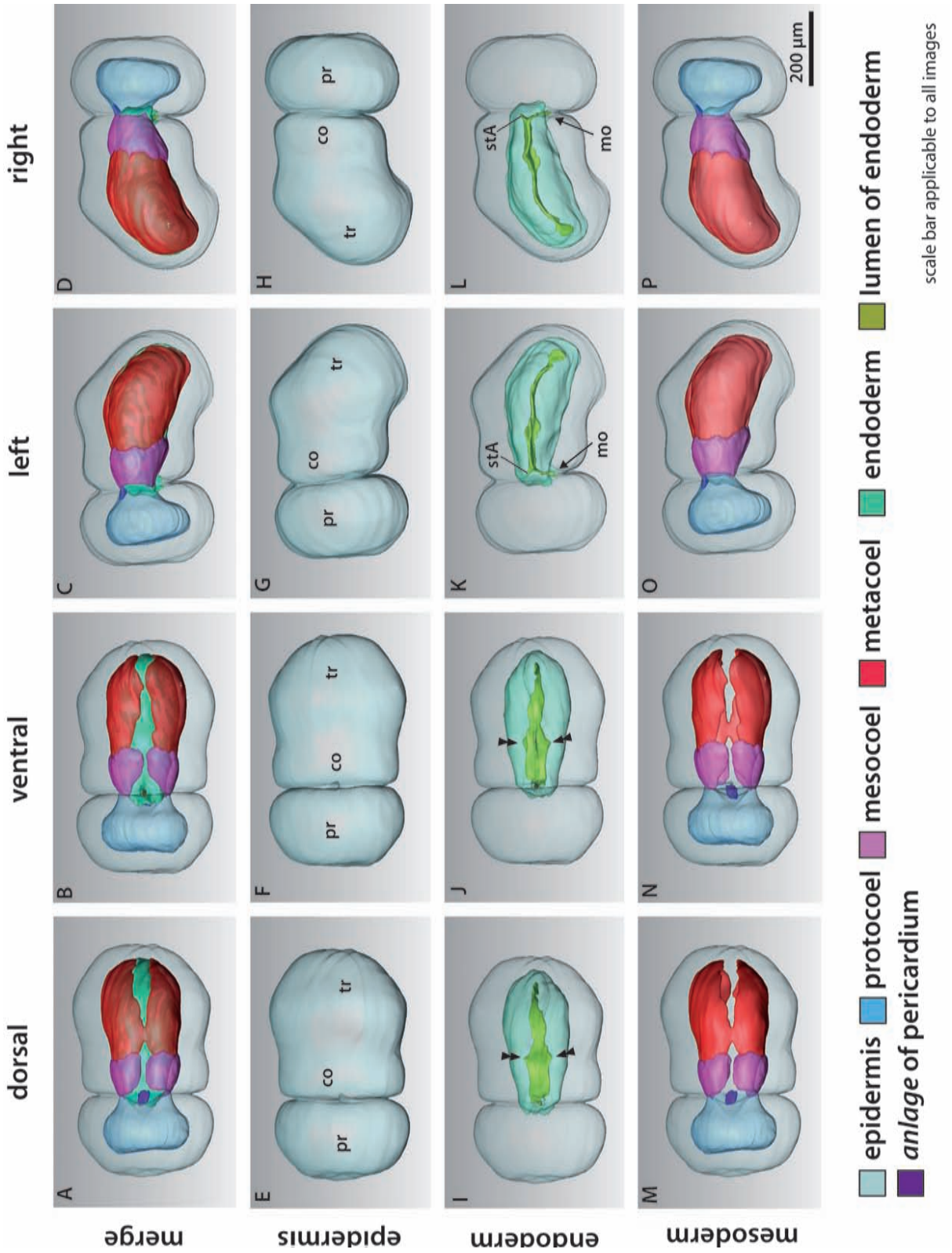
dorsal
ventral
left
right
merge
epidermis
endoderm
mesoderm
A
B
C
D
E
F
G
H
I
J
K
L
M
N
O
P
pr
co
tr
stA
mo
200 µm
scale bar applicable to all images
epidermis
protocoel
mesocoel
metacoel
endoderm
lumen of endoderm
anlage of pericardium

Figure 4

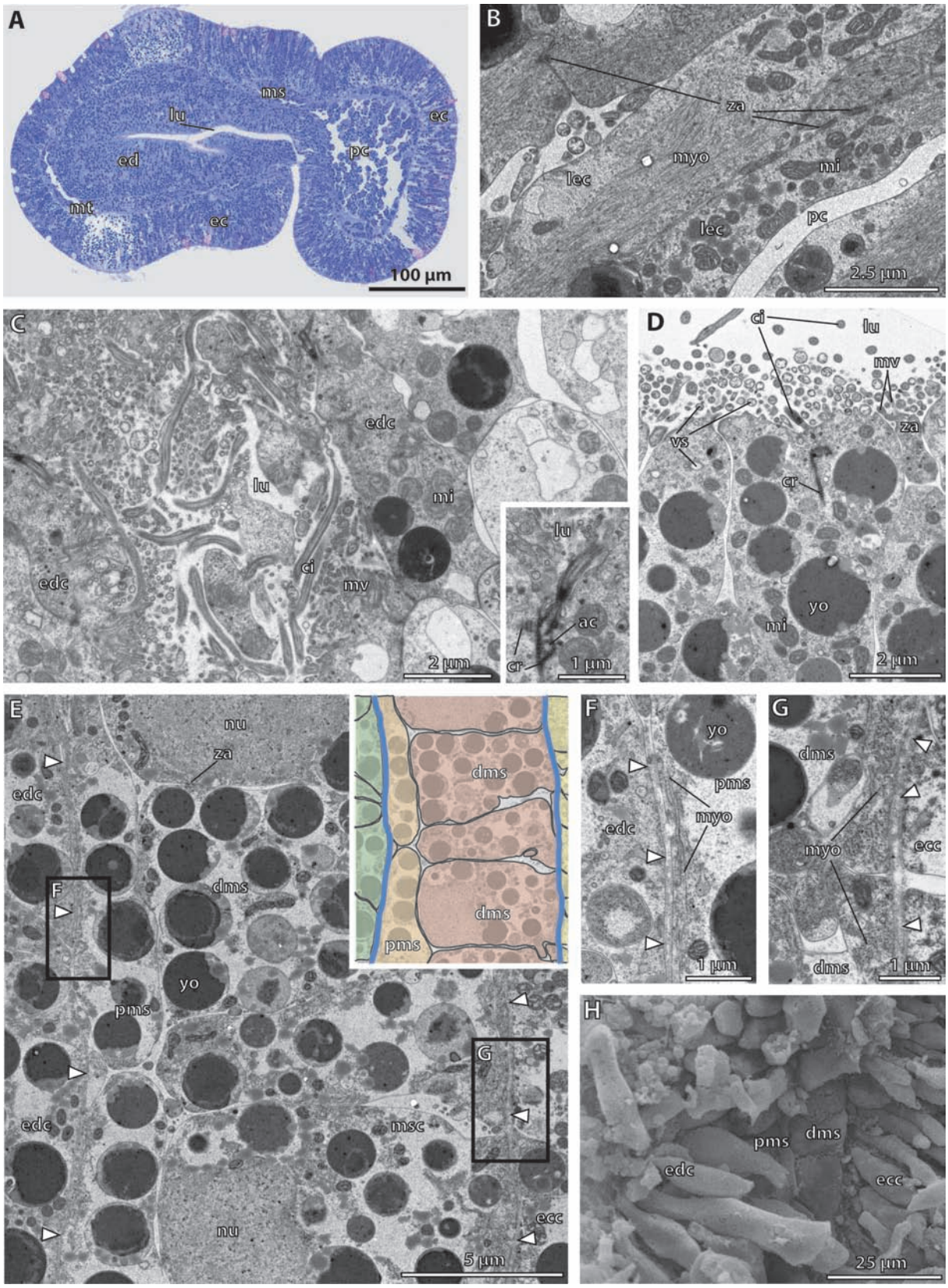
A
ms
lu
ec
ed
pc
mt
ec
100 µm
B
za
myo
mi
lec
lec
pc
2.5 µm
C
edc
lu
mi
ci
edc
mv
2 µm
lu
ac
cr
1 µm
D
ci
lu
mv
za
vs
cr
yo
mi
2 µm
E
nu
za
edc
dms
F
yo
pms
msc
G
edc
nu
ecc
5 µm
dms
dms
pms
F
yo
pms
myo
edc
1 µm
G
dms
myo
ecc
dms
1 µm
H
pms
dms
edc
ecc
25 µm

Figure 5

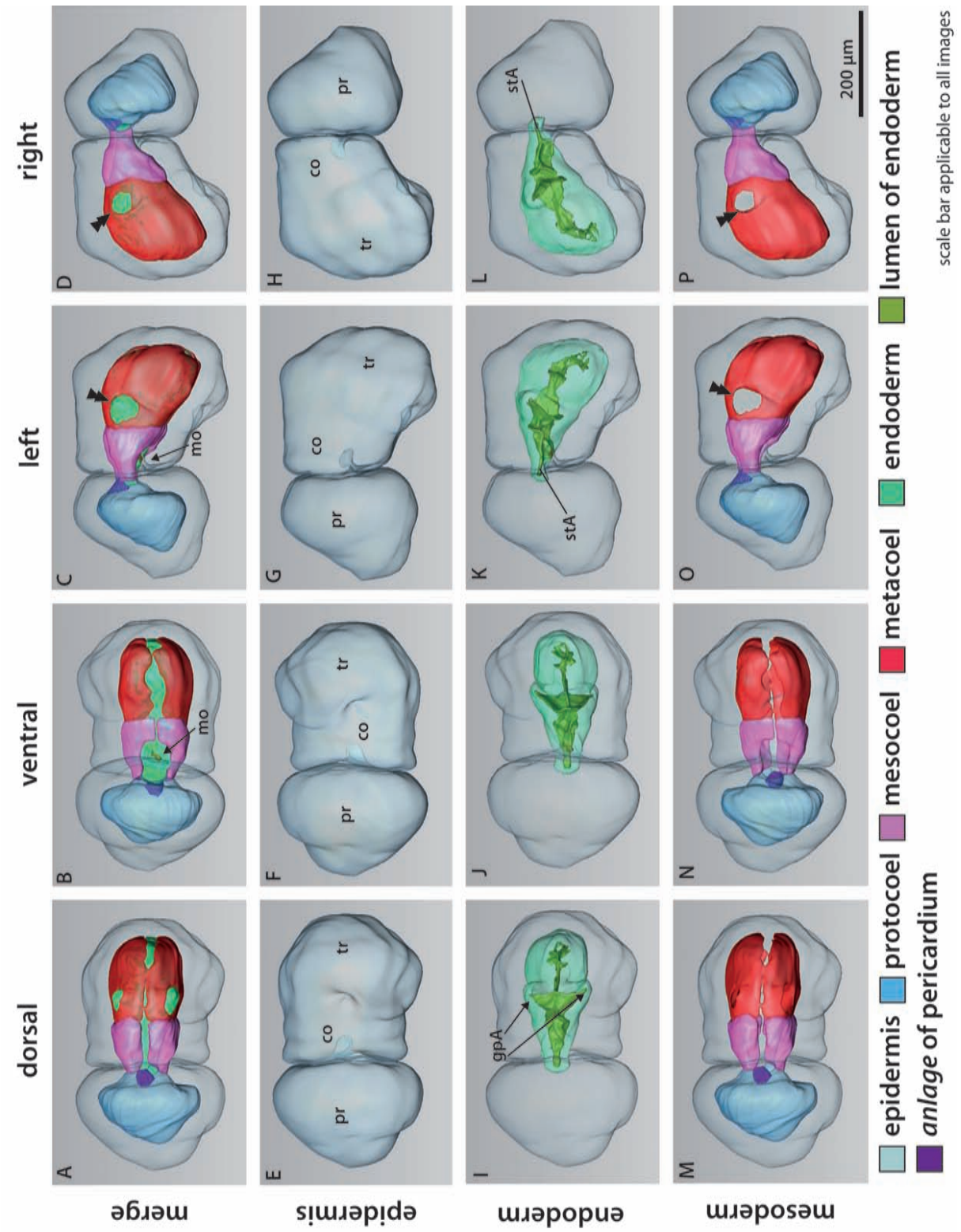
dorsal
ventral
left
right
merge
epidermis
endoderm
mesoderm
A
B
C
D
E
F
G
H
I
J
K
L
M
N
O
P
mo
co
pr
tr
gpA
stA
200 µm
epidermis
protocoel
mesocoel
metacoel
endoderm
lumen of endoderm
anlage of pericardium
scale bar applicable to all images

Figure 6

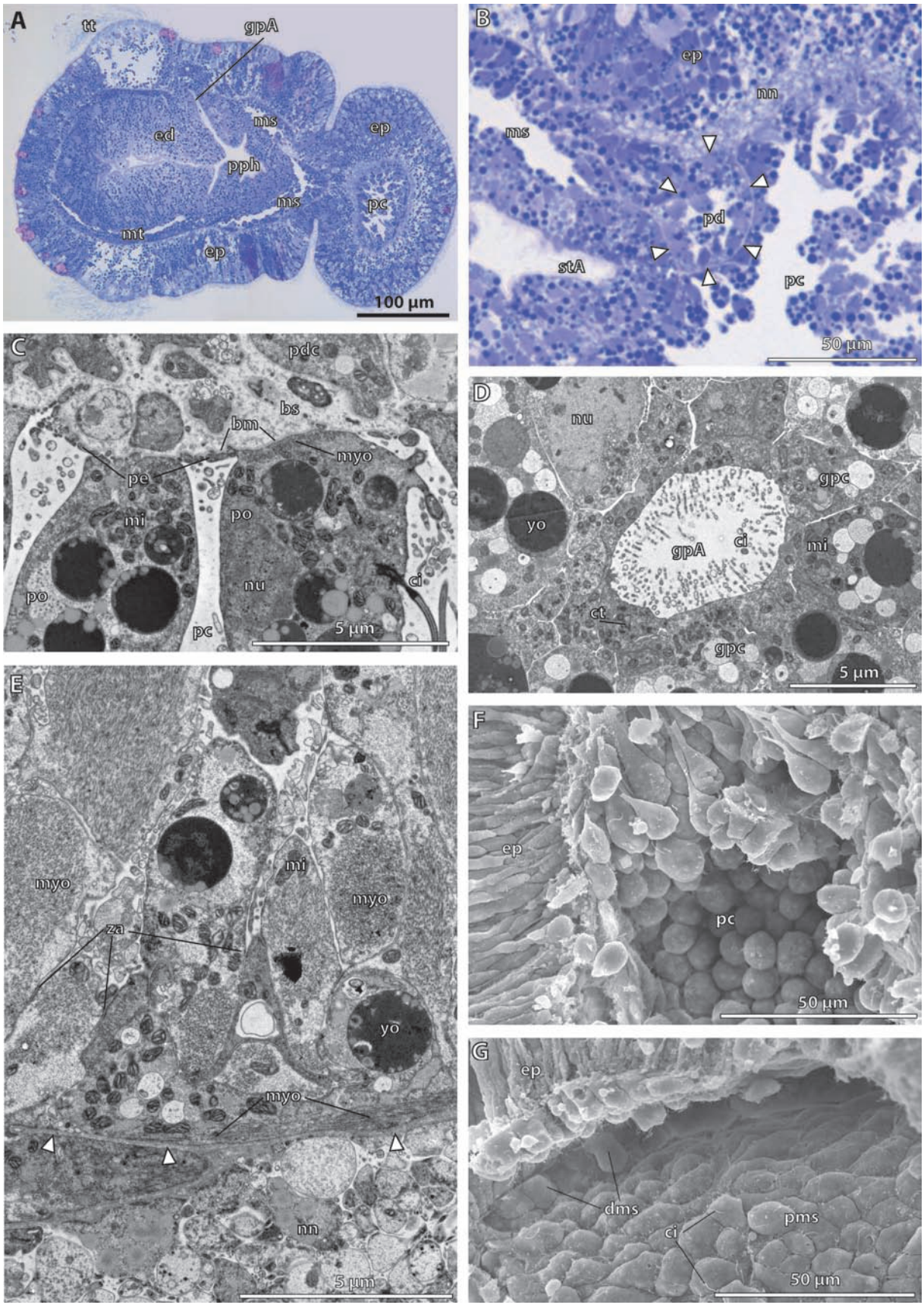
A
tt
gpA
ms
ed
ep
pph
ms
pc
mt
ep
100 µm
B
ep
nn
ms
pd
stA
pc
50 µm
C
pdc
bs
bm
myo
pe
mi
po
ci
po
nu
pc
5 µm
D
nu
gpc
yo
gpA
ci
mi
ct
gpc
5 µm
E
mi
myo
myo
za
yo
myo
nn
5 µm
F
ep
pc
50 µm
G
ep
dms
pms
ci
50 µm

Figure 7

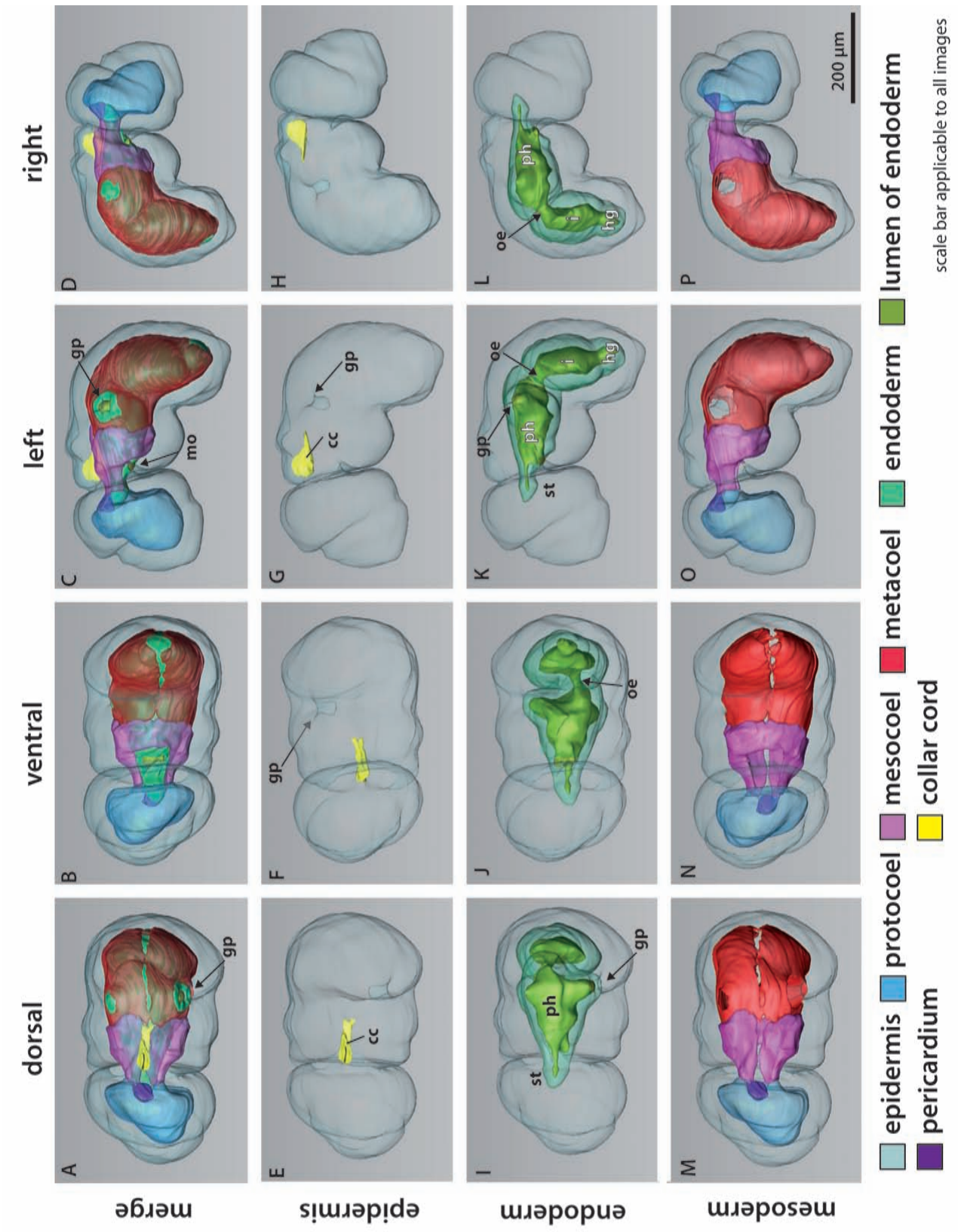
dorsal
ventral
left
right
merge
epidermis
endoderm
mesoderm
A
B
C
D
E
F
G
H
I
J
K
L
M
N
O
P
gp
mo
cc
ph
st
oe
i
hg
200 µm
epidermis
protocoel
mesocoel
metacoel
endoderm
lumen of endoderm
pericardium
collar cord
scale bar applicable to all images

Figure 8

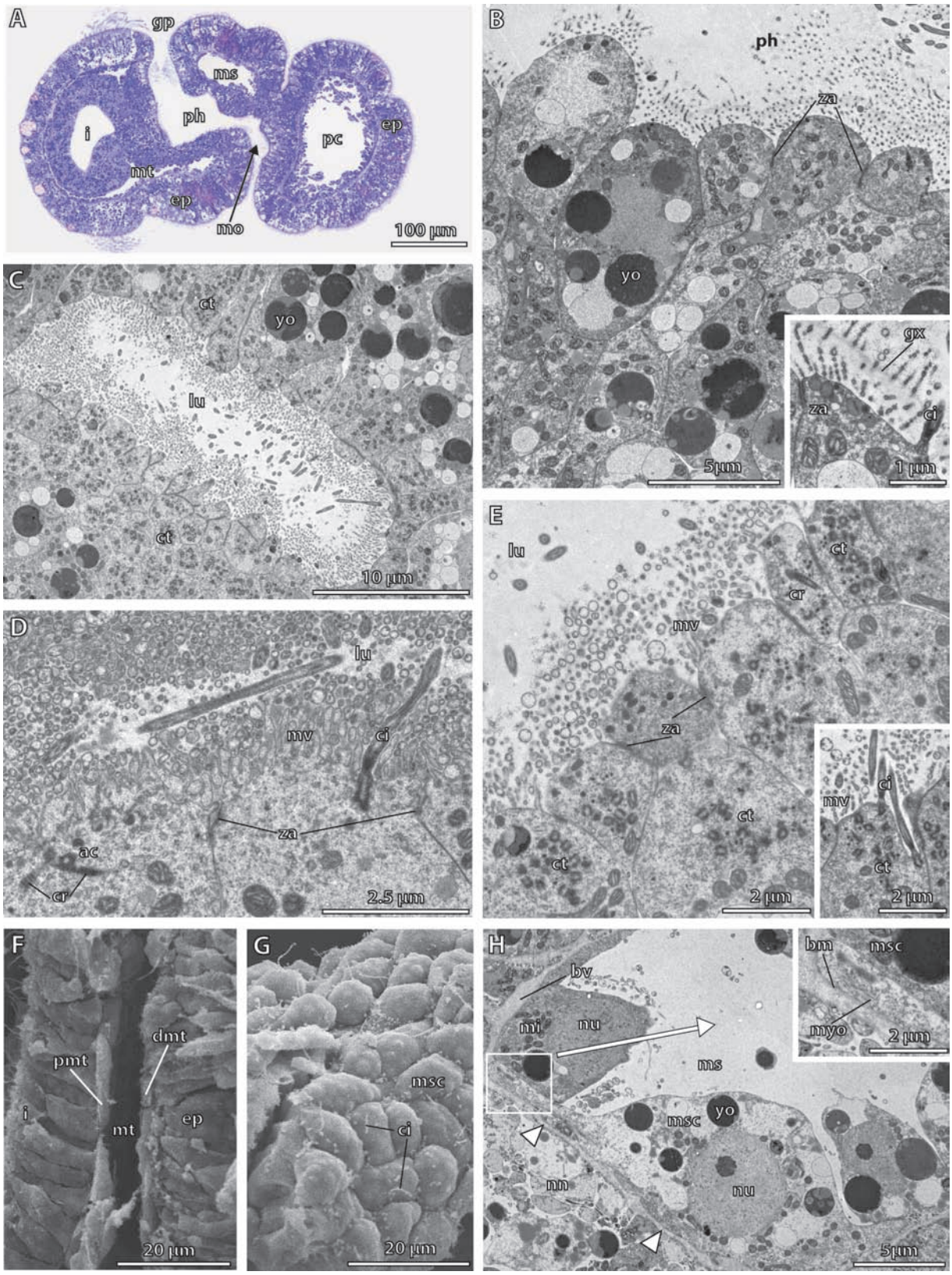
A
gp
ms
ph
i
pc
ep
mt
ep
mo
100 µm
B
ph
za
yo
5µm
gx
za
ci
1 µm
C
ct
yo
lu
ct
10 µm
D
lu
mv
ci
za
ac
cr
2.5 µm
E
lu
ct
cr
mv
za
ct
ct
2 µm
mv
ci
ct
2 µm
F
dmt
pmt
i
mt
ep
20 µm
G
msc
ci
20 µm
H
bv
mi
mu
ms
msc
yo
mn
mu
5µm
bm
msc
myo
2 µm

Figure 9

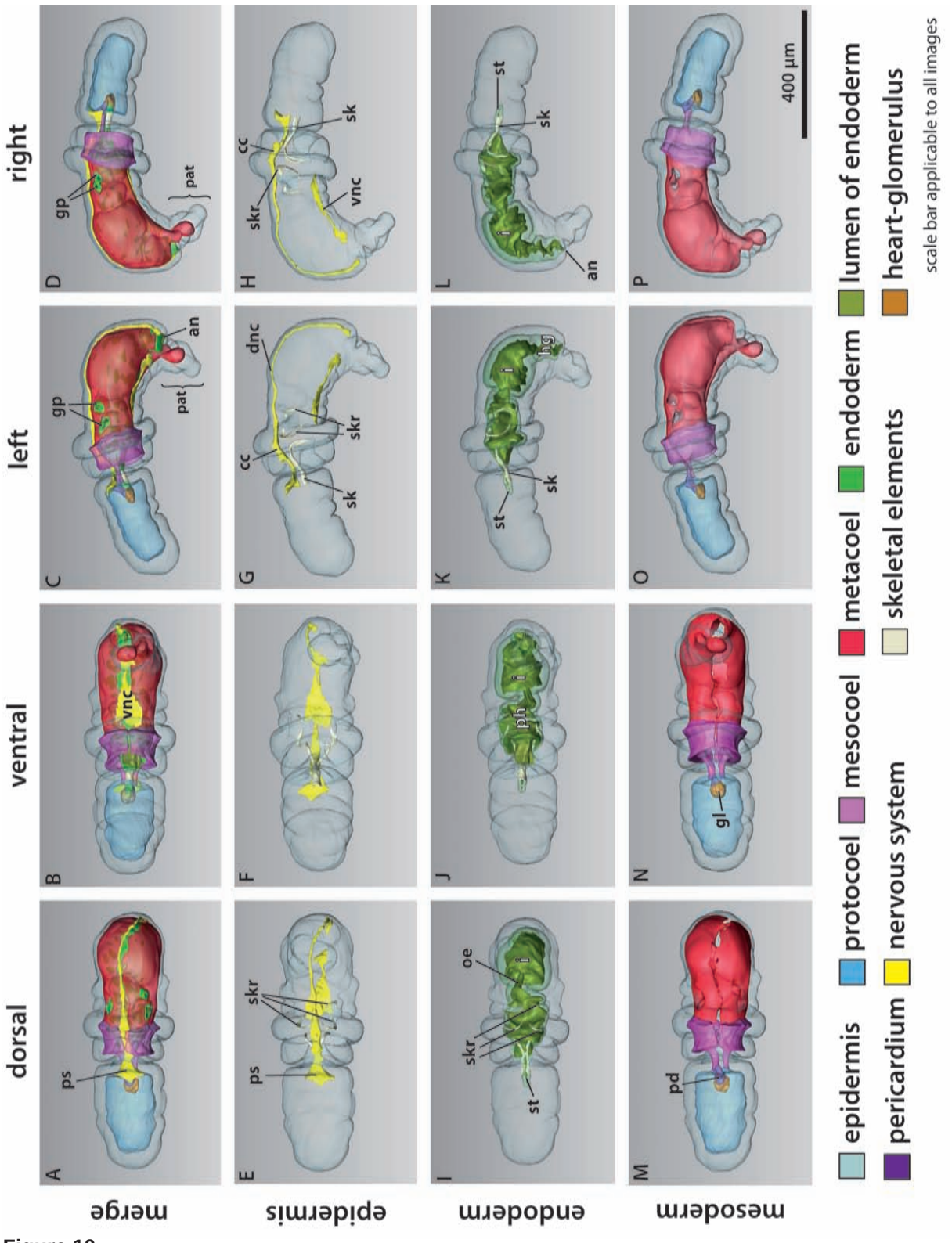
dorsal
ventral
left
right
merge
epidermis
endoderm
mesoderm
A
B
C
D
E
F
G
H
I
J
K
L
M
N
O
P
ps
vnc
gp
pat
an
dnc
cc
skr
sk
oe
i
ph
hg
st
gl
pd
400 µm
epidermis
protocoel
mesocoel
metacoel
endoderm
lumen of endoderm
pericardium
nervous system
skeletal elements
heart-glomerulus
scale bar applicable to all images

Figure 10

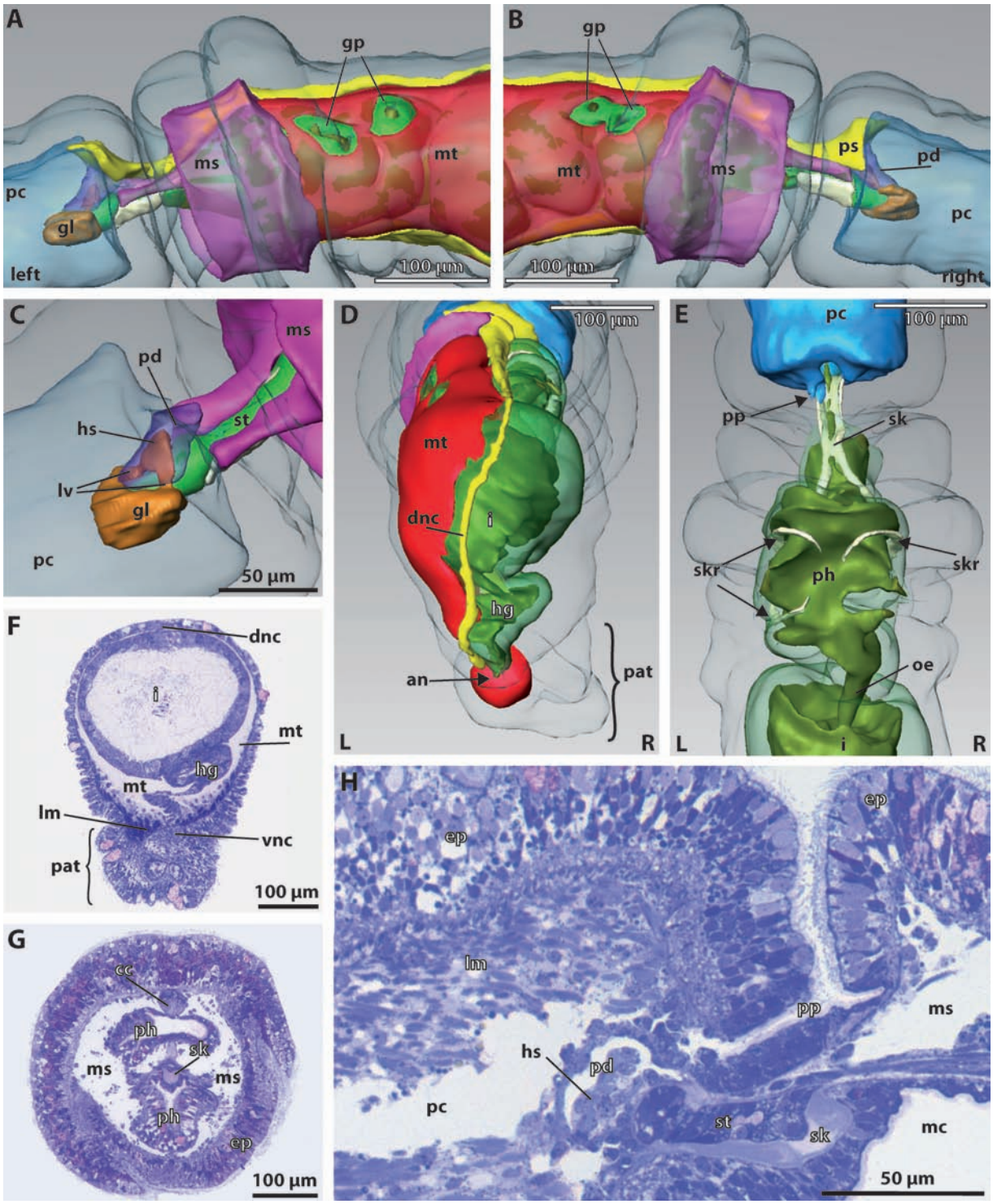
A
gp
ms
mt
pc
gl
left
100 µm
B
gp
mt
ms
ps
pd
pc
100 µm
right
C
ms
pd
hs
st
lv
gl
pc
50 µm
D
100 µm
mt
dnc
i
hg
an
pat
L
R
E
pc
100 µm
pp
sk
skr
ph
skr
oe
L
i
R
F
dnc
i
mt
hg
mt
lm
vnc
pat
100 µm
G
cc
ph
sk
ms
ms
ph
ep
100 µm
H
ep
ep
lm
pp
ms
hs
pd
pc
st
sk
mc
50 µm

Figure 11

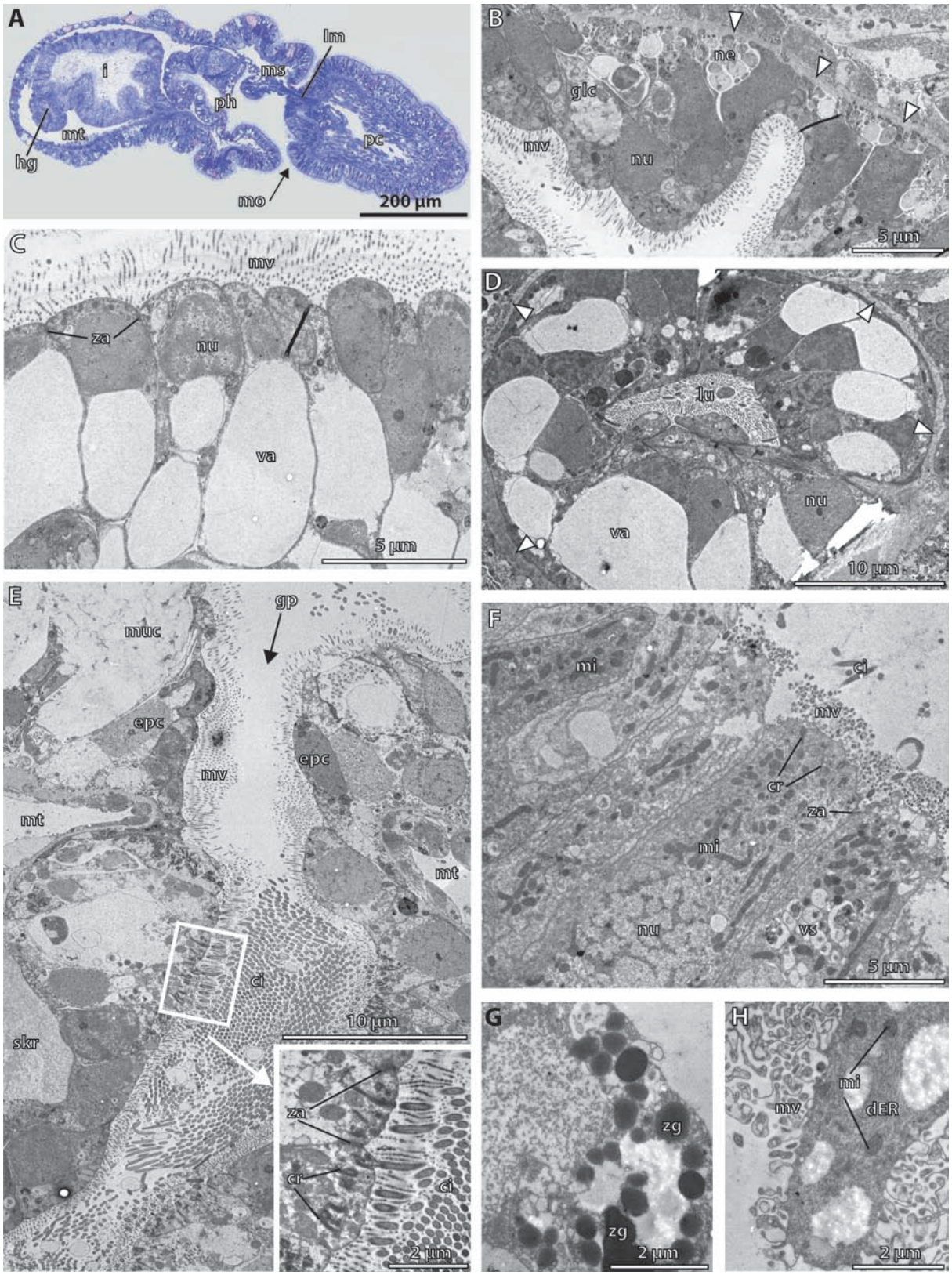
A
i
lm
ms
ph
mt
hg
pc
mo
200 µm
B
ne
glc
mv
nu
5 µm
C
mv
za
nu
va
5 µm
D
lu
nu
va
10 µm
E
gp
muc
epc
mv
epc
mt
mt
ci
skr
10 µm
za
cr
ci
2 µm
F
mi
ci
mv
cr
za
mi
nu
vs
5 µm
G
zg
zg
2 µm
H
mi
mv
dER
2 µm

Figure 12

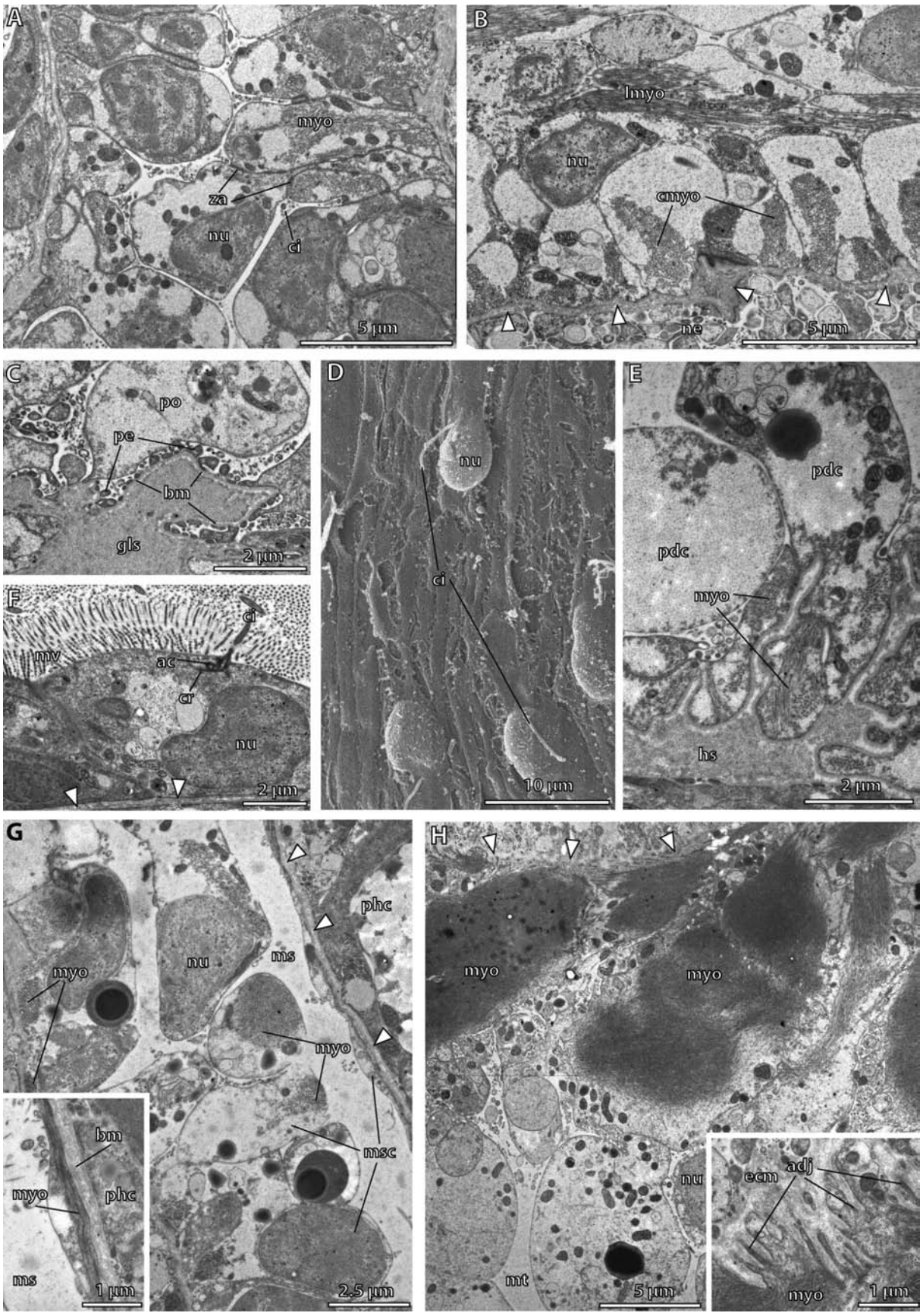
A
myo
za
nu
ci
5 µm
B
lmyo
nu
cmyo
ne
5 µm
C
po
pe
bm
gls
2 µm
D
nu
ci
10 µm
E
pdc
pdc
myo
hs
2 µm
F
ci
mv
ac
cr
nu
2 µm
G
phc
nu
ms
myo
myo
msc
bm
myo
phc
ms
1 µm
2.5 µm
H
myo
myo
nu
mt
5 µm
ecm
adj
myo
1 µm

Figure 13

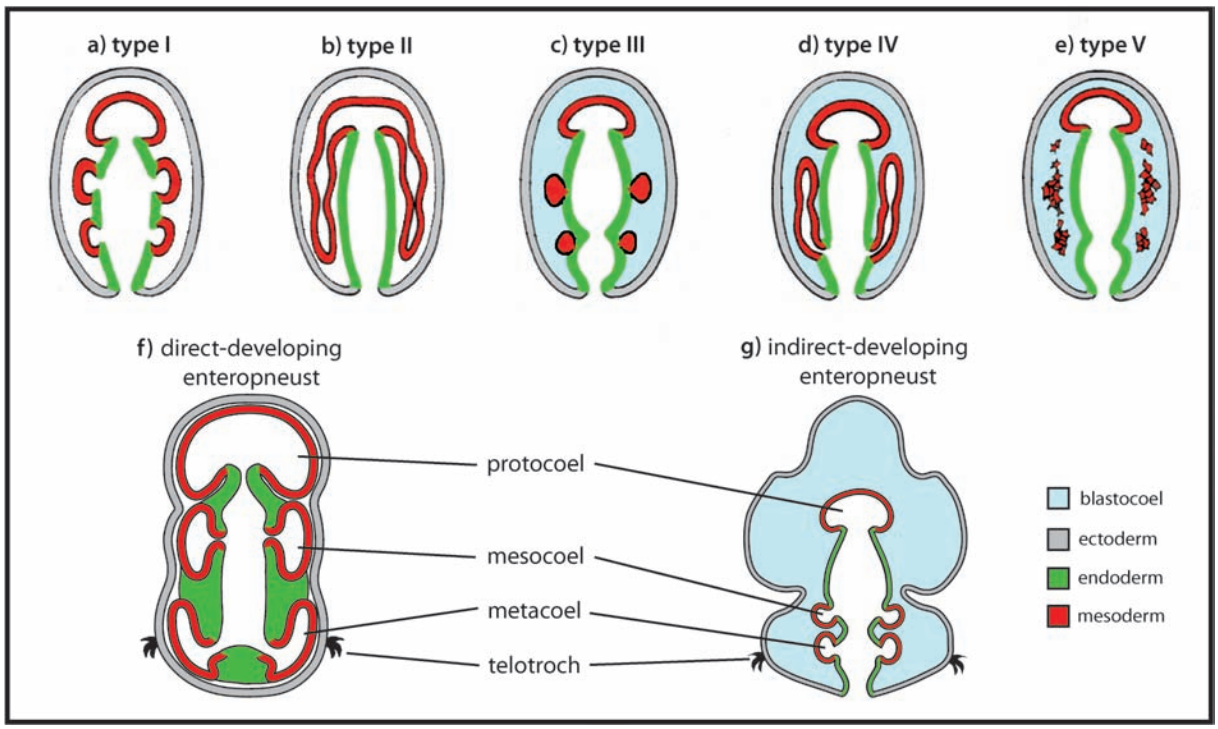
a) type I
b) type II
c) type III
d) type IV
e) type V
f) direct-developing enteropneust
g) indirect-developing enteropneust
protocoel
mesocoel
metacoel
telotroch
blastocoel
ectoderm
endoderm
mesoderm

Figure 14

	characteristics accord. to literature	taxon	source	author's commentary
type I (Fig. 14a)	mesocoela & metacoela form as separated, epithelial outpocketings from the middle and posterior gut regions	*S. kowalevskii* (Harrimaniidae)	Bateson (1884) present study	confirmed by ultrastructural investigations (present study)
type II (Fig. 14b)	a single anterior coelomic sac pinches off from the archenteron and subdivides posterolateral into mesocoel & metacoel	*S. pusillus* (Harrimaniidae)	Davis (1908)	limited light microscopical resolution. TEM study warranted
type III (Fig. 14c)	mesocoela and metacoela form from separated, but *solid* masses of cells from the middle and posterior gut regions	New England Tornaria unknown species (Ptychoderidae)	Morgan (1891)	misinterpretation of the term *solid*, originally described as epithelial enterocoela
type IV (Fig. 14d)	meso- and metacoela originate from a single outpocketing from the posterior gut region that later subdivides	*Glandiceps* sp. (Spengelidae) *B. clavigerus* (Ptychoderidae)	Rao (1953) Bourne (1889) Stiasny (1914) Spengel (1893)	origin of mesocoela is not documented in original literature. origin of metacoela only decribed convincingly
type V (Fig. 14e)	meso- and metacoela originate from multiple clusters of mesenchymatic cells within the blastocoel	tentaculated Tornaria (Ptychoderidae)	Morgan (1894)	limited light microscopical resolution. TEM study warranted

Table 1

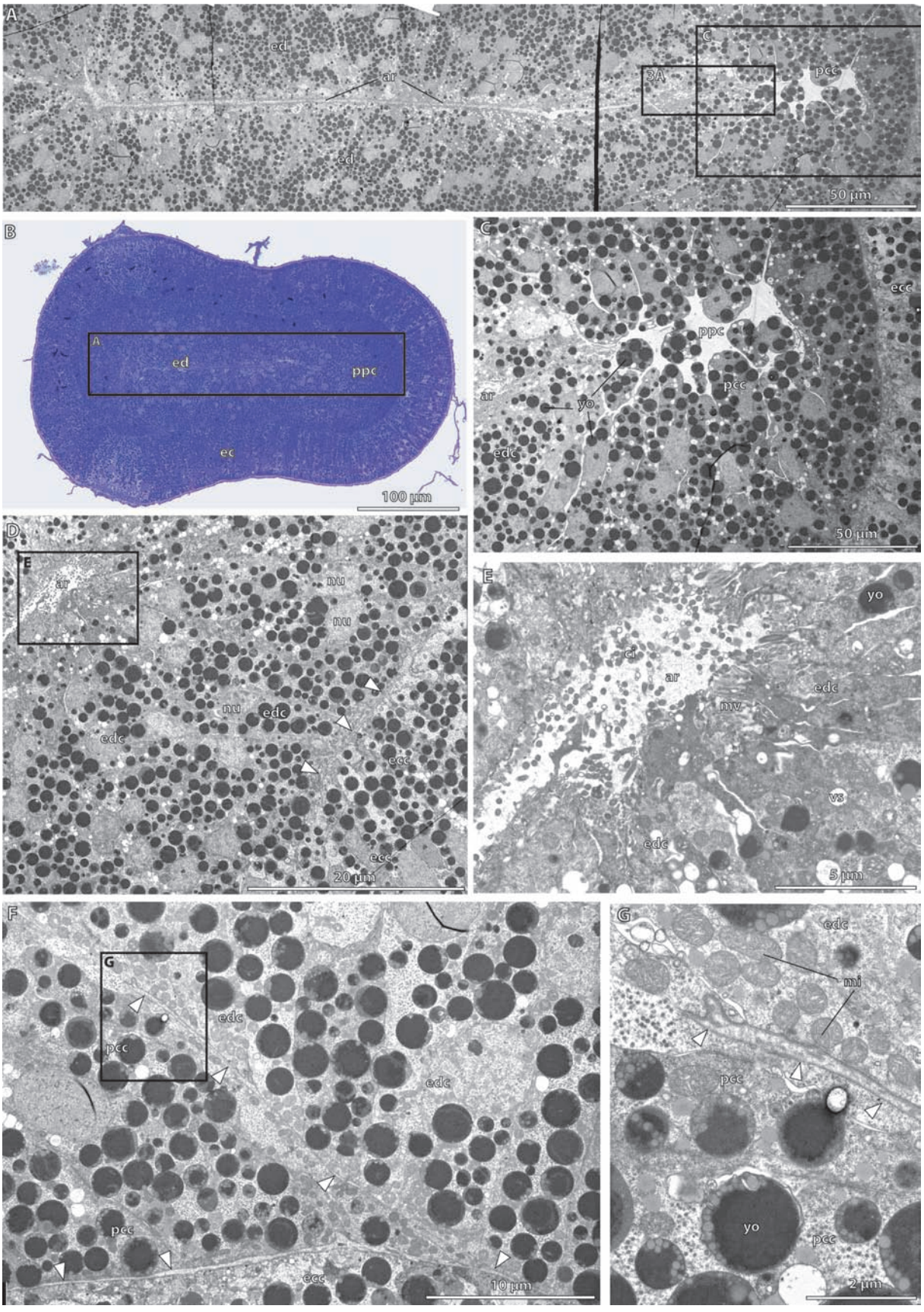

Figure supplementary 1

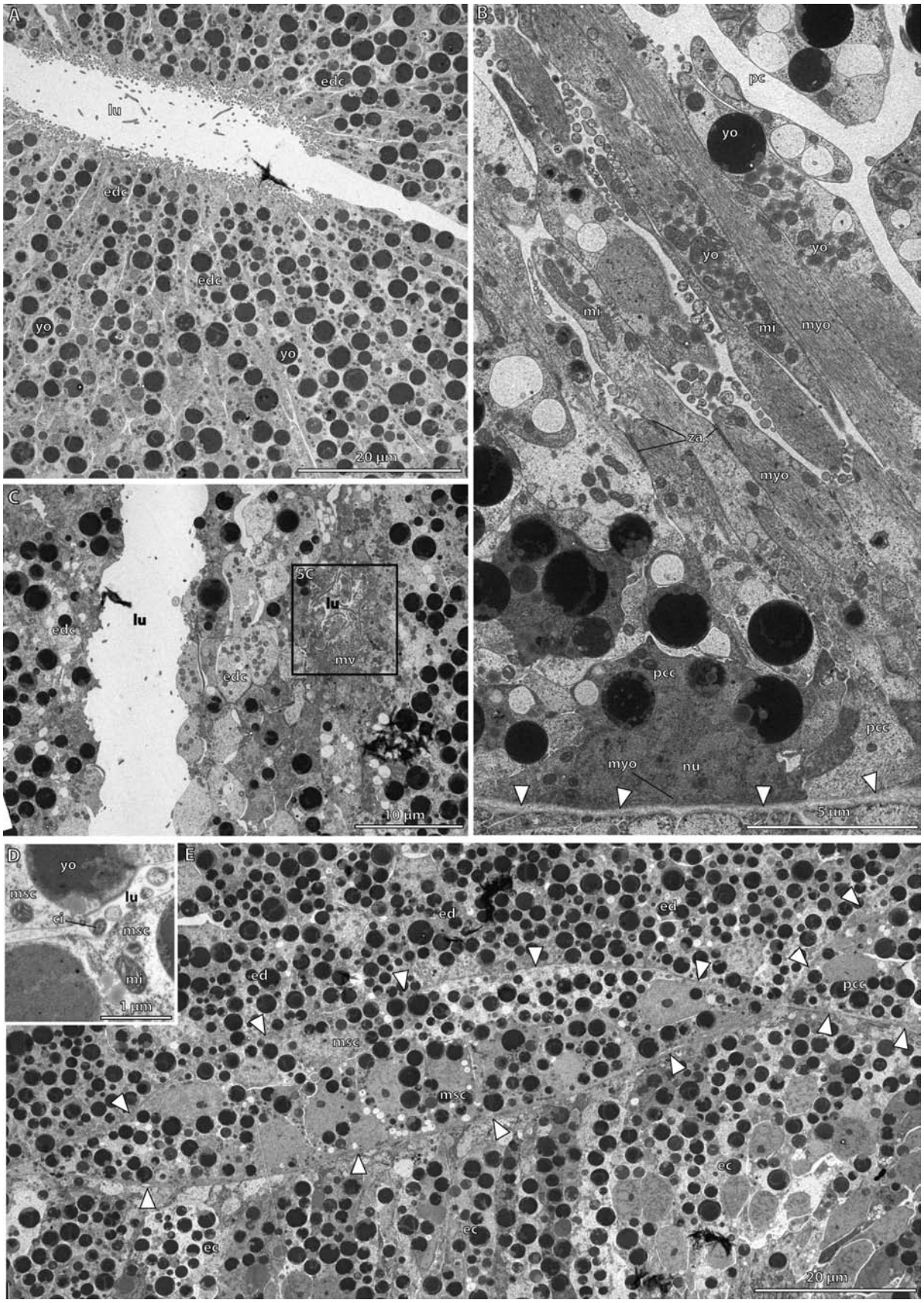

Figure supplementary 2

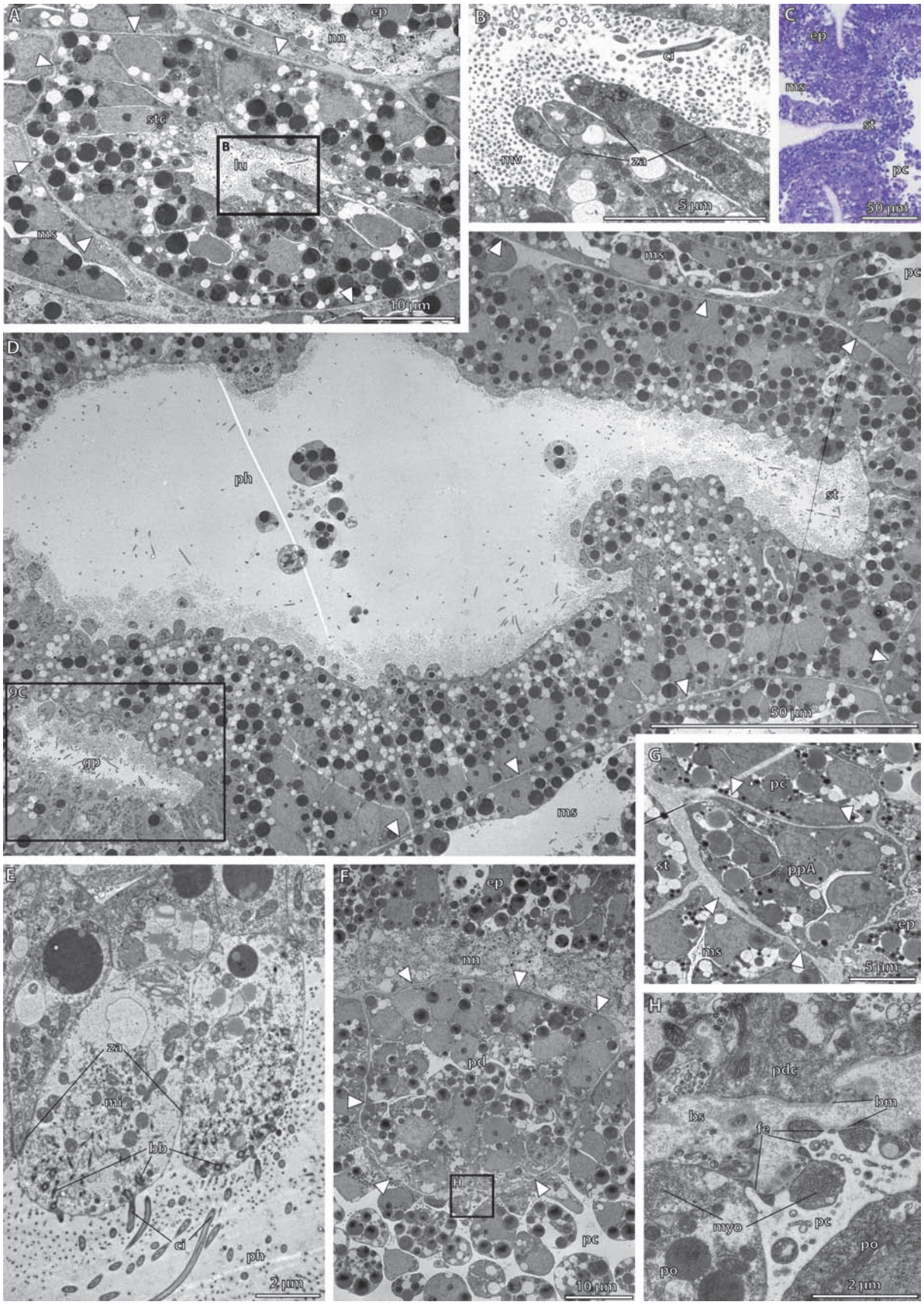

Figure supplementary 3

7. Final discussion

Hemichordata, a small, marine taxon comprising colonial pterobranchs and solitary enteropneusts, is closely related to Chordata and thus may allow insights into the origin of characteristic chordate features, such as notochord, neural tube, or pharyngeal gill slits (Gerhart et al. 2005, Nielsen 2001, Stach 2008). All of these chordate features are currently far from being understood when it comes to homology hypotheses with potentially corresponding structures in early deuterostomes. Given that similarities between these constitutive chordate characters and features in hemichordates have been acknowledged for a long time (Bateson 1885), it is surprising that hemichordates are still widely understudied.

For that reason, the overall aim of the study presented here was to investigate the development of the nervous system and mesoderm in hemichordates by using modern morphological techniques as electron microscopy and immunohistochemistry in order to provide a detailed analysis of the development in hemichordates that were lacking until today. The obtained data will then be compared among deuterostomes as a contribution to elucidate deuterostome evolution. In avoidance of overly repetition of the discussions presented in the previous chapters, I will focus on key features and summarise the main aspects in the following.

7.1 Post-anal tail of ***Saccoglossus kowalevskii***

The homology of the post-anal tail in *S. kowalevskii* and chordates was proposed first by Eaton (1970) and is nowadays more accepted by the assumption that chordates may represent dorso-ventral inversed bilaterians (Geoffrey Saint-Hilaire 1822, Lowe et al. 2006, Nübler-Jung & Arendt 1994). The post-anal tail of chordates contains a central rod-like structure, the notochord (Burighel & Cloney 1997, Conklin 1932, Stach 2000). The notochord is laterally flanked by mesodermal muscles, whereas dorsally a hollow neural tube is situated and ventrally a strand of endodermal tissue (Cloney 1964, Brun & Garson 1984, Hausen & Riebesell 1991, Stach 1999; 2008, Munro and Odell 2002). In contrast, the post-anal tail of *S. kowalevskii* does not contain any specialized skeletal element. Endodermal tissue is likewise not present and a longitudinal neural tube is also lacking (Stach & Kaul 2011, chapter 2). Instead, the post-anal tail of *S. kowalevskii* is comprised by nothing more than posterior extensions of the paired metacoel of the trunk which are filled by mesodermal muscle cells. The post-anal tail in the enteropneust family Harrimaniidae does not contain anatomical structures similar to the one of chordates, i.e. neural tube, strand of endodermal tissue or a notochord as supporting skeletal element. Therefore, from our results we conclude that beyond the general position at the posterior end of the animals there are no additional morphological characters to support the suggested homology with the chordate locomotory tail (Stach & Kaul 2011, chapter 2).

*7.2 Collar cord formation in **S. kowalevskii** and the nervous system of **Cephalodiscus gracilis***

Our study (Kaul & Stach 2010, chapter 3) suggests that the formation leading to the establishment of the collar cord within the mesosome in enteropneusts is homologous to neurulation in chordates. In both cases, a dorsal neural plate produces a subepidermal tube-like structure with a central fluid-filled canal that is accompanied ventrally by endoderm. It should be mentioned here, that the ectoneural system in a derived group of Echinodermata, namely Cryptosyringida (holothuroids, echinoids, ophiuroids) consists of a fluid-filled sinus and is subepidermal in position as well (Byrne 1994, Cavey & Märkel 1994, Mashanov et al. 2006). During development the basiepidermal, ectoneural nerves on the oral side are overgrown by epineural flaps that grow towards the centre of the oral disk where they merge (von Ubisch 1913). Hereby, five pentaradially arranged sinus accompanied by hydrocoel and somatocoel are formed showing paired lateral openings at the base of each tube foot (Cavey & Märkel 1994). Therefore, according to differences in anatomical organization, position, and ontogenetic origin between the ectoneural system in cryptosyringids and the dorsal collar cord of enteropneusts hypothesis of homology between the two structures is rejected by the authors.

Based on the structural separation between somata and neuropil as well as the presence of different neuronal cell types (e.g. ependymal cells, giant cells), elaborate and diverse cell junctions, and probably synaptic vesicles, it is likely that the collar cord in enteropneusts is to some extent a central element of the nervous system, where neuronal integration occurs. The dorsal brain within the mesosome of *C. gracilis* is separated into an anterodorsal cluster of serotonergic somata and a posterior neuropil with a dense network of neurites that run predominantly in transverse direction, although statistical analysis demonstrates that neurite direction differs among brain regions. Furthermore, a pair of branchial nerves projects posteriorly from the brain running to the single pair of gill slits. Additional serotonergic nerves run into each of the tentacles and anteriorly into the mouth shield. Electron microscopy, in addition, revealed the presence of synaptic vesicles throughout the neuropil and a group of a special type of neuronal cells within the posterior region of the brain. The anatomy of the dorsal brain of *C. gracilis* thus is indicative of its function as an integrative centre. Based on the resemblances in their dorsal position in the mesosome, homology of the enteropneust collar cord and the pterobranch dorsal brain is supported as has been previously suggested (Benito & Pardos 1997, Dilly 1975, Dilly et al. 1970). As stated above, according to their anatomy the brain of pterobranchs and the collar cord of enteropneusts both outline neuronal centres performing integrative functions. Taking into account that anterior nerve centres are as well present in stalked crinoids (Akasaka et al. 2005) as in all members of the chordates (Lacalli 1994, Stach 2008), the described structure of the integrative centres of hemichordates support the hypothesis that a centralized part of the nervous system was present in the

last common ancestor of Deuterostomia as was recently also suggested by several authors (Burke 2011, Hay-Schmidt 2000, Nielsen 1999, Nomaksteinsky et al. 2009).

7.3 Pericardium-glomerulus complex

The pericardium in the deuterostome *S. kowalevskii* is ontogenetically derived from the ectoderm and develops by schizocoely (Kaul-Strehlow & Stach 2011, chapter 4), a mode of coelom formation traditionally associated with protostomes (Technau & Scholz 2003). Despite differing ontogenies, homology between the pericardia found in echinoderms and hemichordates is generally accepted (Cameron 2005, Mayer & Bartolomaeus 2003, Ruppert & Balser 1986, Swalla & Smith 2008), because they are part of a nephridial complex that shows numerous distinct similarities. The similarities of the nephridial complex include the contractile pericardium with striated muscle cells, the large anterior protocoel with podocytes and left-sided excretory canal and a glomerulus.

*7.4 Coelom formation in **S. kowalevskii***

The five main coelomic cavities (paired mesocoel and metacoel and single protocoel) are ontogenetically derived from the endoderm by enterocoely. Whereas the protocoel in enteropneusts is pinched off as a single sac from the anterior tip of the endoderm or archenteron, the paired mesocoela and metacoela derive as separated pouches from the middle and posterior regions of the endoderm. A comparable ontogenetic stage where three successive coelomic pouches are developed as described for enteropneusts, can be seen during the ontogeny of the cephalochordate amphioxus (Stach 2002). Here, the early larva recapitulates this tricoelomate stage before additional coelomic sacs are developed posteriorly. In contrast, the common mode of coelom formation described in echinoderms derives all main coelomic cavities from a single anterior outpocketing (MacBride 1903, von Ubisch 1913). Thus, the mode of coelom formation documented in enteropneusts is indicative for a closer relationship of hemichordates and chordates.

*7.5 Left-dominated development of the gill slits and skeletal gill rods in **S. kowalevskii***

The development of the gill slits and associated skeletal rods is left-dominated in enteropneusts. In particular, our data show that the gill pores and skeletal rods on the left side develop slightly earlier than the ones on the right side. Furthermore, the oesophagus connecting pharynx and intestine is shifted to the right body half. *Left-Right (LR) asymmetries* of structures are present in different chordate groups, e.g. the heart or visceral organs in mammals (Brown & Wolpert 1990, Levin 2005, Palmer 2004, Patten 1922) or the asymmetric folded gut in tunicates (Boorman & Shimeld 2002, Burighel & Cloney 1997). In cephalochordates most notable is the mouth that opens on the left larval side while the first row of gill slits (prospective left gill slits) successively arise along the ventral midline (Conklin

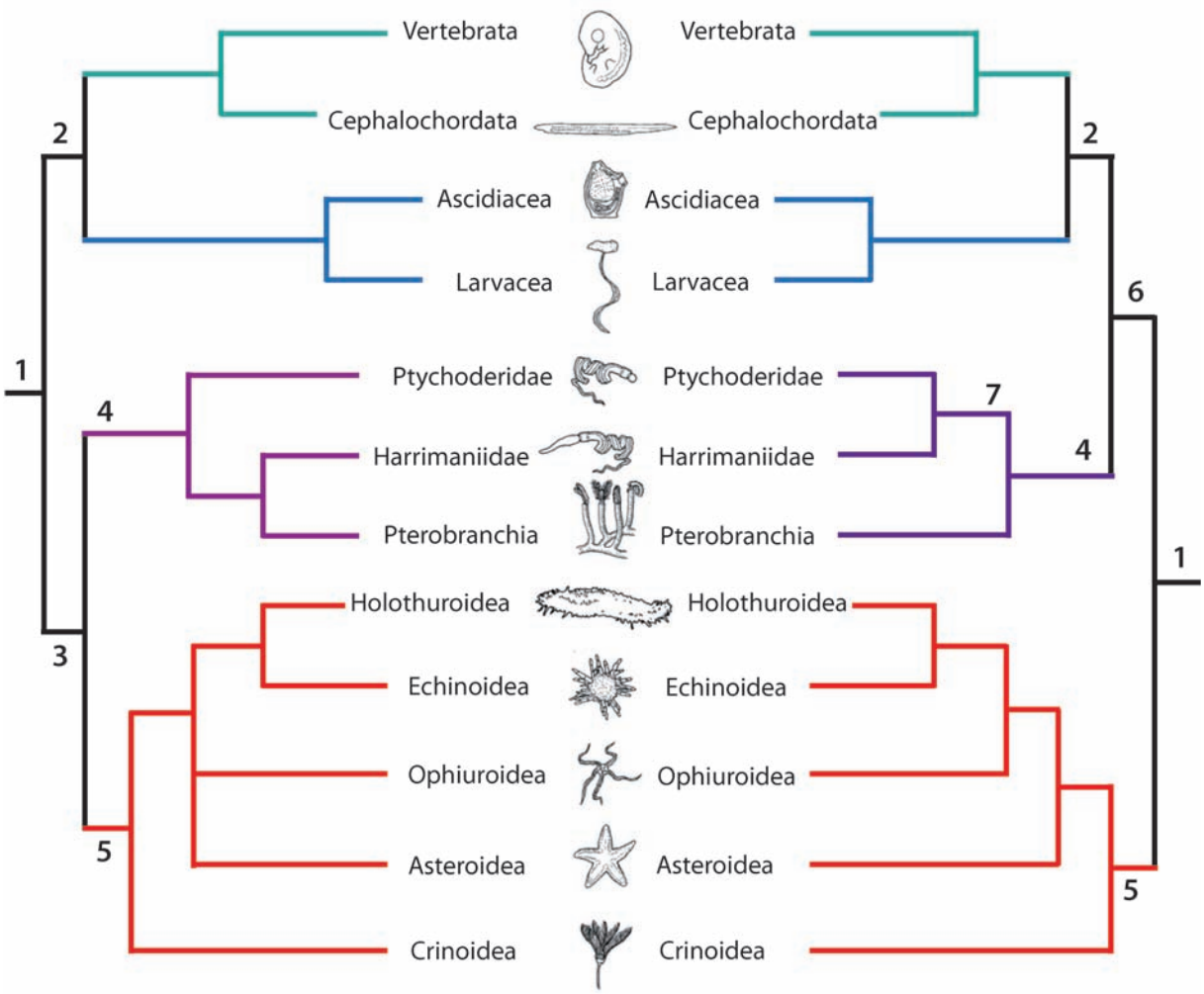

Fig. 7.1: Deuterostome phylogeny. Left side shows a dendrogram compiled from molecular phylogenetic analyses (edited from Zeng & Swalla 2005). Right side shows a diagram inferred from morphological, cladistical analysis (after Schaeffer 1987). 1 = Deuterostomia, 2 = Chordata, 3 = Ambulacraria, 4 = Hemichordata, 5 = Echinodermata, 6 = Pharyngotremata, 7 = Enteropneusta.

1932, Hatschek 1881, Jefferies et al. 1996 , Ruppert 1997b, Stach 2000, Willey 1891). In members of the Echinodermata, we find almost the entire adult body organized asymmetrically in favour of the left side (Gemmill 1914, Hörstadius 1973, MacBride 1903, for review see Hyman 1955). Given the presence of *LR asymmetries* in all major deuterostome groups (Echinodermata, Hemichordata and Chordata) lead us to suggest that at least some degree of *LR asymmetries* was present in the last common ancestor of Deuterostomia. Moreover, the similarities in left-dominated development of the gill slits in *S. kowalevskii* and amphioxus are indicative for a closer relationship of hemichordates and chordates.

7.6 Phylogeny and evolution of the Deuterostomia

Considering the previous listed character complexes, I would like to discuss consequent alternatives for the evolution of Deuterostomia in the following.

There are primarily two competing hypothesis of deuterostome phylogeny which are currently under debate (Fig. 7.1). Both suggested phylogenies are differing in the exact position of the hemichordates and further in the question, if Enteropneusta are monophyletic or if Harrimaniidae may be more closely related to the Pterobranchia. The majority of molecular

phylogenetic analyses (Bourlat et al. 2006, Cameron et al. 2000, Halanych 1995; 2004, Swalla & Smith 2008) as well as some combined analyses (Cameron 2005, Zrzavy et al. 1998) group Hemichordata as the sister taxon to Echinodermata, together comprising the taxon Ambulacraria (Metschnikoff 1881). On the other hand, most of the classical phylogenetic analyses (Ax 2001, Maisey, 1986, Nielsen 2001, Schaeffer 1987) place Hemichordata in a closer relationship to Chordata, a group called Pharyngotremata (sensu Schaeffer 1987).

By using the results obtained during the present study, arguments that support monophyly of the particular groups Hemichordata (7.6.1), Ambulacraria (7.6.2), and Pharyngotremata (sensu Schaeffer 1987) (7.6.3) will be reviewed in detail, and consequences in respect to deuterostome evolution will be evaluated respectively. The monophyly of the Chordata is well supported by a number of constitutive characters (notochord, neural tube, gill slits, myomeric myotomes, a.o.) and will not be called into question (Ax 2001, Bourlat et al. 2006, Dohle 2004, Schaeffer 1987, Stach 2008). Although some scientists have indeed suggested alternatives as well (Gudo 2005, Gutmann 1981), e.g. deriving hemichordates and echinoderms from acrania-like chordate ancestors (Fig. 1.3F).

7.6.1 Hemichordata as a monophyletic group

A sister group relationship of Enteropneusta and Pterobranchia was suggested based on at least four potentially synapomorphic features, namely the tripartite organization of the body and coelom, the structure and position of the brain within the mesosome, the stomochord-pericardium-glomerulus complex, and the presence of mesocoelic ducts and pores (Benito & Pardos 1997, Dohle 2004, Hyman 1959, Schaeffer 1987).

At least the tripartite organisation of the coelom can not be regarded as a synapomorphic feature of Hemichordata, because the coelom in echinoderm larvae and young larvae of amphioxus develops similarly (Nielsen 2001, Stach 2002, von Ubisch 1913). Thus, a tripartite coelomic organisation is likely to be a plesiomorphic feature for Hemichordata that already has been present in the last common ancestor of deuterostomes (Ax 2001, Nielsen 2001).

Similarities in the structure and position of the dorsal brain in hemichordates could further be confirmed during our studies on the ultrastructural and immunohistochemical level as already stated above. In echinoderms, a concentration of nerves is present in the form of a ring nerve around the oesophagus on the ventral side and radial nerves along the ambulacra (Cobb 1995, Cavey & Märkel 1994). The central nervous system in chordates extends along the anterior-posterior axis in the form of the dorsal neural tube and an anterior brain (Nicol & Meinertzhagen 1988, Schroeder 1970, Stach 2000; 2008) and thus is not restricted to a specific body region as seen in hemichordates. Therefore, the mesosomal brain of enteropneusts and pterobranchs is suggested to be a synapomorphic feature uniting them into the group Hemichordata.

Despite the resemblances shared by both brains, one significant difference is puzzling, when it comes to reconstruct the ancestral state in Hemichordata. The dorsal brain in pterobranchs is basiepidermal in position, whereas the collar cord in enteropneusts is invaginated by a

process similar to chordate neurulation. In 18S rDNA analyses, Pterobranchia are positioned as a derived group within the Enteropneusta (Cannon et al. 2009, Halanych 1995, Winchell et al. 2002). According to this, the basiepidermal brain in pterobranchs is likely to represent a derived condition and the invaginated collar cord can be regarded as the ancestral state. This in turn would be consistent with a suggested homology of neurulation processes found in enteropneusts and chordates.

Another feature that is generally assumed to unite Hemichordata as a monophyletic group is the so-called stomochord-pericardium-glomerulus complex (heart-glomerulus complex) (Dohle 2004). As stated in a preceding paragraph, the potential homology of these complexes in enteropneusts and pterobranchs is thoroughly investigated in both groups (Balser & Ruppert 1990, Dilly et al. 1986, Kaul-Strehlow & Stach 2011, chapter 4, Mayer & Bartolomaeus 2003, Welsch et al. 1987) and can hardly being questioned. However, as homologous parts of this excretory complex can as well be found in the axial organ of echinoderms (Mayer & Bartolomaeus 2003, Nielsen 2001, Kaul-Strehlow & Stach 2011, Ruppert & Balser 1986), this excretory complex is suggested to be a plesiomorphic character of Hemichordata. Indeed, such an excretory organ could possibly be inherited from a deuterostome ancestor, as homologous parts of this organ have been suggested to be present in cephalochordates as well (Goodrich 1917, Franz 1927, Nielsen 2001, Stach 2002). Character polarity of the excretory complex will be discussed in the next paragraph in more detail (7.6.2). First, a more detailed consideration of the stomochord, as part of the stomochord-pericardium-glomerulus complex is warranted.

The stomochord is a diverticulum of the buccal cavity that is projecting into the anterior protocoel. It was first proposed as a homologous structure to the chordate notochord by Bateson (1885). Similarities can be found in the ontogenetic origin from the dorsal endoderm and the presence of highly vacuolated cells (Balser & Ruppert 1990, Benito & Bardos 1997, Kaul-Strehlow & Stach 2011, chapter 4 & 6). On the contrary, the stomochord never loses connection to the endodermal tissue as does the notochord in chordates (Ruppert 2005). Moreover, the stomochord is probably not involved in the induction of the neurulation of the collar cord as characteristic for the chordate notochord (Smith & Schoenwolf 1989), because the invaginated collar cord is running within the collar region and therefore touches the stomochord at no particular time (Benito & Pardos 1997, Kaul & Stach 2010, chapter 2). Another difference is that vacuolated cells of the stomochord are restricted to its anterior portion that is positioned within the protocoel. Here, the stomochord is adjoined dorsally by the pericardium and not by the dorsal collar cord (Kaul-Strehlow & Stach 2011, chapter 4). Developmental gene expression data show that the transcription factor *brachyury* is expressed during notochord development in chordates though it is not expressed in the stomochord of hemichordates (Gerhart et al. 2005, Peterson et al. 1999, Ruppert 2005, Rychel et al. 2006).

Given a plethora of differences between the stomochord and notochord, it must be taken into account that the stomochord may represent an innovation of the hemichordates, rather than being a homologue to the notochord of chordates. Nevertheless, the similarities mentioned above cannot completely rule out either, that the stomochord is a precursor and homologue of the chordate notochord.

Concluding the previous paragraph on the suggested monophyly of Hemichordata, Enteropneusta and Pterobranchia can be united as sister groups by only two remaining synapomorphic features, the stomochord as a supporting structure of the pericardium-glomerulus complex and the presence of mesocoelic ducts and pores (Benito & Pardos 1997).

7.6.2 Ambulacraria as a monophyletic group

As previously mentioned, a closer relationship of Hemichordata and Echinodermata is supported by most of the molecular phylogenetic analyses (Bourlat et al. 2006, Cameron et al. 2000, Halanych 2004, Peterson & Eernisse 2001, Winchell et al. 2002) as well as by some morphological, developmental, and molecular characteristics beyond primary sequence similarities (Castresana et al. 1998, Hyman 1959, Metschnikoff 1881, Nielsen 2001, Peterson 2004, Ruppert & Balser 1986). From a morphological point of view, there are two main characters that are consistently mentioned to support the monophyly of Ambulacraria.

On the one hand, both groups develop through pelagic larval stages, by which the larvae are characterized by a specific arrangement of the ciliary bands (neotroch) around the oral field (Cameron 2005, Nielsen 1987; 1998; 2005). The ciliary band consists of separate cilia on monociliated cells and functions as an upstream-collecting system for food capture (Nielsen 1987). In contrast, the ciliary bands described in many protostome larvae are fundamentally different with a downstream-collecting band of compound cilia on multiciliated cells. Given the presence of pelagic larvae with such an upstream-collecting type consisting of separate cilia on monociliated cells in hemichordates, echinoderms and also in lophophorate groups (Phoronida and Brachiopoda) which were traditionally classified closely related to deuterostomes (Ax 2001, Nielsen 2001), such a larval stage was proposed to be a plesiomorphic feature of Echinodermata and Hemichordata (Ax 2001, Hay-Schmidt 2000, Nezlin 2000, Nielsen 2005). However, molecular phylogenetic analyses have shown that phoronids and brachiopods are likely to be protostomes and should therefore be excluded from the deuterostome clade (Dunn et al. 2008, Edgecombe et al. 2011, Goloboff et al. 2009, Halanych et al. 1995). Consequently, ciliary bands consisting of separate cilia on monociliated cells within brachiopod and phoronid larvae must have been evolved convergently. Hence, within the deuterostomes pelagic larvae with circumoral ciliary bands (neotroch) consisting of separate cilia on monociliated cells are only present in echinoderms and hemichordates and may be regarded as an apomorphy supporting the Ambulacraria (Cameron 2005).

Another putative synapomorphy uniting Echinodermata and Hemichordata as sister groups is suggested by the homology of the axial complex in echinoderms and the pericardium-glomerulus complex in hemichordates. While the homology of these excretory complexes

among echinoderms and hemichordates is indeed well established (Cameron 2005, Mayer & Bartolomaeus 2003, Hyman 1955; 1959, Nielsen 2001, Kaul-Strehlow & Stach 2011, chapter 4, Ruppert & Balser 1986, Swalla & Smith 2008), a potential homology with different structures present in lancelets has also been suggested by Nielsen (2001) and Stach (2002). In particular, based on the anterior position, homology with Hatschek's left diverticulum or Hatschek's pit is traditionally suggested (Goodrich 1917, Franz 1927, Nielsen 2001), whereas according to similarities in structure, ontogenetic position, and excretory function, homology with Hatschek's nephridium is suggested by Stach (2002). In any case, if the excretory complexes or parts thereof of non-chordate deuterostomes have homologies in chordates, then it has to be concluded that these homologies are plesiomorphic characters within deuterostome taxa. Consequently, these plesiomorphies cannot be used to support a closer relationship of Echinodermata and Hemichordata.

As mentioned above, our studies of the nervous system in enteropneusts revealed that the process leading to the formation of the collar cord is homologous to chordate neurulation. Hence, the last common ancestor of Ambulacraria and Chordata could have had a neurulated part of the dorsal nervous system. As discussed in a preceding paragraph, the ectoneural system in derived echinoderms, namely the Cryptosyringida (ophiuroids, echinoids and holothuroids), is indeed subepidermal in position, but according to differences in anatomical organisation (not associated with endodermal tissue), position (circumoral on the ventral side) and ontogenetic origin (oral ectoderm instead of dorsal ectoderm), the process forming the ectoneural system in cryptosyringids is suggested to be homoplasious compared with chordate or enteropneust neurulation (Kaul & Stach 2010, chapter 3). Even if the precise anatomy of the nervous system of the last common ancestor of Ambulacraria and Chordata cannot be resolved yet, statements regarding the presumed level of organization are possible. To put it plainly, the presence of nervous centres in all deuterostome groups as stated above (Akasaka et al. 2005, Kaul & Stach 2010, Lacalli 1994, Stach et al. submitted, chapter 5), leads to the conclusion that a centralized part of the nervous system was present in the last common ancestor of Deuterostomia (Burke 2011, Hay-Schmidt 2000, Nielsen 1999). This assumption in turn supports the homology between the centralized nervous systems of protostomes and deuterostomes as suggested by Arendt et al. (2008) and Nomaksteinsky et al. (2009).

It follows from the above that a sister group consisting of Echinodermata and Hemichordata is supported morphologically only by the presence of the dipleurula larval type (Semon 1888), with an upstream-collecting system consisting of separate cilia on monociliated cells (Nielsen 1987). The larval excretory system on the other hand represents a plesiomorphic feature (Nielsen 2001, Stach 2002), inherited from the last common ancestor of the Deuterostomia.

7.6.3 Pharyngotremata (sensu Schaeffer) as a monophyletic group

The name "hemichordates" already implies that affinities with the chordates persist as has been recognized early by several morphological systematists (Ax 2001, Bateson 1885, Garstang 1928, Maisey 1986, Nielsen 2001, Romer 1967, Schaeffer 1987). Namely the neural tube, pharyngeal gill slits and the stomochord led Bateson (1885) to propose a closer relationship of hemichordates and chordates. Recent support for a group comprising Pharyngotremata comes from developmental data that indicates homology between the postanal tail of hemichordates and chordates and similarities in the axial patterning (Gerhart et al. 2005, Lowe et al. 2003, Lowe et al. 2006).

The neurulation process in chordates leads to the formation of a dorsal tube-like structure with a fluid-filled central canal that is subepidermal in position (Holland 2009, Nieuwenhuys 2002). As has been discussed explicitly above, the results of the study presented here (Kaul & Stach 2010, chapter 3) show that the collar cord in enteropneusts derives in a similar pattern and, thus homology of the neurulation processes in hemichordates and chordates is suggested. According to this, a neurulation process leading to an invaginated part of the nervous system can congruently be used as a synapomorphy uniting Hemichordata and Chordata.

The gill slits in enteropneusts develop as paired pharyngeal pouches that open dorsolaterally by fusion of the endoderm and ectoderm within the anterior trunk region (chapter 6). This is similar to what is described for cephalochordates (Conklin 1932, Hatschek 1881, Stach 2000). The presumed homology of pharyngeal gill slits found in hemichordates and chordates is further supported by similarities in the gene expression pattern of *pax1/9*, *eya*, *six1* (Gillis et al. 2011, Lowe et al. 2003, Ogasawara et al. 1999), structure and position (Ruppert 2005, Schaeffer 1987), and composition of the pharyngeal cartilage (Rychel et al. 2006). In extant echinoderms no such pharyngeal gill slits are present and the reports of slit-like openings from so-called calcichordate fossils (Jefferies 1968, Jollie 1982, Smith 2008) remain questionable. Therefore, pharyngeal gill slits illustrate a well established synapomorphy uniting Hemichordata and Chordata as sister groups.

Our data from the development of gill slits in enteropneusts additionally show that the left and right side of gill slits and skeletal gill rods form asymmetrically (chapter 6). In particular, gill slits and rods on the left body half in enteropneusts developed earlier compared to the right side. In cephalochordates, gill slit development is a prominent example of developmental *LR asymmetries* in chordates (Conklin 1932, Jefferies 1986). Here, the first row of gill slits successively arises along the ventral midline (Hatschek 1881, Ruppert 1997b, Willey 1891, for review see Jefferies 1986, Jefferies et al. 1996). These gill slits phylogenetically correspond to the left gill slits of tunicates and craniates (Conklin 1932, Willey 1894, Jefferies et al. 1996) and eventually shift to the left body half whereas the right row of gill slits develop later on during metamorphosis. Although there are indeed differences between the left-dominated development of gill slits in enteropneusts and cephalochordates, in both cases

the opening of the pharyngeal gill slits initially starts on the left body side. This similarity further supports a closer relationship of hemichordates and chordates.

The stomochord, which has been discussed above, shows many differences to the chordate notochord, e. g. it is always continuous with the endodermal tissue, it is probably not involved in the induction of the invagination of the collar cord, no *brachyury* expression is expressed, and is therefore suggested to be an apomorphic invention of the Hemichordata, rather than a homologue to the chordate notochord (Cameron et al. 2000, Gerhart et al. 2005, Ruppert 2005, Rychel et al. 2005). However, similarities can be found in the ontogenetic origin from the dorsal endoderm and the presence of highly vacuolated cells (Balser & Ruppert 1990, Benito & Bardos 1997, Kaul-Strehlow & Stach 2011, chapter 4). Therefore, under consideration of a grouping of Hemichordata and Chordata as sister groups, one cannot rule out the possibility that the stomochord is homologous to the chordate notochord as first proposed by Bateson (1885).

Last but not least it is necessary to discuss a putative homology between the ventral post-anal tail in hemichordates and the dorsal post-anal tail in chordates, as it has been proposed due to similar expression patterns of the Hox genes *hox11/13* (Lowe et al. 2003), can be further supported by additional morphological features. Whereas the differences in position of both structures, i.e. ventral in harrimaniid hemichordates and dorsal in chordates, seem to contradict this hypothesis, a mutual explanation for this incongruence is given by the assumption that chordates may represent dorsoventrally inversed bilaterians (Geoffrey Saint-Hilaire 1822, Nübler-Jung & Arendt 1994). From a combination of morphological, embryological and molecular data from annelids, arthropods and chordates, Nübler-Jung and Arendt (1994) concluded, that chordates are inverted protostomes. And an inversion could have happened between enteropneusts and chordates (Nübler-Jung & Arendt 1996), what is recently supported by an extensive study of gene expression patterns during development in the hemichordate *S. kowalevskii* (Lowe et al. 2006). The assumption that Enteropneusta has not undergone axis inversion is further supported by morphological arguments, e.g. position of gill slits and presence of ventral nerve cord (Gerhart et al. 2005, Nübler-Jung & Arendt 1996, Nielsen 1999, Ruppert et al. 1999). On the contrary, others found no sign of a shift in the dorsal-ventral orientation by comparison of serotonergic nervous systems among different bilaterians (Hay-Schmidt 2000).

However, as mentioned at the beginning of this chapter, the post-anal tail of *S. kowalevskii* does not contain any specialized skeletal element as the notochord in chordates. Endodermal tissue is likewise not present ventrally and a longitudinal neural tube is also lacking (Stach & Kaul 2011, chapter 2). Instead, the post-anal tail of *S. kowalevskii* is comprised by posterior extensions of the paired metacoel of the trunk which are filled by mesodermal muscle cells. Since these results show no additional morphological characters to support the suggested homology with the chordate locomotory tail beyond the general position at the posterior end of the animals, the authors reject a putative homology (Stach & Kaul 2011, chapter 2).

According to this, one must conclude that the ventral post-anal tail of enteropneusts and the dorsal post-anal tail of chordates cannot be used as indicative for a dorsoventral inversion within the line leading to chordates. Actually, the similarities of left-dominated development of gill slits described for enteropneusts (present study) and cephalochordates (Conklin 1932, Stach 2000) and the congruent dorsal position of neurulated nervous systems in both groups, clearly contradict the dorsoventral inversion-theory. Considering that Harrimaniidae is suggested to be the sister group of Pterobranchia according to 18S rRNA analyses (Cameron 2005, Cannon et al. 2009, Halanych 1995, Winchell et al. 2002), the stalk of pterobranchs should be further investigated to see if similarities with the post-anal tail of harrimaniid enteropneusts persist.

7.7 Concluding remarks

The aim of the present study was to investigate the development of the nervous system and mesoderm in Enteropneusta and Pterobranchia by using modern ultrastructural and immunohistochemical methods in order to contribute to the evaluation of early deuterostome evolution. Hemichordata were chosen in particular, because modern morphological studies and especially on phylogenetically informative structures as the nervous tissue and mesoderm were lacking until today. Moreover, hemichordates share some characteristic chordate features, such as notochord, neural tube and pharyngeal gill slits, thus the phylogenetic position of Hemichordata is crucial in order to reveal insights into early chordate evolution.

The detailed analysis of the development of the collar cord, pharyngeal gill slits and formation of the coelomic cavities in hemichordates altogether support previously acknowledged similarities with corresponding structures found in chordates, i.e. neural tube, gill slits, and coelom formation. Furthermore, the data presented here lead to suggest homology between those structures, rejecting the assumptions of homoplasy previously made by others (e.g. Cameron 2005, Cameron & Mackie 1996, Ruppert 2005). Following this, morphological data from this study support a closer relationship between Hemichordata and Chordata (Ax 2001, Maisey 1986, Nielsen 2001, Schaeffer 1987). Therefore, a grouping of Hemichordata and Echinodermata as suggested by 18S rRNA analyses (Bourlat et al. 2006, Cameron et al. 2000, Cannon et al. 2009, Halanych 1995; 2004, Winchell et al. 2002) is not supported here by morphology.

The present study demonstratively shows that deploying modern morphological techniques on previously understudied groups is necessary and reveals new insights by consolidating our knowledge. In the future, it is recommended to integrate this new morphological data into combined (total-evidence) analyses in order to test competing phylogenetic hypotheses and to overcome the existing incongruence between molecular and morphological data.

Bibliography

Akasaka K, Omori A, Amemiya S (2005) Primitive central nervous system of stalked crinoids (*M. rotundus*). Zool Sci 22: 13-89.

Arendt D, Denes AS, Jekely G, Tessmar-Raible K (2008) The evolution of nervous system centralization. Phil Trans R Soc B 363: 1523-1528.

Ax P (2001) Das System der Metazoa III. Ein Lehrbuch der phylogenetischen Systematik. Spektrum Akademischer Verlag, Heidelberg.

Anderson K (1907) Die Pterobranchier der schwedischen Südpolar-Expedition 1901-1903. Wiss Ergeb schwed Südpolarexpedition 5: 1-122.

Balser EJ, Ruppert EE (1990) Structure, ultrastructure and function of the preoral heart-kidney in Saccoglossus kowalevskii (Hemichordata, Enteropneusta) including new data on the stomochord. A Zool 71: 235-249.

Barrington EJ (1965) The Biology of Hemichordata and Protochordata. WH Freeman, San Francisco.

Bateson W (1884) The early stages of the development of *Balanoglossus* (sp. incert.). Q J Microsc Sci, NS 24: 208-236, pls 18-21.

Bateson W (1885) The later stages in the development of *Balanoglossus kowalevskii*, with a suggestion on the affinities of the Enteropneusta. Q J Microsc Sci 25: 81-128.

Benito J, Pardos F (1997) Hemichordata. In: Harrison FW, Ruppert EE (eds) Microscopic anatomy of invertebrates, vol 15. Wiley-Liss, New York, Chichester, Weinheim, Brisbane, Singapore, Toronto, pp 15-101.

Boorman CJ, Shimeld SM (2002) The evolution of left-right asymmetries in chordates. BioEssays 24: 1004-1011.

Bourlat SJ, Juliusdottir T, Lowe CJ, Freeman R, Aronowicz J, Kirschner M, Lander ES, Thorndyke M, Nakano H, Kohn AB, Heyland A, Moroz LL, Copley RR and Telford MJ (2006) Deuterostome phylogeny reveals monophyletic chordates and the new phylum Xenoturbellida. Nature, 444: 85-88.

Bourlat SJ, Nielsen C, Lockyer AE, Littlewood DTJ, Telford MJ (2003). *Xenoturbella* is a deuterostome that eats molluscs. Nature 424: 925–928.

Bourne GC (1889) On a Tornaria found in British seas. Journ Mar Biol Assoc (2), 1: 63-68, pls 7-8.

Bullock TH (1946) The anatomical organization of the nervous system of enteropneusts. Q J Micros Sci 86: 55-111, pls2-8.

Bullock TH (1965) The nervous system of hemichordates. In: Structure and Function in the nervous system of invertebrates. San Francisco: WH Freeman and Co.

Burighel P, Cloney RA (1997) Urochordata: Ascidiacea. In: Harrison FW, Ruppert EE (eds) Microscopic anatomy of invertebrates, vol 15. Wiley-Liss, New York, Chichester, Weinheim, Brisbane, Singapore, Toronto, pp 221-347.

Burke RD (2011) Deuterostome neuroanatomy and the body plan paradox. Evolution & Development 13: 110-115.

Bromham LD, Degnan BM (1999) Hemichordates and deuterostome evolution: robust molecular phylogenetic support for a hemichordate + echinoderm clade. Evol Dev 1: 166-171.

Brown FD, Prendergast A, Swalla BJ (2008). Man is but a worm: chordate origins. Genesis 46: 605–613.

Brown NA, Wollpert L (1990) The development of handedness in left/right asymmetry. Development 109: 1-9.

Brusca RC, and Brusca G J (1990) Invertebrates. Sinauer Associates, Sunderland, MA.

Burdon-Jones C (1952) Development and biology of the larva of *Saccoglossus horsti* (Enteropneusta). Phil Trans R Soc B 236: 553-590.

Burdon-Jones C (1956) Observations on the enteropneust, *Protoglossus koehleri* (Caullery and Mesnil). Proc Zool Soc Lond 127: 35-59.

Brun RB, Garson JA (1984) Notochord formation in the mexican salamander (*Ambystoma mexicanum*) is different from notochord formation in *Xenopus laevis*. J Exp Zool 229: 235-240.

Byrne M (1994) Ophiuroidea. In: Harrison FW, Chia F-S, editors. Microscopic Anatomy of Invertebrates. New York: Wiley-Liss. pp 247-343.

Cameron CB (2002) The anatomy, life habits, and later development of a new species of enteropneust, *Harrimania planktophilus* (Hemichordata: Harrimaniidae). Biol Bull 202: 182-191.

Cameron CB (2005) A phylogeny of the hemichordates based on morphological characters. Canadian Journal of Zoology 83: 196-215.

Cameron CB, Garey JR, Swalla BJ (2000) Evolution of the chordate body plan: new insights from phylogenetic analyses of deuterostome phyla. Proc Natl Acad Sci USA 97: 4469-4474.

Cameron CB, Mackie GO (1996) Conduction pathways in the nervous system of *Saccoglossus* sp. (Enteropneusta). Can J Zool 74: 15-19.

Cameron RA, Hinegardner RT (1974) Initiation of metamorphosis in laboratory cultured sea-urchins. Biol Bull 146: 335-342.

Cannon JT, Rychel AL, Eccleston H, Halanych KM (2009) Molecular phylogeny of hemichordata, with updated status of deep-sea enteropneusts. Mol Phylogenet Evol 52: 17-24.

Castresana J, Feldmaier-Fuchs G, Yokobori S, Satoh N, Paabo S (1998) The mitochondrial genome of the hemichordate *Balanoglossus carnosus* and the evolution of deuterostome mitochondria. Genetics 150: 1115–1123.

Cavey J, Märkel K (1994) Echinoidea. In: Harrison FW, Chia F-S, editors. Microscopic Anatomy of Invertebrates. New York: Wiley-Liss. pp 247-343.

Chia FS, Burke RD (1978) Echinoderm metamorphosis: fate of larval structures. In F. Chia and M.Rice (eds.). Settlement and Metamorphosis of Marine Invertebrate Larvae. Elsevier-North Holland Biomedical Press, New York, pp. 219-2.3

Chia FS, Harrison FW (1994) Introduction to the Echinodermata. In: Harrison FW, Chia FS (eds) Microscopic anatomy of invertebrates, vol 14. Wiley-Liss, New York, Chichester, Weinheim, Brisbane, Singapore, Toronto, pp 1-8.

Cloney RA (1964) Development of the ascidian notochord. A Embryol Morphol Exp 7: 111-113.

Cobb JLS (1995) The nervous systems of Echinodermata: Recent results and new approaches. In: Breidbach O, Kutsch W, editors. The Nervous System of Invertebrates: An evolutionary and Comparative Approach. Basel: Birkhäuser. pp 407–424.

Colwin Al, Colwin LH (1953) The normal embryology of *Saccoglossus kowalevskii*. J Morphol 92: 401-453.

Conklin EG (1932) The embryology of *Amphioxus*. J Morphol 54: 69-118.

Dautov SS, Nezlin LP (1992) Nervous system of the tornaria larva (Hemichordata: Enteropneusta). A histochemical and ultrastructural study. Biol Bull 183: 463-475.

Davis BM (1908) The early life history of *Dolichoglossus pusillus* Ritter. Univ Calf Publs Zool 4: 187-226, pls 4-8.

Delage Y, Hérouard E (1903) Traité de Zoologie Concrète, Vol 3: Les Échinodermes. Schleicher Paris.

Delsuc F, Brinkmann H, Chourrout D, Philippe, H (2006) Tunicates and not cephalochordates are the closest living relatives of vertebrates. Nature 439: 965-968.

Dilly PN (1975) The pterobranch *Rhabdopleura compacta*: its nervous system and phylogenetic position. Symposium of the zoological Society of London 36: 1-16.

Dilly PN, Welsch U, Rehkämper G (1986) Fine structure of heart, pericardium and glomerular vessel in *Cephalodiscus gracilis* M'Intosh, 1882 (Pterobranchia, Hemichordata). A Zool 67: 173-179.

Dilly PN, Welsch U, Storch V (1970) The Structure of the nerve fibre layer and neurocord in the enteropneusts. Zeitschrift für Zellforschung 103: 129-148.

Dohle W (2004) Die Verwandtschaftsbeziehungen der Großgruppen der Deuterostomier: Alternative Hypothesen und ihre Begründungen. Sber Ges Naturf Freunde Berlin 43: 123-162.

Eaton TH (1970) The stem-tail problem and the ancestry of chordates, J Paleon 44: 969-979.

Edgecombe G, Giribet G, Dunn C, Hejnol A, Kristensen R, Neves R, Rouse G, Worsaae K, Sørensen M (2011) Higher-level metazoan relationships: recent progress and remaining questions. Org Div & Evol 11: 151-172.

Fiala-Médioni A (1978a) A scanning electron microscope study of the branchial sac of benthic filter-feeding invertebrates (ascidians). A Zool 59: 1-9.

Fiala-Médioni A (1978b) Filter-feeding ethology of benthic invertebrates (Ascidians). IV. Pumping rate, filtration rate, filtration efficiency. Mar Biol 48: 243-249.

Franz V (1927) Morphologie der Akranier. Zeitschr ges Anat 27: 464-692.

Garstang W (1928) The morphology of the Tunicata and its bearing on the phylogeny of the Chordata. Q J Microsc Sci 72: 51-187.

Gemmill JF (1912) The development of the star fish *Solaster endeca* Forbes. Trans Zool Soc Lond 20: 1-71.

Gemmill JF (1914) The development and certain points in the adult structure of the starfish *Asterias rubens*, L. Phil Trans R Soc B 205: 213-294.

Geoffrey St-Hilaire E (1822) Considérations générales sur la vertèbre. Mémoires, Mus d'His Nat 9:89-119.

Gerhart J, Lowe C, Kirschner M. 2005. Hemichordates and the origin of chordates. Curr Opin Genet Dev 15:461–467.

Gillis JA, Fritzenwanker JH, Lowe CJ (2011) A stem-deuterostome vertebrate pharyngeal transcriptional network. Proc R Soc Lon B doi:10.1098/rspb.2011.0599.

Goldschmid A (2007) Echinodermata. In: Westheide W, Rieger R, eds. Spezielle Zoologie, Vol. 1: Einzeller und wirbellose Tiere. 2. Auflage. Elsevier GmbH, Spektrum Akademischer Verlag, Heidelberg.

Goloboff PA, Catalano SA, Marcos Mirande J, Szumik CA, Salvador Arias J, Källersjö M, Farris JS (2009) Phylogenetic analysis of 73 060 taxa corroborates major eukaryotic groups. Cladistics 25: 211-230.

Goodrich ES (1917) 'Proboscis pores' in craniate vertebrates, a suggestion concerning the premandibular somites and hypophysis. Q J Microsc Sc 62: 539–553.

Grobben K (1908) Die systematische Einteilung des Tierreiches. Verhand Königl Zool Bot Gesell Wien 58: 491-511.

Gudo M (2005) An evolutionary scenario for the origin of pentaradial echinoderms – implications from the hydraulic principles of form determination. A Biotheo 53: 191-216.

Gutmann WF (1981) Relationships between invertebrate phyla based on functional-mechanical analysis of the hydrostatic skeleton. Am Zool 21: 63-81.

Halanych KM (1995) The phylogenetic position of the pterobranch hemichordates based on 18S rDNA sequence data. Mol Phylogenet Evol 4: 72-76.

Halanych KM (2004) The new view of animal phylogeny. Annu Rev Ecol Evol Syst 35: 229-256.

Halanych KM, Bacheller JD, Aguinaldo AM, Liva SM, Hillis DM, Lake JA (1995) Evidence from 18S ribosomal DNA that the lophophorates are protostome animals. Science 267**:** 1641–1643.

Hatschek B (1881) Studien über die Entwicklung des *Amphioxus*. Arb Zool Inst Univ Wien 4: 1-88, pls 1-9.

Hausen P, Riebesell M (1991) The Early Development of *Xenopus laevis*: An Atlas of the Histology. Springer Verlag, Berlin/Heidelberg.

Hay-Schmidt A (2000) The evolution of the serotonergic nervous system. Phil Trans R Soc Lon B 267: 1071-1079.

Hejnol A, Obst M, Stamatakis A, Ott M, Rouse GW, Edgecombe GD, Martinez P, Baguñà J, Bailly X, Jondelius U, Wiens M, Müller WE, Seaver E, Wheeler WC, Martindale MQ, Giribet G, Dunn CW (2009) Assessing the root of bilaterian animals with scalable phylogenomic methods. Proc R Soc Lon B 276: 4261-4270.

Hirakow R, Kajita N (1994) Electron microscopic study of the development of amphioxus, *Branchiostoma belcheri tsingtauense*, the neurula and larva. Acta Anat Nippon 69: 1-13.

Hörstadius S (1973) Experimental Embryology of Echinoderms. Clarendon Press, Oxford.

Holland LZ (2009) Chordate roots of the vertebrate nervous system: Expanding the molecular toolkit. Nat Rev Neurosci 10: 736-746.

Holland ND, Clague DA, Gordon DP, Gebruk A, Pawson DL, Vecchione M (2005) 'Lophenteropneust' hypothesis refuted by collection and photos of new deep-sea hemichordates. Nature 434: 374-376.

Holland PWH, Hacker AM, Williams NA (1991) A molecular analysis of the phylogenetic affinities of *Saccoglossus cambrensis* Brambell & Cole (Hemichordata). Phil Trans R Soc Lon B 332: 185-189.

Holland PW, Koschorz B, Holland LZ, Herrmann BG (1995) Conservation of *Brachyury* (T) genes in amphioxus and vertebrates: developmental and evolutionary implications. Development 121: 4283-4291.

Horie T, Shinki R, Ogura Y, Kusakabe TG, Satoh N, Sasakura Y (2011) Ependymal cells of chordate larvae are stem-like cells that form the adult nervous system. Nature 469: 525-528.

Hyman LH (1951) The Invertebrates, Vol.2: Platyhelminthes and Rhynchocoela: The acoelomate Bilateria. McGraw-Hill, New York.

Hyman LH (1955) The Invertebrates, Vol.4: Echinodermata. McGraw-Hill, New York.

Hyman LH (1959) The Invertebrates, Vol.5: Smaller coelomate groups. McGraw-Hill Book Company, Inc., New York.

Jefferies RPS (1968) The subphylum Calcichordata (Jefferies 1967) – primitive fossil chordates with echinoderm affinities. Bull Brit Mus 16: 243-339.

Jefferies RPS (1986) The ancestry of the vertebrates. British Museum & Cambridge University Press, London and Cambridge.

Jefferies RPS, Brown NA, Daley PEJ (1996) The early Phylogeny of Chordates and Echinoderms and the Origin of Chordate Left-Right Asymmetry and Bilateral Symmetry. A Zool 77: 101-122.

Jenner RA (2004) Towards a phylogeny of the Metazoa: evaluating alternative phylogenetic positions of Platyhelminthes, Nemertea, and Gnathostomulida, with a critical reappraisal of cladistic characters. Contributions to Zoology 73: 3-163.

Jollie M (1973) The origin of the chordates. A Zool 54: 81-100.

Jollie M (1982) What are the 'calcichordata'? And the larger question of the origin of chordates. Zool J Lin Soc 75: 167-188.

Jorgensen CB (1966) Acrania. New York: Pergamon.

Kaul S, Stach T (2010) Ontogeny of the collar cord: Neurulation in the hemichordate *Saccoglossus kowalevskii*. J Morph 271: 1240-1259.

Kaul-Strehlow S, Stach T (2011) The pericardium in the deuterostome *Saccoglossus kowalevskii* (Enteropneusta) develops from the ectoderm via schizocoely. Zoomorphology 130: 107-120.

Keller RE (1975) Vital dye mapping of the gastrula and neurula of *Xenopus laevis*. I. Prospective areas and morphogenetic movements of the superficial layer. Dev Biol 42: 222-241.

Keller RE (1976) Vital dye mapping of the gastrula and neurula of *Xenopus laevis*. II. Prospective areas and morphogenetic movements of the deep layer. Dev Biol 51: 118-137.

Knight-Jones EW (1952) On the nervous system of *Saccoglossus cambrensis* (Enteropneusta). Philos Trans R Soc Lond B 236: 315-354.

Komai T (1951) The homology of the notochord in pterobranchs and enteropneusts. Am Nat 85: 270-271.

Lacalli TC (1994) Apical organs, epithelial domains, and the origin of the chordate central nervous system. Am Zool 34: 533-541.

Lacalli TC (2010) The emergence of the chordate body plan: some puzzles and problems. A Zool 91: 4-10.

Lake JA (1990) Origin of the Metazoa. Proc Nat Acad Sci USA 87: 763-766.

Lemaire P, Smith WC, Nishida H (2008) Ascidians and the Plasticity of the Chordate Developmental Program. Curr Biol 18: 620-631.

Levin M (2005) Left-right asymmetry in embryonic development: a comprehensive review. Mechan Dev 122: 3-25.

Lankester ER (1884) A Contribution of the knowledge of *Rhabdopleura*. Q J Micros Sci 96: 622-647.

Lester SM (1985) Cephalodiscus sp. (Hemichordata: Pterobranchia): observations of functional morphology, behavior and occurrence in shallow water around Bermuda. Mar Biol 85: 263-268.

Lester SM (1988) Ultrastructure of adult gonads and development and structure of the larva of *Rhabdopleura normani* (Hemichordata: Pterobranchia). AZool 69: 95-109.

Lowe CJ, Terasaki M, Wu M, Freeman RM, Runft L, Kwan K, Haigo S, Aronowicz J, Lander E, Gruber C, Smith M, Kirschner M, Gerhart J (2006) Dorsoventral patterning in hemichordates: insights into early chordate evolution. PLoS Biol 4: e291.

Lowe CJ, Wu M, Salic A, Evans L, Lander E, Stange-ThomannN, Gruber CE, Gerhart J, Kirschner M. (2003) Anteroposterior patterning in hemichordates and the origin of the chordate nervous system. Cell 113: 853–865.

Lowery LA, Sive H (2004) Strategies of vertebrate neurulation and a re-evaluation of teleost neural tube formation. Mech Dev 121: 1189-1197.

MacBride EW (1896) The development of *Asterina gibbosa*. Q J Microsc Sci 38: 339-411.

MacBride EW (1903) The development of *Echinus esculentus* together with some points of the development of *E. miliaris* and *E. acutus*. Philos Trans R Soc Lond B 195:285–327.

Maisey JG (1986) Heads and tails: A chordate phylogeny. Cladistics 2: 201-256.

Mallat J (1979) Surface morphology and functions of pharyngeal structures in the larval lamprey *Petromyzon marinus*. J Morphol 162: 249-274.

Mallatt J (1981) The suspension feeding mechanism of the larval lamprey *Petromyzon marinus*. J Zool 194: 103-142.

Mashanov VS, Zueva OR, Heinzeller T, Dolmatov IY (2006) Ultrastructure of the circumoral nerve ring and the radial nerve cords in holothurians (Echinodermata). Zoomorphology 125: 27-38.

Mayer G, Bartolomaeus T (2003) Ultrastructure of the stomochord and the heart-glomerulus complex in *Rhabdopleura compacta* (Pterobranchia): phylogenetic implications. Zoomorphology 122: 125-133.

Metschnikoff E (1881) Über die systematische Stellung von *Balanoglossus*. Zool Anz 4: 139-157.

Mierzejewski P, (2004) Classification of the Cephalodiscoidea. iNet: Graptolite Net: http://pterobranchia.graptolite.net/Cephalodiscoidea.html

Morgan TH (1891) The growth and metamorphosis of Tornaria. J Morphol 5:407-458

Morgan TH (1894) The development of *Balanoglossus*. J Morphol 9: 1–86.

Müller F, O'Rahilly R (1985) The development of the human brain, the closure of the caudal neuropore, and the beginning of secondary neurulation at stage 12. Anat Embryol 176: 413-430.

Munro EG, Odell GM (2002) Polarized basolateral cell motility underlies invagination and convergent extension of the ascidian notochord. Development 129: 13-24.

Nezlin LP (2000) Tornaria of hemichordates and other dipleurula-type larvae: a comparison. J Zool Syst Evol Res 38: 149-156.

Nicol D, Meinertzhagen IA (1988) Development of the central nervous system of the larva of the ascidian. *Ciona intestinalis* L. II. Neural plate morphogenesis and cell lineages during neurulation. Dev Biol 130:737–766.

Nielsen C (1987) Structure and Function of metazoan ciliary bands and their phylogenetic significance. A Zool 68: 205-262.

Nielsen C (1998) Origin and Evolution of animal life cycles. Biol Rev 73: 125-155.

Nielsen C (1999) Origin of the chordate central nervous system - and the origin of the chordates. Dev, Genes and Evol 209: 198-205.

Nielsen C (2001) Animal Evolution. Interrelationships of the Living Phyla. New York: Oxford University Press.

Nielsen C (2005) Trochophora Larvae: Cell-Lineages, Ciliary Bands and Body Regions. 2. Other Groups and General Discussion. J exp Zool 304B: 401-447.

Nieuwenhuys R (2002) Deuterostome brains: Synopsis and commentary. Brain Res Bull 57: 257-270.

Nomaksteinsky M, Roettinger E, Dufour HD, Chettouh Z, Lowe CJ, Martindale MQ, Brunet J-F (2009) Centralization of the Deuterostome Nervous System Predates Chordates. Curr Biol 19:1264-1269.

Nübler-Jung K, Arendt D (1994) Is ventral in insects dorsal in vertebrates? Roux' Arch Dev Biol 203: 357-366.

Nübler-Jung K, Arendt D (1996) Enteropneusts and chordate evolution. Curr Biol 6:352-353.

Ogasawara M, Wada H, Peters H, Satoh N (1999) Developmental expression of Pax1/9 genes in urochordate and hemichordate gills: insight into function and evolution of the pharyngeal epithelium. Development 126: 2539-2550.

Olsson R (1963) Endostyles and endostylar secretions: a comparative histochemical study. A Zool (Stockholm) 44: 299-328.

Palmer AR (2004) Symmetry Breaking and the Evolution of Development. Science 306: 828-833.

Patten BM (1922) Formation of the cardiac loop in the chick. Am J Anat 30: 373–397.

Peterson KJ (2004) Isolation of *Hox* and *Parahox* genes in the hemichordate *Ptychodera flava* and the evolution of deuterostome *Hox* genes. Mol Phylogenet Evol 31: 1208–1215.

Peterson KJ, Eernisse DJ (2001) Animal phylogeny and the ancestry of bilaterians: inferences from morphology and 18S rDNA sequences. Evolution & Development 3:170-205.

Philippe H, Lartillot N, eBrinkmann H (2005) Multigene analyses of bilaterian animals corroborate the monophyly of Ecdysozoa, Lophotrochozoa and Protostomia. Mol Biology Evol 22: 1246-1253.

Rehkämper G, Welsch U, Dilly PN (1987) Feinstrukturelle Beobachtungen zur funktionellen Bedeutung der Trimerie (Archimerie) bei *Cephalodiscus* (Pterobranchia, Hemichordata).

Riisgard HU, Svane I (1999) Filter feeding in lancelets (amphioxus), *Branchiostoma lanceolatum*. Invertebr Biol 118: 423-432.

Romer AS (1967) Major steps in vertebrate evolution. Science 158: 1629-1637.

Ruppert EE (1997a) Introduction: Microscopic Anatomy of the Notochord, Heterochrony, and Xhordate Evolution. In: Harrison FW, Ruppert EE (eds) Microscopic anatomy of invertebrates, vol 15. Wiley-Liss, New York, Chichester, Weinheim, Brisbane, Singapore, Toronto, pp 349-504.

Ruppert EE (1997b) Cephalochordata (Acrania). In: Harrison FW, Ruppert EE (eds) Microscopic anatomy of invertebrates, vol 15. Wiley-Liss, New York, Chichester, Weinheim, Brisbane, Singapore, Toronto, pp 349-504.

Ruppert EE (2005) Key characters uniting hemichordates and chordates: Homologies or homoplasies? Can J Zool 83: 8–23.

Ruppert EE, Balser EJ (1986) Nephridia in the larvae of hemichordates and echinoderms. Biol Bull 171: 188-196.

Ruppert EE, Cameron CB, Frick JE (1999) Endostyle-like features of the dorsal epibranchial ridge of an enteropneusts and the hypothesis of dorso-ventral inversion in chordates. Inv Biol 118: 202-212.

Rychel AL, Smith SE, Shimamoto HT, Swalla BJ (2006) Evolution and Development of the Chordates: Collagen and Pharyngeal Cartilage. Mol Biol Evol 23: 541-549.

Saveliev SV (2009) Evolution of brain development in amphibians. Biol Bull 36: 128-138.

Salvini-Plawen Lv (2000) On the phylogenetic significance of the neurenteric canal (Chordata). Zoology 102: 175-183.

Schoenwolf GC, Smith JL (1990) Mechanisms of neurulation: Traditional viewpoint and recent advances. Development 109: 243-270.

Schaeffer B (1987) Deuterostome monophyly and phylogeny. Evol Biol 21: 179-235.

Schepotieff A (1907) Die Pterobranchier. Anatomische und histologische Untersuchungen über *Rhabdopleura normani* Allman und *Cephalodiscus dodecalophus* M'int. 1. Teil. *Rhabdopleura normani*. 1. Abschnitt. Die Anatomie von *Rhabdopleura*. Zool. Jahrb. Anat. 23: 463-534.

Schroeder TE (1970) Neurulation in *Xenopus laevis*. An analysis and model based upon light and electron microscopy. J Embryol exp Morphol 23: 427-462.

Semon R (1888) Die Entwicklung der *Synapta digitata* und die Stammesgeschichte der Echinodermen. Jenaische Z Naturwiss 22: 1-135, Taf 1-6.

Silén L (1950) On the nervous system of *Glossobalanus marginatus* Meek (Enteropneusta). A Zool 31: 149-175.

Smith AB (2008) Deuterostomes in a twist: the origins of radical new body plan. Evol Dev 10: 493-503.

Smith JL, Schoenwolf GC (1989) Notochordal Induction of Cell Wedging in the Chick Neural Plate and its Role in Neural Tube Formation. J Exp Zool 250: 49-62.

Spengel JW 1893 Die Enteropneusten des Golfes von Neapel und der angrenzenden Meeres-Abschnitte. Fauna und Flora des Golfes von Neapel. Vol. 18. Engelmann, Leipzig.

Stach T (1999) The ontogeny of the notochord of *Branchiostoma lanceolatum*. A Zool 80: 25-33.

Stach T (2000) Microscopic anatomy of developmental stages of *Branchiostoma lanceolatum* (Cephalochordata, Chordata). Bonn Zool Monogr 47: 1-111.

Stach T (2002) Minireview: On the homology of the protocoel in Cephalochordata and 'lower' Deuterostomia. A Zool 83: 25-31.

Stach T (2008) Chordate phylogeny and evolution: A not so simple three-taxon problem. J Zool 276: 117–141.

Stach T, Gruhl A, Kaul-Strehlow S (20xx) The central and peripheral nervous system of *Cephalodiscus gracilis* (Pterobranchia, Deuterostomia). Zoomorphology submitted.

Stach T, Kaul S (2011) The postanal tail of the enteropneust *Saccoglossus kowalevskii* is a ciliarly creeping organ without distinct similarities to the chordate tail. A Zool 92: 150-160.

Stiasny G (1914) Studium über die Entwicklung des *Balanoglossus clavigerus* Delle Chiaje. II. Darstellung der weiteren Entwicklung bis zur Metamorphose. Mitt zool Stat Neapel 22: 255-290.

Swalla BJ, Smith AB (2008) Deciphering deuterostome phylogeny: molecular, morphological and palaeontological perspectives. Phil Trans R Soc B 363: 1557-1568.

Technau U, Scholz CB (2003) Origin and evolution of endoderm and mesoderm. Int J Dev Biol 47: 531-539.

Turbeville JM, Field KG, Raff RA (1992) Phylogenetic position of phylum Nemertini, inferred from 18S rRNA sequences: molecular data as a test of morphological character homology. Mol Biol Evol 9: 235-249.

van der Horst CJ (1939) Hemichordata. Bronn HG, editor. Leipzig: Akademische Verlagsgesellschaft mbH 737 p.

von Ubisch L (1913) Die Entwicklung von *Strongylocentrotus lividus* (*Echinus microtuberculatus, Arbacia pustulosa*). Z Wiss Zool 106: 409-448, pls 405-407.

Watters C (2006) Video views and reviews: neurulation and the fashioning of the vertebrate central nervous system. CBE - Life Sciences Education 5: 99-103.

Welsch U (1968) Über den Feinbau der Chorda dorsalis von *Branchiostoma lanceolatum*. Z Zellforschg Mikrosk Anat 87: 69-81.

Welsch U, Dilly PN, Rehkämper G (1987) Fine structure of the stomochord in *Cephalodiscus gracilis* M'Intosh, 1882 (Hemichordata, Pterobranchia). Zool Anz 218: 209-218.

Welsch U, Storch V (1969) Zur Feinstruktur der Chorda dorsalis niederer Chordaten *Dendrodoa grossularia* (v. Beneden) und *Oikopleura dioika* (Fol.). Z Zellforschg Mikrosk Anat 93: 547-559.

Westheide W, Rieger R (2007) Spezielle Zoologie, Vol. 1: Einzeller und wirbellose Tiere. 2. Auflage. Elsevier GmbH, Spektrum Akademischer Verlag, Heidelberg.

Wilkinson DG, Bhatt S, Herrmann BG (1990) Expression pattern of the mouse T gene and its role in mesoderm formation. Nature 343: 657-659.

Willey A (1891) The later larval development of *Amphioxus*. Q J Microsc Sci 32: 183-234, pls 13-15.

Winchell CJ, Sullivan J, Cameron CB, Swalla BJ, Mallatt J (2002) Evaluating hypotheses of deuterostome phylogeny and chordate evolution with new LSU and SSU ribosomal DNA data. Mol Biol Evol 19: 762-776.

Woodwick KH, Sensenbaugh T, (1985) *Saxipendium coronatum*, new genus, new species (Hemichordata: Enteropneusta): the unusual spaghetti worms of the Galapagos Rift hydrothermal vents. Proc Biol Soc Wash 98: 351-365.

Yasuo H, Satoh N (1994) An ascidian homolog of the mouse *Brachyury* (T) gene is expressed exclusively in notochord cells at the fate restricted stage. Dev Growth Differ 36: 9-18.

Young JZ (1962) The life of vertebrates. 2nd edition. Oxford University Press, Oxford.

Zeng L, Swalla BJ (2005) Molecular phylogeny of the protochordates: chordate evolution. Can J Zoology 83: 24-33.

Summary

Deuterostomia consists of three higher taxa, Echinodermata, Hemichordata, and Chordata. Members of the Chordata are characterized by a number of features, e.g. notochord, neural tube, pharyngeal gill slits, post-anal tail, or characteristic left-right (*LR*) *asymmetries* in the organization of certain structures. However, the evolutionary origin of each of the aforementioned features is still far from being understood. Until today, no consensus has been reached regarding phylogenetic relationships among deuterostome taxa, especially regarding non-chordate deuterostomes. While analyses of molecular data in general support a taxon Ambulacraria consisting of Hemichordata and Echinodermata, most morphological studies foster arguments to unite Enteropneusta (or Hemichordata) and Chordata. These arguments include the presence of a dorsal hollow neural tube, pharyngeal gill slits and a trimeric organization of the coelomic cavities. Although most of these morphological similarities between Hemichordata and Chordata have long been acknowledged, the development and ultrastructure of these organ systems remain largely understudied in hemichordates. For this purpose, the present study elucidates the development of the mesoderm and nervous system in *Saccoglossus kowalevskii* (Enteropneusta) and *Cephalodiscus gracilis* (Pterobranchia) using TEM, SEM, histology, computer aided 3D-reconstruction, and immunohistochemical analyses using confocal laser scanning microscopy.

The data from this study show that the collar cord within the mesosomal region in *S. kowalevskii* develops by invagination of a middorsal plate that is closed in a posterior to anterior direction by enclosing a central fluid-filled canal. The final collar cord is surrounded by a sheath of *extracellular matrix* and lies subepidermal in position. The dorsal brain within the mesosome of *C. gracilis* consists of an anterodorsal cluster of serotonergic somata and a posterior neuropil with a dense network of neurites. According to further ultrastructural details as synaptic vesicles, different neuronal cell types and a separation into somata and neuropil, the collar cord of enteropneusts and the dorsal brain of pterobranchs are suggested to represent integrative centres of the nervous system.

During early development of *S. kowalevskii* the five main coelomic cavities (single protocoel, paired mesocoel and metacoel) derive as separate outpocketings from the endoderm via enterocoely. In contrast, the pericardium, a small sixth coelomic cavity within the anterior protocoel derives from the ectoderm via schizocoely. Later on, pharyngeal gill slits develop as endodermal pouches that fuse with the ectoderm to form dorsolateral openings within the trunk region of *S. kowalevskii*. Moreover, the gill slits and skeletal rods develop asymmetrically, i.e. faster on the left body half.

The ventral post-anal tail of the harrimaniid *S. kowalevskii* comprises a posterior extension of the paired metacoel of the trunk and is filled by mesodermal muscle cells. There is no specialized skeletal element, no strand of endodermal tissue, and no accompanying neural tube present as seen in the dorsal post-anal tail of chordates.

Concluding, the detailed analysis of the development of the collar cord, pharyngeal gill slits and formation of the coelomic cavities in hemichordates altogether support previously acknowledged similarities with the corresponding structures found in chordates, i.e. neural tube, gill slits, and coelom formation. Furthermore, the data presented here lead to suggest homology between these structures, rejecting the assumptions of homoplasy previously made by others. Following this, morphological data from this study support a closer relationship between Hemichordata and Chordata.

Zusammenfassung

Die Deuterostomia umfassen drei höhere Taxa, Echinodermata, Hemichordata und Chordata. Dabei zeichnen sich Mitglieder aus der Gruppe der Chordata durch eine Mehrzahl von charakteristischen Eigenschaften aus, so z.B. Notochord, Neuralrohr, Kiemenspalten, post-analer Schwanz oder links-rechts Asymmetrien bestimmter Strukturen. Der evolutionäre Ursprung jeder dieser Eigenschaften ist jedoch nicht einmal ansatzweise verstanden. Bis heute sind die Verwandtschaftsverhältnisse der einzelnen Deuterostomiertaxa ungeklärt, insbesondere die Stellung der nicht-chordaten Deuterostomier. Während die molekularen Analysen ein Taxon Ambulacraria unterstützen, sehen die meisten morphologischen Studien Argumente für ein näheres Verwandtschaftsverhältnis zwischen Enteropneusten (bzw. Hemichordaten) und Chordaten.

Obwohl es seit langem Hinweise auf morphologische Übereinstimmungen zwischen Hemichordaten und Chordaten gibt, sind die Entwicklung und die Ultrastruktur dieser Organsysteme bei den Hemichordaten bislang zu wenig untersucht. Aus diesem Grund ist es Gegenstand dieser Studie, die Entwicklung des Mesoderms und Nervensystems in *Saccoglossus kowalevskii* (Enteropneusta) und *Cephalodiscus gracilis* (Pterobranchia) mittels TEM, REM, Histologie, computergestützter 3D-Rekonstruktion und Immunohistochemie zu untersuchen.

Die Ergebnisse dieser Studie zeigen, dass sich das Kragenmark in der Mesosomaregion bei *S. kowalevskii* durch Invagination der dorsalen Neuralplatte bildet. Dabei schließt sich das Kragenmark in posteriorer nach anteriorer Richtung und umschließt einen zentralen, flüssigkeitsgefüllten Kanal. In seiner endgültigen Position ist das Kragenmark von *ecm* umgeben und liegt subepidermal im Mesocoel. Das dorsale Gehirn im Mesosoma von *C. gracilis* besteht aus einer anterodorsalen Ansammlung von serotonergen Somata und einem posterioren Neuropil mit einem dichten Netzwerk an Neuriten. Darüber hinaus sprechen weitere ultrastrukturelle Details wie synaptischen Vesikeln, verschiedenen Neuronentypen und einer Unterteilung in Somata- und Neuropilbereich dafür, dass es sich sowohl bei dem Kragenmark der Enteropneusten als auch bei dem dorsalen Gehirn der Pterobranchier um integrative Teile des Nervensystems handelt.

Während der frühen Ontogenese von *S. kowalevskii* entstehen die fünf Coelomräume (einzelnes Protocoel, jeweils paarige Meso- und Metacoele) als voneinander getrennte Darmtaschen vom Endoderm durch Enterocoelie. Das Perikardium als kleines, sechstes Coelom hingegen stammt aus dem Ektoderm und wird durch Schizocoelie gebildet. Später in der Entwicklung von *S. kowalevskii* entstehen die Kiemespalten als Ausbuchtungen des Endoderms, die durch Zusammenwachsen mit dem Ektoderm im Rumpfbereich dorsolaterale Öffnungen bilden. Die Bildung der Kiemenspalten und zugehörigen Kiemenspangen geschieht asymmetrisch, d.h. diese Strukturen entwickeln sich auf der linken Körperseite schneller bzw. zuerst.

Der ventrale post-anale Schwanz des harrimaniiden *S. kowalevskii* besteht aus einer posterioren Erweiterung des Metacoels des Rumpfes und ist mit mesodermalen Muskelzellen ausgefüllt. Im post-analen Schwanz von *S. kowalevskii* konnte ganz im Gegensatz zum dorsalen Chordatenschwanz kein spezieller Skelettstab, kein endodermaler Gewebestrang und auch kein begleitendes Neuralrohr dokumentiert werden.

Zusammenfassend kann festhalten werden, dass die detaillierte Untersuchung der Entwicklung des Kragenmarks, der Kiemenspalten und der Bildung der Coelomräume in Hemichordaten, die

zuvor erkannten Gemeinsamkeiten zu entsprechenden Strukturen bei Chordaten, d.h. Neuralrohr, Kiemenspangen und Coelomentwicklung, weiter unterstützen. Die hier präsentierten Ergebnisse stärken als weitere Argumente eine Homologie zwischen den genannten Strukturen, und schwächen zugleich die Annahmen von Homoplasien, wie von anderen Autoren vorgeschlagen. Auf der Basis von morphologischen Daten wird demzufolge ein Schwestergruppenverhältnis von Hemichordata und Chordata vorgeschlagen.